(12) INTERNATIONAL APPLICATION PUBLISHED UNDER THE PATENT COOPERATION TREATY (PCT)

(19) World Intellectual Property Organization

International Bureau





(10) International Publication Number WO 2013/108045 A2

(43) International Publication Date 25 July 2013 (25.07.2013)

(51) International Patent Classification: **B01J 37/02** (2006.01)

(21) International Application Number:

PCT/GB2013/050122

(22) International Filing Date:

21 January 2013 (21.01.2013)

(25) Filing Language:

English

(26) Publication Language:

English

(30) Priority Data:

20 January 2012 (20.01.2012) 1201086.4 1201305.8 25 January 2012 (25.01.2012) GB

GB

- (71) Applicant: UNIVERSITY OF NEWCASTLE UPON TYNE [GB/GB]; SAgE Enterprise Team, 1st Floor, Devonshire Building, Research and Enterprise Services, Newcastle Upon Tyne NE1 7RU (GB).
- (72) Inventor: AKAY, Galip; School of Engineering and Advanced Materials, Newcastle University, Newcastle Upon Tyne, Tyne and Wear NE1 7RU (GB).
- (74) Agent: STUTTARD, Garry; Tower North Central, Merrion Way, Leeds, West Yorkshire LS2 8PA (GB).

- (81) Designated States (unless otherwise indicated, for every kind of national protection available): AE, AG, AL, AM, AO, AT, AU, AZ, BA, BB, BG, BH, BN, BR, BW, BY, BZ, CA, CH, CL, CN, CO, CR, CU, CZ, DE, DK, DM, DO, DZ, EC, EE, EG, ES, FI, GB, GD, GE, GH, GM, GT, HN, HR, HU, ID, IL, IN, IS, JP, KE, KG, KM, KN, KP, KR, KZ, LA, LC, LK, LR, LS, LT, LU, LY, MA, MD, ME, MG, MK, MN, MW, MX, MY, MZ, NA, NG, NI, NO, NZ, OM, PA, PE, PG, PH, PL, PT, QA, RO, RS, RU, RW, SC, SD, SE, SG, SK, SL, SM, ST, SV, SY, TH, TJ, TM, TN, TR, TT, TZ, UA, UG, US, UZ, VC, VN, ZA, ZM. ZW.
- (84) Designated States (unless otherwise indicated, for every kind of regional protection available): ARIPO (BW, GH, GM, KE, LR, LS, MW, MZ, NA, RW, SD, SL, SZ, TZ, UG, ZM, ZW), Eurasian (AM, AZ, BY, KG, KZ, RU, TJ, TM), European (AL, AT, BE, BG, CH, CY, CZ, DE, DK, EE, ES, FI, FR, GB, GR, HR, HU, IE, IS, IT, LT, LU, LV, MC, MK, MT, NL, NO, PL, PT, RO, RS, SE, SI, SK, SM, TR), OAPI (BF, BJ, CF, CG, CI, CM, GA, GN, GQ, GW, ML, MR, NE, SN, TD, TG).

Published:

without international search report and to be republished upon receipt of that report (Rule 48.2(g))



(54) Title: PROCESS INTENSIFICATION IN THE CATALYTIC SYNTHESIS OF SUPPORTED CATALYSTS WITH HIER-ARCHIC PORE STRUCTURE

<u>Process intensification in the catalytic synthesis of supported catalysts with hierarchic pore structure</u>

The present invention relates to a process for preparing a metal catalyst precursor or a decomposition product thereof supported on a microporous solid support which can be used to obtain a metal catalyst supported on a microporous solid support.

The benefits of a metal catalyst supported on a porous solid support are well known. The porous solid support is typically composed of a highly porous particulate or monolithic material such as carbon or an oxide of aluminium (alumina) or silicon (silica). In conventional processes for the preparation of a metal catalyst supported on a porous solid support, an aqueous solution of a metal catalyst precursor salt such as a nitrate of nickel, cobalt, iron or ruthenium is used to impregnate a porous solid support. The resulting system is treated at an elevated temperature (typically 600°C) to decompose the metal catalyst precursor salt in situ to obtain metal oxide supported on the porous solid support. The metal oxide is then reduced to metal catalyst by heating at a similar elevated temperature. The metal catalyst is activated to an extent which is dependent on the catalyst size. As a result the catalyst loading on the support is often low (a few wt%). Catalyst agglomeration and size enlargement is caused by the blockage of the pores of the support, inaccessibility of the pores to the catalyst precursor molecules and calcination at high temperature during catalyst activation. Furthermore catalyst loading is mainly on the outer surface of the support and the accessibility of the catalyst particles to the reactants is non-uniform with catalysts on the support surface being the primary contributors to the reactions.

The present invention is based on the recognition that exposing a solution of a metal catalyst precursor and a surface-modified nanoparticulate to a high energy source such as microwave or thermal energy can lead to the formation of a supported metal catalyst precursor (or a decomposition product thereof) with a high surface area. The solid support is microporous and the distribution of metal catalyst precursor across the solid support is substantially uniform on the nanometer scale (*ie* the metal catalyst supported on the microporous support is nanostructural) whilst accessibility to all the sites is provided through a hierarchy of pores.

Thus viewed from a first aspect the present invention provides a process for preparing a metal catalyst precursor or a decomposition product thereof supported on a microporous solid support comprising:

- (A) adding together a metal catalyst precursor and surface-modified nanoparticles of the material of the microporous solid support to form an aqueous supportedcatalyst precursor solution; and
- (B) subjecting the aqueous supported-catalyst precursor solution to a source of energy at a power sufficient to cause repeated formation and collapse of films in the supported-catalyst precursor solution and to facilitate the emergence of the metal catalyst precursor or the decomposition product thereof supported on the microporous solid support.

Without wishing to be bound by theory, the source of energy causes rapid evaporation (eg vigorous boiling) of the aqueous solution leading to continuous formation and collapse of liquid films with increasing viscosity. When sufficient water has evaporated, the microporous solid support becomes stable which leads to the formation of a nanostructural metal catalyst precursor supported on the microporous solid support with large interconnecting pores. If the source of energy is of a sufficiently high power, the decomposition of the metal catalyst precursor (typically to metal oxide) begins within the thin walls of the microporous material.

Preferably step (B) is carried out by subjecting the aqueous supported-catalyst precursor solution to a source of energy at a power instantly sufficient to cause repeated formation and collapse of films in the supported-catalyst precursor solution and to facilitate the emergence of the metal catalyst precursor or the decomposition product thereof supported on the microporous solid support.

Step (B) generally involves the rapid evaporation of water which may be followed by the onset of the decomposition of metal catalyst precursor into the decomposition product thereof.

Preferably in step (B) the source of energy is at a power sufficient to facilitate the emergence of the decomposition product supported on the microporous solid support. The decomposition product is typically a metal oxide.

The nanoparticles of the material of the microporous solid support may be surface-modified with organic surface modifiers. The organic surface modifiers may remain intact during step (B) or during any subsequent high temperature treatment of the metal catalyst precursor or decomposition product thereof supported on the microporous solid support in an inert atmosphere (eg nitrogen). For example if step (B) is carried out at low temperature (eg with microwave irradiation or thermal decomposition at 300°C), there may be incomplete combustion of the organic surface modifiers on the surface-modified nanoparticles. When the catalyst is then used for reactions involving compounds of carbon, residual carbon deposits on the catalyst will reduce its activity.

Preferably the process further comprises: (C1) removing organic surface modifiers from the surface-modified nanoparticles of the material of the microporous solid support.

Particularly preferably step (C1) is carried out by applying an electric field to the metal catalyst precursor or decomposition product thereof supported on the microporous solid support in the presence of plasma.

The electric field serves to regenerate the metal catalyst precursor or decomposition product thereof supported on the microporous solid support by removing organic surface modifiers from the microporous solid support which would otherwise reduce catalytic activity. This may be carried out at low temperature through the application of the electric field in the presence of plasma to oxidise carbon with ozone generated by air passing through the catalyst bed.

Alternatively step (C1) may be carried out by calcining the metal catalyst precursor or decomposition product thereof supported on the microporous solid support. Calcining is typically carried out at high temperature (eg about 600°C).

Preferably the process further comprises: (C2) applying an electric field to the metal catalyst precursor supported on the microporous solid support in the presence of plasma whereby to decompose the metal catalyst precursor into the decomposition product thereof.

Preferably the process further comprises: (D) reducing the decomposition product (eg metal oxide) supported on the microporous solid support to a metal catalyst supported on the microporous solid support.

Typically step (D) is carried out in the presence of a reducing agent such as hydrogen. Step (D) may be carried out thermally at an elevated temperature (eg about 300 to 600°C) or at low temperature in the presence of plasma.

Preferably step (D) is carried out thermally in the presence of hydrogen at a temperature of 400°C or more, particularly preferably 550°C or more.

Preferably step (D) is carried out using hydrogen by applying an electric field in the presence of plasma at a temperature of 250°C or less.

In a preferred embodiment, step (B) is carried out in a continuously curved vessel. In a particularly preferred embodiment, step (B) is carried out in a round bottomed flask or watchglass. This further promotes formation and/or collapse of films in the supported-catalyst precursor solution and/or the emergence of the metal catalyst precursor or the decomposition product thereof supported on the microporous solid support.

In a preferred embodiment, step (B) is carried out in the presence of a bubbling gas. The bubbling gas may advantageously further promote film formation. The bubbling gas may be exogenous or generated *in situ* (*eg* through thermal or microwave assisted degradation). The bubbling gas may be generated by a blowing agent. The bubbling gas may be generated by decomposition of a film-forming promoter (*eg* polyacrylamide).

The bubbling gas may be carbon dioxide, nitrogen, oxygen, a nitrogen oxide (eg nitric oxide) or air. The gas (eg nitric oxide) may activate the metal catalyst.

In step (B), the source of energy capable of achieving the requisite power may be selected from one or more of the group consisting of microwave irradiation, thermal energy (eg radiative thermal energy), ultrasound, solar irradiation and ultra-violet irradiation.

The power which is sufficient to cause repeated formation and collapse of films in the supported-catalyst precursor solution and to facilitate the emergence of the metal catalyst precursor or the decomposition product thereof supported on the microporous solid support may be determined empirically by the man skilled in the art. Generally speaking, as the concentration of metal catalyst precursor in the supported-catalyst precursor solution

increases, the requisite power increases. If the power is low, the evaporation of water takes a long time before the onset of the decomposition of metal catalyst precursor. However, if the power is high, the evaporation of water is completed rapidly but decomposition of metal catalyst precursor may not begin until the temperature exceeds about 220°C.

The source of energy may be (or include) thermal energy. The thermal energy may be viscous heat.

The thermal energy may be provided in an environment at high temperature. The high temperature is typically a temperature of 300°C or more, preferably 300°C to 650°C, particularly preferably 450 °C to 600 °C (eg about 600°C). The environment may be a vessel such as a furnace.

Preferably the source of energy is (or includes) microwave irradiation.

The source of energy may be (or include) ultrasound.

The power of microwave irradiation is typically in the range 200 to 1500W, preferably in the range 800 to 1200W (eg about 1000W).

Microwave irradiation is generally ceased when the temperature reaches 225°C.

In step (B) the period during which the supported-catalyst precursor solution is subjected to microwave irradiation is typically 60 to 300 seconds.

Typically the pH of the supported-catalyst precursor solution is 5.5 which is the natural pH of most of the solutions used in embodiments of the invention.

The aqueous supported-catalyst precursor solution may be an aqueous dispersion.

The metal catalyst may contain one or more metal elements. In a preferred embodiment, the (or each) metal element has a valency of II, III, IV or V, preferably II, III or IV.

The (or each) metal element may be selected from the group consisting of alkaline earth metal elements, group IVA metal elements, group B transition metal elements (eg first row group B transition metal elements) and lanthanide metal elements. Preferably the (or each) metal element is selected from the group consisting of group IVA, IVB, VB, VIB, VIIB and VIIIB metal elements. Particularly preferably the (or each) metal element is a group VIIIB metal element.

In a preferred embodiment, the (or each) metal element is selected from the group consisting of Ca, Ba, Pb, Ru, Rh, Pd, Pt, Ir, Ti, Zr, Cr, Nb, V, Co, Ta, Fe, Ni, La and Mn. In a particularly preferred embodiment, the (or each) metal element is selected from the group consisting of Ru, Ti, Fe, Co, Cr, Cu and Ni. In an especially preferred embodiment, the (or each) metal element is selected from the group consisting of Co, Fe and Ni.

The metal catalyst precursor may be a metal salt. The metal catalyst precursor may be a metal halide, carbonate, bicarbonate, hydrogen sulphide, hydrogen sulphate, nitrate, chlorate or sulphate.

Preferably the metal catalyst precursor in the aqueous supported-catalyst precursor solution is capable of decomposition in step (B) into a gas.

Preferably the metal catalyst precursor is a metal nitrate.

Preferably step (B) is carried out in the presence of a film-forming promoter.

Particularly preferably step (B) is preceded by:

(B0) adding the film-forming promoter to the aqueous supported-catalyst precursor solution;

(B00) allowing the formation of a gel part and a solution part in the supported-catalyst precursor solution and

(B000) discarding the gel part, wherein step (B) is then carried out on the solution part.

The film-forming promoter may be a foam generator.

Preferably the film-forming promoter raises the extensional viscosity of the supportedcatalyst precursor solution. This may serve to stabilise film formation in step (B).

The film-forming promoter may be a polymer such as a homopolymer, copolymer (*eg* a random copolymer, a statistical copolymer, a block copolymer or an alternating copolymer), oligomer or co-oligomer (*eg* a random co-oligomer, a statistical co-oligomer, a block co-oligomer or an alternating co-oligomer).

The film-forming promoter may be a non-ionic polymer. The non-ionic polymer may be selected from the group consisting of a polyacrylamide, polyethylene oxide, polyethylene glycol and derivatives thereof (*eg* carboxy derivatives thereof).

The film-forming promoter may be an ionic polymer. The ionic polymer may be selected from the group consisting of a polyacrylamide copolymer (eg a polyacrylamide-acrylic acid copolymer), polyacrylic acid, hydrolysed polymethylmethacrylate and derivatives thereof (eg carboxy derivatives thereof). An ionic polymer may advantageously have the additionally capability to bind metal ions and promote better dispersion of the metal catalyst on the microporous solid support.

The film-forming promoter may be a water soluble polymer. The water soluble polymer is preferably a hydrophobically-modified water soluble polymer.

The hydrophobically-modified water soluble polymer may be characterised by a hydrophilic polymer backbone to which is attached hydrophobic groups. Hydrophobic groups may be

attached to the termini of the hydrophilic polymer backbone. Alternatively or additionally hydrophobic monomers (for example C_{12-22} -alkyl methacrylate monomers) may be grafted along the hydrophilic polymer backbone.

The hydrophilic polymer backbone may be an acrylic polymer (eg an acrylamide, acrylic acid, methacrylate or ethacrylate polymer or a salt thereof), an amine-functional polymer (eg an allylamine, ethyleneimine or oxazoline polymer), an ether polymer, a maleic anhydride polymer, a styrene polymer (eg a polystyrene sulphonic acid or salt thereof), a vinyl alcohol polymer, a vinyl acid polymer (eg a vinylsulphonic or vinylphosphonic polymer) or a salt thereof.

The hydrophobic monomer may be an acrylic monomer (eg an acrylonitrile, acrylamide, maleic anhydride or acrylate (eg butylacrylate, methacrylate or ethacrylate) monomer), an amide monomer, an imide monomer, a carbonate monomer, a diene monomer, an ester monomer, an ether monomer, a fluorocarbon monomer, an olefinic monomer (eg an ethyleneic or propyleneic monomer), a styreneic monomer, a vinylacetal monomer, a vinyl chloride monomer, a vinylidene chloride monomer, a vinyl ether monomer, a vinyl ketone monomer, a vinylpyridine monomer or a vinylpyrrolidone monomer.

The hydrophobically-modified water soluble polymer may be selected from the group consisting of a hydrophobically-modified polyacrylic acid, hydrophobically-modified polyacrylate, hydrophobically-modified polyethylene glycol, hydrophobically-modified hydroxyethyl cellulose, hydrophobically-modified ethyl hydroxyethyl cellulose, hydrophobically-modified ethoxylated urethane copolymer and derivatives thereof (*eg* carboxy derivatives thereof).

In a preferred embodiment, the hydrophobically-modified water soluble polymer is a hydrophobically-modified polyacrylic acid. In a particularly preferred embodiment, the hydrophobically-modified water soluble polymer is an acrylic acid/ C_{12-22} -alkyl methacrylate copolymer. In a more preferred embodiment, the hydrophobically-modified water soluble polymer is an acrylic acid/ C_{12-18} -alkyl methacrylate copolymer (eg an acrylic acid/lauryl methacrylate copolymer or an acrylic acid/stearyl methacrylate copolymer).

In step (B) the film-forming promoter may be added to the supported-catalyst precursor solution in an amount in the range 1:5 to 1:3 (eg about 1:4) by weight.

The material of the microporous solid support may be silica and/or alumina. Preferably the material of the microporous solid support is silica. Alternatively preferably the material of the microporous solid support is silica and alumina (a binary support).

Preferably the nanoparticles of the material of the microporous solid support are surface modified with one or more of the group of organic surface modifiers consisting of silanol groups, silyl ether groups (eg methoxy silane or ethoxysilane groups), acetoxysilane groups, epoxy functionalised silyl or silyl ether groups, hydroxy groups, ureido groups, amino groups, amido (eg methacrylic amido) groups and alkoxy groups.

The nanoparticles of the material of the microporous solid support may be surface-modified with an organofunctional silane. The organofunctional silane may have the following formula:

$$X-R-Si(R')_{3-n}R''_n$$

wherein n is 0, 1 or 2;

R is a C_{1-6} -alkylene group optionally interrupted by an epoxy group;

each of R' and R'' is a hydrolyzable group; and

X is an organofunctional group.

Each of R' and R'' may be independently selected from a C_{1-6} -alkoxy group or acetoxy. Preferably each of R' and R'' is independently methoxy, ethoxy or acetoxy, particularly preferably methoxy or ethoxy.

X may be an epoxy, amino, methacryloxy or sulfido group.

The diameter of the nanoparticles is typically in the range 1 to 100nm, preferably in the range 1 to 40nm, particularly preferably in the range 1 to 10nm.

The surface-modified nanoparticles of the material of the microporous solid support are typically in an aqueous dispersion. Alternatively the surface-modified nanoparticles of the material of the microporous solid support form a composite with an inert support and decompose during step (B).

The amount of material in the aqueous dispersion of nanoparticles of the material of the microporous solid support may be in the range 25 to 45wt% (preferably 30 to 40wt%).

The aqueous dispersion of nanoparticles of the material of the microporous solid support may be prepared as required or may be available commercially (*eg* Bindzil CC30, Bindzil CC40 or Bindzil CC301).

In step (A) the molar ratio of metal to material of microporous solid support is typically in the range 1:9 to 1:3, preferably 1:5 to 1:3 (eg about 1:4).

The surface area of the metal catalyst (or metal catalyst precursor or decomposition product thereof) supported on the microporous solid support may be $120 \text{m}^2/\text{g}$ or more, preferably $150 \text{m}^2/\text{g}$ or more, particularly preferably $175 \text{m}^2/\text{g}$ or more, more preferably $200 \text{m}^2/\text{g}$ or more.

The metal catalyst supported on the microporous solid support may have a hierarchically interconnected micro-mesoporous architecture or a micro-meso-macroporous architecture.

The metal catalyst supported on the microporous solid support may have layered, particulate, spherical, ribbon-like or tubular nanostructures.

Viewed from a further aspect the present invention provides a metal catalyst supported on a microporous solid support obtained or obtainable from a process as hereinbefore defined.

Viewed from a yet further aspect the present invention provides the use of a metal catalyst supported on a microporous solid support obtained or obtainable from a process as hereinbefore defined for cleaning syngas, producing syngas or converting syngas into liquid hydrocarbons.

The syngas may result from the gasification of biomass or waste.

Preferably the use of the metal catalyst supported on a microporous solid support is for producing syngas or converting syngas into liquid hydrocarbons.

Preferably the use of the metal catalyst supported on a microporous solid support for producing syngas is in carbon dioxide reforming.

Preferably the use of the metal catalyst supported on a microporous solid support for converting syngas into one or more liquid hydrocarbons is in a Fischer-Tropsch synthesis.

Particularly preferably the Fischer-Tropsch synthesis is carried out in the presence of plasma (preferably non-thermal plasma). Typically the Fischer-Tropsch synthesis is carried out in the presence of plasma at a temperature of 250°C or less, preferably 200°C or less.

This embodiment has the advantage that the non-thermal plasma assisted Fisher-Tropsch process can reach higher CO conversions at low temperature and ambient pressure compared with conventional processes carried out at relatively high temperature and pressure. Moreover carbon formation on the surface of catalysts is strongly inhibited by plasma. Non-thermal plasma is uniquely able to improve metal dispersion on the catalyst as well as reduce metal particle size to less than 10nm.

Viewed from a still even further aspect the present invention provides a method for preparing a metal catalyst precursor or a decomposition product thereof supported on an alumina support comprising:

- (A) adding together a metal catalyst precursor and an aluminium salt (eg nitrate) to form an aqueous supported-catalyst precursor solution; and
- (B) subjecting the aqueous supported-catalyst precursor solution to a source of energy at a power sufficient to cause repeated formation and collapse of films in the supported-catalyst precursor solution and to facilitate the emergence of the metal catalyst precursor or the decomposition product thereof supported on the alumina support.

The present invention will now be described in a non-limitative sense with reference to Examples and Figures in which:

Figures 1a-d show the XRD patterns of samples A-1, A-2, A-3 and A-4 respectively;

Figures 2a-c show electron microscopy images of sample A-1 at a magnification of 10000, 50000 and 450000 respectively;

Figures 3a-c show electron microscopy images of sample A-3 at a magnification of 10000, 50000 and 450000 respectively;

Figures 4a-c show electron microscopy images of sample A-4 at a magnification of 10000, 50000 and 450000 respectively;

Figure 5 illustrates SEM images of a Cu/Co/SiO₂ catalyst at two magnifications;

Figures 6a and 6b illustrate schematically equipment for the production of agglomerated dense supported catalysts;

Figures 7a and 7b illustrate the variation of temperature with time during microwave irradiation of the catalyst and support precursor solutions (a) at 1kW power with cobalt or nickel catalyst precursor and (b) at various power ratings for cobalt catalyst precursor;

Figures 8a-c illustrates XRD patterns of various nickel/Si and Co/Si catalysts in Examples 5 and 10;

Figure 9 illustrates the formation of nano-sized platelets after the decomposition under microwave irradiation of binary supported catalyst based on [Co]/[Cu]/[Si] = 1:1:8;

Figure 10 shows XRD patterns of silica supported nickel or iron-manganese catalysts produced under combined thermal and microwave irradiation: (a) Ni/Si 2 minutes, (b) Ni/Si 5 minutes and (c) Fe/Mn/Si 2 minutes;

Figure 11 shows XRD patterns of alumina supported cobalt catalysts using Al(NO₃) and Co(NO₃)₂ solution microwave irradiated under NO₂ atmosphere for 5 minutes;

Figure 12a-c show XRD pattern of silica supported iron catalyst produced from FeCl₃ catalyst precursor after microwave irradiation (a) and after heat treatment (b) and with Fe(NO₃)₃ after microwave irradiation followed by heat treatment at 600^oC (c);

Figure 13 illustrates various micro-capillary reactors formed by macro-porous metal foams filled with supported catalysts;

Figure 14 illustrates scanning electron microscopy of silica supported cobalt catalyst macroporous nickel foam: A) overall appearance of the fracture surface of the foam with catalyst (scale bar = 100 microns) and B) at large magnification showing the walls of the nickel foam in a large pore with porous supported catalyst;

Figure 15 shows XRD patterns of silica supported cobalt catalyst in macro-porous nickel foam;

Figure 16a illustrates a comparison of solar (UV)-irradiated catalyst support and catalyst precursor solutions (samples before and after washing are denoted by the letters A and AW and the samples are identified as:

```
Ph2-Fe-Si-14; [Fe]:[Si]=1:4 with method -1.

Ph3-Fe-Si-14; [Fe]:[Si]=1:4 with method -2.

Ph3-Fe-Ca-Si-118; [Fe]:[Ca]:[Si]=1:1:8 method -1.

Ph3-Fe-Mn-Si-118; [Fe]:[Mn]:[Si]=1:1:8 method -1;
```

Figure 16b illustrates peak identification conducted on the washed sample in [Fe]:[Si] = 1:4 after UV radiation before and after washing;

Figure 16c illustrates peak identification in [Fe]:[Si] = 1:4 after UV radiation and washing followed by heat treatment at 600° C for 20 min in a preheated oven;

Figure 16d illustrates peak identification in [Fe]:[Mn]:[Si] = 1:1:8 after UV radiation and washing of the combined silica support precursor and catalyst precursor solutions;

Figure 16e illustrates peak identification in [Fe]:[Mn]:[Si] = 1:1:8 after combined thermal and microwave irradiation of the silica support precursor and catalyst precursor solutions produced according to Example 5-6;

Figure 17 illustrates a plasma reactor;

Figure 18 illustrates a plasma reactor used to demonstrate the activity of catalysts of the invention and a process flow diagram of gas-to-liquid conversion by Fischer –Tropsch synthesis using the plasma reactor;

Figure 18b illustrates various electrode arrangements in the plasma reactor in which a) both electrodes are isolated; b) both electrodes are non-isolated and in contact with the catalyst and/or plasma catalysis promoter (PCP); c) the high voltage electrode is isolated but the earth electrode is not isolated and is in contact with the catalyst and/or plasma catalysis promoter (PCP);

Figure 19a shows the influence of plasma on CO conversion over catalyst PR1;

Figure 19b shows the influence of reduction temperature on the reaction in plasma;

Figures 20a-d illustrate SEM images of various dense silica supported catalysts (a, b) Ni:Si = 1:5 with scale bar 1200 microns and 1 micron respectively and (c, d) Ni:Si = 1:4 with scale bar 5 microns and 500nm respectively;

Figure 20e is a TEM image of Bindzil CC 301 after exposure to UV showing tubular structures with some bar-code strands which also appear extensively in silica supported catalysts (scale bar 20nm);

Figure 20f is a TM image of silica supported catalyst Ni:Si = 1:4 obtained from Bindzil CC 30 and Ni(NO₃)₂ (pH 0.2) without full decomposition and subsequently heat treated at 600° C for 2 hours (scale bar 20nm);

Figure 20g is a TM image of silica supported catalyst Ni:Si = 1:5 obtained from Bindzil CC 30 and Ni(NO₃)₂ with a hydrophobically modified water soluble polymer treated with microwave and subsequently heat treated at 600° C for 2 hours (scale bar 100nm);

Figure 20h is a TM image of silica supported catalyst Co:Si = 1:4 obtained from Bindzil CC 30 and $Co(NO_3)_2$ treated with microwave and subsequently heat treated at 600° C for 2 hours and reduced with hydrogen at 550° C (scale bar 100nm);

Figure 20i is a TM image of silica supported catalyst Fe:Si = 1:4 obtained from Bindzil CC 301 and FeCl₃ treated with microwave at 1kW (scale bar 20nm); and

Figure 20j illustrates schematically various structures observed in the TEM images of several samples.

Characterisation

Catalysts at various stages of processing were characterised using the following techniques:

- 1. Scanning Electron Microscopy (SEM) was used to determine the pore structure in the micrometre to nanometre size range.
- 2. Energy-Dispersive X-ray (EDX) spectroscopy was used to determine concentrations at various locations during SEM analysis.
- 3. Transmission Electron Microscopy (TEM) was used to determine the catalyst support structure at nanometre size range from which catalyst crystallite structure could be evaluated.
- 4. Surface area analysis using the BET method was used to determine the overall admissible surface area provided by the catalyst precursor and catalyst.
- 5. X-ray diffraction (XRD) was used to determine the presence of crystallite structures as well as the average crystallite size using the so-called Scherrer method.
- 6. Catalytic chemical reactions were used to test the activity of the catalyst.

Equipment

- 1. Rotating disk reactor.
- 2. Haake internal mixer with water evaporation.
- 3. Rapid thermal decomposition.
- 4. Microwave treatment.

- 5. Combined microwave and thermal decomposition.
- 6. Combined microwave and ultrasonic treatment.
- 7. Plasma induced catalyst generation.
- 8. Solar radiation or solar radiation simulant.

<u>EXAMPLE 1</u> – Preparation of a nanostructural metal catalyst supported on a microporous solid support

Materials

 SiO_2 source = Bindzil CC30 (an epoxy functional methoxysilane modified silica dispersion in the form of a clear solution containing 30 wt% silica with a particle size of 7nm)

Metal source (M) = $Ni(NO_3)_2$ or $Co(NO_3)_2$

Molar ratio of M:Si = 1:4 or 1:5

Foam generator = hydrophobically modified water soluble polymers (HMWSPs)

A1: Acrylic acid/lauryl methacrylate copolymer (molar ratio 25:1; molecular weight = 4kD)

A2: Acrylic acid/lauryl methacrylate copolymer (molar ratio 8:1; molecular weight = 3kD)

A3: Acrylic acid/stearyl methacrylate copolymer (molar ratio 8:1; molecular weight = 3kD)

Experimental:

(a) No HMWSPs

A clear solution of the metal source M in a stabilised silica dispersion (molar ratio Si:M = 4:1 or 5:1) was placed on a round bottomed Petri dish with a diameter of 9.5cm and a total water holding capacity of 50 ml. The dish was put at the centre of the rotating tray of a microwave kitchen oven. The solution was irradiated continuously for 60 seconds. Vigorous boiling was observed with nitrous oxide evolution which caused the formation of a film. After irradiation, a black crust was observed. Solid deposits of unreacted nickel nitrate (green) or unreacted cobalt nitrate (red) were present around the edge.

Nickel catalyst: A solution of nickel nitrate and Bindzil CC30 at 1:5 Ni:Si molar ratio yielded only flakes of black catalyst powder (sample A-1) which could be easily identified on the light green dry nickel nitrate even when the volume of the solution was decreased from 5 to 2.5 ml or when the irradiation period was increased from 60 seconds to 180 seconds. However when the diameter of the container was decreased to 2 cm, black nickel oxide powder was obtained. When the Ni:Si molar ratio was 1:4, a 5 ml solution (6.2 g) yielded 2.1g of black nickel oxide catalyst even when the diameter of the round bottom Petri dish was 9.5 cm.

Cobalt catalyst: A 5 ml solution of cobalt nitrate + Bindzil CC30 at 1:5 Co:Si molar ratio yielded ca 2.5 g of supported catalyst as a black powder which was highly porous (sample B-1). There was ca 0.2g of unreacted cobalt.

For the purposes of comparison with sample B1, an additional 5 ml solution of cobalt nitrate and Bindzil CC30 at 1:5 Co:Si molar ratio was not irradiated with microwaves but calcined in air at 600°C in an oven for 1 hour to produce sample B-2. XRD, SEM and TEM analysis of samples B-1 and B-2 indicated that cobalt nitrate decomposition in the presence of a silica support yield very similar results to those obtained for nickel.

The above results indicate that the formation of a film is important for the decomposition of metal nitrate under microwave irradiation to form catalytic metal oxides. In the present Example, film formation is achieved by the evolution of the nitrate decomposition products (oxides of nitrogen). If the volume of oxides produced is insufficient, film growth is not possible and decomposition under microwave irradiation stops.

(b) With HMWSPs

The HMWSP used was PPE 1362. 5g of PPE 1362 was mixed with 20g of a solution of nickel nitrate and Bindzil CC30 at 70°C at a molar ratio of 1:4 Ni:Si. There was separation into a top gel part (ca 5g) and a bottom solution part (ca 20g). The two parts were separated.

The gel part was microwaved for 2 minutes. It remained green and was then calcined at 600°C for 1 hour in air and formed a black powder (sample A-2). The solution part was microwave irradiated for 2 minutes and formed a black crust (sample A-3). Sample A-3 was calcined at 600°C in air to form sample A-4.

Figures 1a-d illustrate the XRD of samples A-1, A-2, A-3 and A-4 respectively. They clearly show that nickel oxide peaks are broad when nickel nitrate was microwave irradiated and the broadness does not disappear even after thermal degradation as shown in Figures 1c and 1d. Figure 1d compared with Figure 1c shows that subsequent calcination fails to change the structure of the catalyst.

Figures 2a-c show electron microscopy images of sample A-1 at magnifications of 10000, 50000 and 450000 respectively.

Figures 3a-c show electron microscopy images of sample A-3 at magnifications of 10000, 50000 and 450000 respectively.

Figures 4a-c show electron microscopy images of sample A-4 at magnifications of 10000, 50000 and 450000 respectively.

The use of the HMWSP allows the initial decomposition to be sustained and large yields of supported metal oxide to be obtained. This is achieved by stabilisation of the film which is formed during microwave irradiation.

EXAMPLE 2

A mixed catalyst system was prepared using copper, cobalt and silica at a molar ratio of: 0.25:0.75:4 by dissolving $Cu(NO_3)_2$ and $Co(NO_3)_2$ precursor salts in a SiO_2 dispersion (Bindzil CC30). The pH of the solution was reduced to 0.2 by adding concentrated nitric acid. 5ml of the resulting solution was microwaved in a round bottom watch glass at 1000W for 3 minutes. The resulting material was examined under SEM (see Figure 5) which indicated the presence of nanofibre structure which subsequently collapsed upon thermal treatment at $600^{\circ}C$. The surface area of this catalyst was found to be $175m^2/g$.

EXAMPLE 3

A binary support system containing Ni, Al_2O_3 and SiO_2 at a molar ratio of 1:1:8 was prepared by microwave irradiation of a solution of $Al(NO_3)_3$ and $Ni(NO_3)_2$ in a SiO_2 dispersion (Bindzil CC30) as described in Example 2. The resulting catalyst had a higher surface area than the silica only system.

EXAMPLE 4 – Preparation of low porosity supported catalysts particles

Example 4-1: Uncoated silica particles as support (Classical Method)

A Haake internal mixer (50 ml capacity) fitted with two sigma rotary blades was equipped with a gas/vapour extraction facility which was connected to a fume extraction system (see G Akay and L Tong, Journal of Colloid and Interface Science, Vol. 239 pp. 42-357 (2001)). 100 ml of 1M cobalt nitrate solution in deionised water and a sufficient amount of uncoated colloidal silica particles (Aerosil 380 with average particle size of 7 nm supplied by Degussa) were mixed in a beaker to obtain a Co:Si ratio of 1:5. A highly viscous paste was formed. Approximately 50 g of the material was placed into the internal mixer while mixing at 60 rpm at room temperature. The mixer temperature was increased to 120°C. Mixing was continued for 20 minutes whilst evaporating water. As the level of material dropped due to the evaporation of water, more of the stock dispersion was added. The resulting highly viscous paste-like material was recovered and calcined at 600°C. The initial furnace temperature was ca. 20°C. The heating rate was 10°C/min. After reaching 600°C, calcination was continued for another hour at this temperature before switching off the heating to allow the furnace to cool down over a period of 24 hours. Afterwards the sample was recovered for surface area and XRD analysis from which the size of the catalyst crystallites was evaluated. The surface area was found to be 218 m²/g while the crystal size based on the strongest peak was 23.3 nm.

Example 4-2: Coated silica particles as catalyst support using a high torque mixer

The above experiment was repeated using coated silica particles. A stock solution of catalyst precursor (nickel nitrate) and Bindzil CC30 was prepared to obtain a molar ratio of Ni:Si = 1:5. 50 ml of the stock solution was mixed in the Haake internal mixer at 120°C with a rotational speed of 60 rpm. The level of catalyst and support precursor dispersion in the mixer was reduced due to the evaporation of water. As a result more stock solution was added to keep the level constant. Initially the torque on the mixer blades was low but with the

evaporation of water and increasing amount of solid, the torque increased. After 20 minutes of mixing, a sufficient amount of water was evaporated and the resulting highly viscous paste was recovered. If the mixing continued further, some cobalt nitrate underwent decomposition around the mixer surface where the mixing blades formed a thin catalyst/support precursor film. The resulting highly viscous paste-like material was recovered and calcined at 600°C. The initial furnace temperature was ca. 20°C. The heating rate was 10°C/min. After reaching 600°C, calcination was continued for another hour before switching off heating to allow the furnace to cool down over a period of 24 hours. Afterwards, the sample was recovered for surface area and XRD analysis from which the size of the catalyst crystallites could be evaluated. The surface area was found to be 214 m²/g whilst the crystal size based on the strongest peak was 18.2 nm. The catalysts could be calcined in monolithic form or could be crushed into powder for use in packed bed reactors.

Example 4-3: Coated silica particles as catalyst support using an agglomerator

Example 4-2 was repeated except that a purpose built agglomerator was used to convert liquid phase reactants into particulate product with desired agglomerate size. This allowed the formation of supported catalyst particles with a desired size so that no size reduction was necessary after calcination.

The equipment is shown in Figures 6a and 6b and described in Akay et al, Process intensification in particle technology: Production of powder coatings produced by non-isothermal flow- induced phase inversion. Ind. Eng. Chem. Res., 50: 3239-3246 (2011). The equipment comprises a rotor and stator disks with cavities to mix and transfer/pump liquids or solids or their mixtures. Part of the stator (top disk) where heating takes place can be constructed from porous stainless steel in order to facilitate the continuous escape of vapours and decomposition gases.

The entrance to the rotor was kept at 90°C while the rest of the disks were kept at 120°C. The rotational speed was 30 rpm. Bindzil CC 30 containing 30 w% silica (with a primary particle size of 7 nm) was fed at room temperature into the equipment at a rate of 10 ml/min. Vapour was allowed to escape from the vapour ports as well from the gap between the disks at the outlet. The dispersion went through a highly viscous phase as water content decreased. Due to constant mixing, primary particles agglomerated and were discharged at the exit between the disks and were collected in the collection tray. The particle size measurements indicate that the average particle size was $D_{50} = 155 \mu m$ and that the particle size at 10% and 90% cumulative was $D_{10} = 42 \mu m$ and $D_{90} = 320 \mu m$ respectively. The particle size span was S=1.08 indicating a very narrow size distribution.

The supported catalyst surface area was $238 \text{ m}^2/\text{g}$ whilst the cobalt oxide size based on the strongest XRD-peak was 21.1 nm.

EXAMPLE 5 - Highly porous supported catalyst generation by rapid film formation at high energy

Example 5 illustrates embodiments of the invention for comparison with Example 4.

Example 5-1: Structure evaluation as a function of processing conditions

A microwave reactor (Ethos One) supplied by Milesone Srl, Italy was used to evaluate the effect of microwave power on properties of a supported catalyst. Either cobalt nitrate or nickel nitrate was used as catalyst precursor and Bindzil CC 30 as support precursor. The molar ratio of [Co]:[Si] and [Ni]:[Si] was 1:5. The equipment allowed the measurement of temperature during microwave irradiation and microwave radiation power could be controlled.

20 ml of a solution of the catalyst precursor and support precursor was placed in a 250 ml round bottom flask fitted with a temperature probe. The flask was placed on a rotating stand and the fumes generated were extracted continuously. The temperature of the sample was not allowed to rise above 225°C. At this cut-off temperature, microwave radiation was stopped, fumes were allowed to be fully extracted and the sample was removed. Typical time-temperature profiles for cobalt and nickel are shown in Figure 7a and 7b which indicates that the rate of reaction for cobalt is faster than that for nickel. At the maximum power input, the reaction is complete within 90s for cobalt and 120s for nickel.

The surface area of the samples was measured and XRD data was obtained (see Figure 8a) from which the catalyst size was evaluated based on the most dominant peak/line. Table 1 summarises the catalyst crystallite size and surface area as a function of power.

Table 1: Variation of surface area and catalyst crystallite size with microwave power

	Ni:Si = 1:5								
Power	200	300	400	500	800	1000			
(W)									
Surface Area (m²/g)	-	-	-	-	-	209			
Crystallite Size (nm)	3.35	3.62	3.60	-	-	3.72			

			Co:Si = 1:5			
Power (W)	200	300	400	500	800	1000
Surface Area	_	-	-	-	_	158

(m^2/g)						
Crystallite Size (nm)	7.75	7.74	6.53	6.65	7.75	6.56

Example 5-2 - Effect of superimposed ultrasound power on crystallite size and surface area

A microwave reactor (Ethos One) supplied by Milesone Srl, Italy was used to evaluate the effect of the superimposition of two energy sources, namely microwave and ultrasound on the characteristics of a supported catalyst. The microwave reactor was fitted with an ultrasonic probe to deliver ultrasound irradiation at 40W. The ultrasonic probe extended into the solution of Bindzil CC30 and catalyst precursor (nickel nitrate or cobalt nitrate) at the centre of the round bottom flask. The microwave power rating was 400W and the amount of liquid was 35 ml. Both power sources were switched on and off at the same time when the temperature reached 225 °C.

The solution of nickel catalyst precursor and Bindzil CC30 was provided with 5 wt% polyethylene glycol with a molar mass of 10000 Da. The solution of cobalt catalyst precursor and Bindzil CC30 contained no additive. The molar ratio was [Co]:[Si] = [Ni]:[Si] = 1:5.

The surface area and crystallite size data shown in Table 2 compared with Table 1 indicates that neither the addition of polyethylene glycol nor the presence of ultrasonic field affects the catalyst properties significantly. Although the presence of ultrasound is expected to produce better dispersion of particles during particle generation (hence smaller catalyst size) it also suppresses film formation which results in larger catalyst crystallites. These two effects cancel each other out and crystallite size and surface area are not significantly affected. These observations are valid for nickel and cobalt catalysts. The effect of polyethylene glycol is to reduce the crystallite size as a result of enhanced film formation in the precursor solution.

Table 2: The effect of ultrasound on supported catalyst characteristics

Variable	Ni:Si = 1:5 (wit	h PEG 10,000)*	Co:Si = 1:5		
	Microwave P	ower= 400 W	Microwave P	ower= 400 W	
Ultrasound		**************************************			
Power (W)	0	40	0	40	
Surface Area (m ² /g)	199	197	-	-	

Crystallite Size				
(nm)				
	3.19	3.42	6.53	6.56

Example 5-3: Supported catalyst characteristics as a function of catalyst:support ratio and processing method

Various supported catalysts were prepared using Bindzil CC 30 as the support precursor and Ni(NO₃)₂ as the catalyst precursor. An appropriate amount of nickel nitrate powder was dissolved in Bindzil CC 30 solution so as to obtain a range of [Ni]:[Si] molar ratios from 0 to 2. When the [Ni]:[Si] ratio = 0, Bindzil CC30 was used at pH=5.5. When the [Ni]:[Si] ratio was greater than 1, it was necessary to add deionised water to the Bindzil CC 30 to dissolve the catalyst precursor. After processing the solution, the resulting silica supported nickel oxide catalyst was analysed using a BET surface area analyser SEM, TEM, EDX and XRD which was subsequently used to obtain the catalyst crystallite size. Before this supported catalyst oxide could be used, it was reduced using hydrogen. The following 3 protocols were used:

- 1. Microwave irradiation: 4ml solution in a 9 cm diameter watch glass (round bottom dish) was irradiated for 4 minutes at 1 kW using a Panasonic kitchen microwave oven. At the end of the irradiation time (when the temperature had reached 225°C), the colour of nickel nitrate changed from green to black indicating full nickel nitrate decomposition and the formation of nickel oxide. A small amount of non-decomposed nickel nitrate remained around the central region. Decomposed nickel nitrate was highly puffed/porous/expanded and formed layers as a result of repeated film formation during boiling. After the evaporation of water and formation of green puffed structure, brown nitrogen oxide gases started forming during the oxidation/decomposition stage. When the [Ni]:[Si] ratio was > 1:3, no decomposition of nickel nitrate took place despite the formation of puffed/highly porous nickel nitrate. Prolonged microwave irradiation did not result in nitrate decomposition.
- 2. Thermal decomposition with boiling at 300°C: 20 ml of the precursor solution containing Bindzil CC 30 and nickel nitrate in a 1 litre beaker was placed in a high temperature furnace. The temperature was raised from room temperature to 300 °C at a rate of 10°C/min. The sample was kept at this temperature for another 30 minutes before heating was switched off. After a period of ca. 0.1 hours, the sample was recovered in the form of puffed black solid and subsequently analysed for surface area, crystallite size and micro-to-nano size structure.
- 3. Thermal decomposition with boiling at 600°C with rapid heating-rapid cooling: 20 ml of the precursor solution containing Bindzil CC 30 and nickel nitrate was placed in a 1

litre beaker. The temperature of the furnace was raised to 600 0 C and the sample was put into the furnace. After a period of 0.1 hours, the sample was removed and allowed to cool at room temperature.

4. Thermal decomposition with boiling at 600 °C with slow heating-slow cooling: After placing the precursor solution into the furnace, its temperature was raised from room temperature to 600 °C at a rate of 10°C/min. The sample was kept at this temperature for another 60 minutes before the heating was switched off. After a period of 24 hours (slow cooling), the sample was recovered in the form of puffed black solid and subsequently analysed for surface area, crystallite size and micro-to-nano size structure.

It can be seen from the results in Table 3 that increasing [Ni]:[Si] ratio results in a decrease in surface area and increasing catalyst size. Thermal treatment of the catalyst increases both the catalyst size and surface area determined from XRD data (see Figure 8a).

Table 3: Summary of the results for silica supported nickel oxide catalyst production at different molar ratios of [Ni]:[Si]. Crystallite size is obtained from the only XRD peak for SiO₂. Cooling time is approximate when the microwave irradiated sample or the thermally treated solution is removed after the heating time is completed

Temp	Heat Time	Cool Time				[Ni]:[Si0	O ₂] Ratio				Notes
(C)	(min)	(h)	0	1:9	1:5	1:4	1:3	1:2	1:1	2:1	
		[App]				Surface A	rea (m ² /g)				
					(Crystallite	Size (nm))			_
225	4	0.0	234	227	212	208	201	100	-	-	1-Area
225	4	0.0	1.13	2.98	3.72	3.50	3.89	-	-	-	1-Size
300	60	0.1	212	208	206	167	159	130	65.6	-	2-Area
300	60	0.1	_	4.76	5.08	8.94	13.9	17.5	21.9	-	2-Size
600	60	0.1	249	228	211	205	203	164	105	80.9	3-Area
600	60	0.1	1.13	3.43	4.04	4.38	5.69	9.88	17.2	20.8	3-Size
600	120	24	289	246	230	217	209	166	123	83.2	4-Area
600	120	24	1.16	5.63	5.80	7.65	10.3	13.9	19.0	22.9	4-Size

Notes:

- 1. Microwave irradiation
- 2. Thermal decomposition with boiling at 300 °C
- 3. Thermal decomposition with boiling at 600^{0} C with rapid heating-rapid cooling

4. Thermal decomposition with boiling at 600 °C with slow heating-slow cooling

Example 5-4: Effect of incomplete catalyst precursor decomposition during microwave irradiation

During microwave irradiation of a support and catalyst precursor solution, incomplete decomposition of catalyst precursor can take place. Nevertheless the solution solidifies and forms a highly porous material. Incomplete decomposition is observed as absence of nitrous oxide evolution and as absence of colour change from green (nickel nitrate) to black (nickel oxide).

Example 5-4 compared the characteristics of supported nickel oxide prepared through either full decomposition or no decomposition after microwave irradiation at 1 kW for 150s using 5 ml solution in a 9 cm diameter round bottom watch glass. The ratio of Bindzil CC30 and catalyst precursor (nickel nitrate) was [Ni]:[Si] = 1:3. As a result of a short microwave irradiation time, the central part of the watch glass only had decomposed black nickel oxide surrounded by green nickel nitrate. The two regions were removed and calcined at 600°C in air. The furnace containing the samples was heated from room temperature at a rate of 10 °C. After reaching 600 °C, heating was continued so that the total heating time was 2 hours. Afterwards, the furnace was switched off and it was allowed to cool for 24 hours before the samples were recovered. Surface area and crystallite size of NiO were determined (see Table 4).

Table 4: Effect of catalyst precursor decomposition by microwave irradiation on the catalyst oxide characteristics after heat treatment at 600 °C

Sample description	Surface area	Crystallite
	(m^2/g)	size (nm)
Complete decomposition	173	4.16
[Ni]:[Si] = 1:3		
No decomposition	177.	4.92
[Ni]:[Si] = 1:3		

The results indicate that the important catalyst property (catalyst size) is not affected significantly by incomplete decomposition of the catalyst precursor.

Example 5-5: Mixed supported catalysts

A mixed catalyst system was prepared using cobalt, copper and silica at a molar ratio of [Co]:[Cu]:[Si] = 1:1:8 using cobalt nitrate and copper nitrate salts and Bindzil CC30. The pH of the solution was reduced to 0.2 by adding concentrated nitric acid. 5 ml of the resulting solution was microwaved in a round bottom watch glass at 1000 W for 4 minutes. The resulting material was examined under SEM (see Figure 9) which indicated the presence of nano-platelet structures in the form of flowers. It was found by EDX analysis carried out by scanning electron microscopy that the nano-platelets had significantly higher Co and Cu content than the bulk.

EDX analysis indicated that the average atomic percentage of various elements was:

Oxygen = 53.3 % Silicon = 26.2 Cobalt = 8.4 and Copper = 12.1 which yielded:

$$\{[Co] + [Cu]\} : [Si] = 0.78.$$

The surface area of the mixed oxide was $175 \text{ m}^2/\text{g}$. The size of the crystallites was $\text{Co}_3\text{O}_4 = 6.48 \text{ nm}$ and CuO = 12.5 nm.

In order to ascertain that the nano-platelets were not copper or cobalt nitrate, microwave irradiated oxidised samples were washed in de-ionized water for two days and then dried before analysis by SEM with EDX. No significant changes were seen in the observations made before washing. The nano-platelets were still present and their composition remained very similar to their un-washed state.

Upon thermal treatment at 600 °C (1 hour heating time at a rate of 10 °C/min followed by another hour at this temperature and 24 hours cooling time), SEM examination revealed the collapse of nano-platelets though their presence was still identifiable. The surface area of the resulting mixed catalyst was reduced to 139 m²/g. The concentration distribution within the sample became uniform reflecting the theoretical value of [Co]:[Cu]:[Si] = 1:1:8.

Example 5-6: Combined thermal and microwave treatment of support and catalyst precursor solution

A Milestone microwave reactor (Pyro XL) was used for the microwave irradiation of Bindzil CC301 and nickel nitrate precursor solution at 600 0 C. 5 ml solution was placed in ceramic crucibles and inserted into a high temperature microwave reactor. Microwave irradiation continued for either 120 sec or 300 sec at the end of which the samples were removed immediately and allowed to cool at room temperature. Samples were then analysed for surface area, XRD and carbon as well as for SEM and TEM for comparison with the thermal or microwave only methods. The results are shown in Table 5.

The above method was repeated using a binary catalyst system (Fe/Mn/Si) in which the support precursor was Bindzil CC301. The iron and manganese catalyst precursors were Fe(NO₃)₃ and Mn(NO₃)₂ respectively.

Table 5: The effect of treatment time on catalyst and support characteristics during thermal and microwave radiation of [Ni]:[Si] = 1:4 and [Fe]:[Mn]:[Si] = 1:1:8 solutions

Catalyst system	Time (sec)	Surface Area (m²/g)	Crystallite Size (nm)	Carbon (wt%)
[Ni]:[Si]=1:4	120	214	3.81	0.18
[Ni]:[Si]=1:4	300	184	5.09	0.05
[Fe]:[Mn]:[Si]=1:1:8	120	233	*See note	0.44

^{*}Two very broad and weak peaks were observed for the Fe/Mn/Si system indicating very small/amorphous structure compared with the Ni/Si system. The XRD spectra of the above samples are shown in Figure 10.

The presence of carbon arises from the surface coating of the silica precursor particles.

Example 5-7: In-situ generation of support during microwave decomposition of support and catalyst precursor solution

Various forms of alumina (Al_2O_3) are commonly used as catalyst support due to their very large surface area. However in spite of its very large surface area, the use of pre-prepared alumina does not result in a large catalyst surface area and small and controllable catalyst size especially at high catalyst loadings. In Example 5-7.1 a solution of an alumina precursor $Al(NO_3)_3$ and a catalyst precursor (cobalt nitrate) is used to obtain a mixed oxide with alumina acting as support. The XRD patterns of the samples in Examples 5-7.1, 5-7.2, 5-7.3 and 5-7.4 are shown in Figures 11a-d.

Example 5-7.1

4ml of a solution containing 1 M Al(NO₃)₃ and 1 M Co(NO₃)₂ was placed in a 50 ml glass beaker on the turntable of a kitchen microwave with a power of 1 kW. The 50 ml beaker was covered with a 150 ml glass beaker to stop decomposition gases escaping freely and to generate a blanket of nitrous oxides over the solution during decomposition. These gases escape through small openings between the turntable and the 150 ml beaker. Irradiation time was 3 minutes. After boiling and thin film formation, nitrous oxides appeared to fill the space above the decomposing solution. After about 100 sec of irradiation, a glow (plasma generation) started emanating from the sample which lasted the course of irradiation. The XRD pattern is shown in Figure 11a and indicates the formation of cobalt aluminium oxide with a crystallite size of 40.9 nm based on the dominant peak.

Example 5-7.2

This is a repeat of Example 5-7.1 except that the solution contained 4 M Al(NO₃)₃ and 1 M $Co(NO_3)_2$. After the recovery of the mixed aluminium cobalt oxide, it was heat treated at 600 0 C for 1 hour heating time at a rate of 10 0 C/min and 1 hour dwell time at 600 0 C followed by 24 hour of cooling. The surface area of the resulting sample was 134 m²/g and the crystallite size was 17.1 nm based on the dominant peak.

Example 5-7.3

This is a repeat of Example 5-7.2 except that the solution additionally contained 0.01% chemical blowing agent (Azodicarboxamide) which generates nitrogen gas above 170^{0} C. The resulting sample after microwave irradiation was heat treated as in Example 5-7.2 and had a surface area of $151 \text{ m}^{2}/\text{g}$ and the crystallite size was 14.4 nm based on the dominant peak indicating the importance of film formation through the addition of the blowing agent in enhancing the surface area and reducing the crystallite size compared with Example 5-7.2.

Example 5-7.4

This is a repeat of Example 5-7.2 except that the microwave power was reduced to 900 W as a result of which cobalt nitrate decomposition was incomplete. The resulting sample was then heat treated at 600°C as in Example 5-7.2. The crystallite size was found to be 14.6 nm.

Example 5-8: Mixed supported catalysts

Silica and alumina support precursors (Bindzil CC30 and Al(NO₃)₃) were mixed and either $Co(NO_3)_2$ or $Ni(NO_3)_2$ precursors were then added to obtain [Co]:[Al]:[Si] = 1:1:8 or [Ni]:[Al]:[Si] = 1:1:8. 5 ml of the solution was microwave irradiated in a kitchen microwave oven at 1kW for 4 minutes. The resulting mixed oxides were heat treated at 600 0 C (with 1 hour heating time at a rate of 10 0 C/min and 1 hour dwell time at 600 0 C followed by 24 hours of cooling). The surface area of the resulting samples was $153m^2/g$ for [Co]:[Al]:[Si] = 1:1:8 and $158 m^2/g$ for [Ni]:[Al]:[Si] = 1:1:8. For use as a catalyst, these mixed oxides need to be reduced using (for example) hydrogen to form Co or Ni on a SiO₂ and Al₂O₃ support.

Example 5-9: Choice of catalyst precursor

4ml of a solution of 1 M FeCl₃ and 4M SiO₂ (Bindzil CC 301) was placed in a round bottom watch glass and irradiated for 4 minutes in a kitchen microwave oven at 1 kW. The resulting mixed oxide sample was calcined at 600°C (with 1 hour heating time at a rate of 10 °C/min and 1 hour dwell time at 600 °C followed by 24 hour of cooling). The XRD pattern of this catalyst is shown in Figures 12a-b where it is compared with the XRD pattern of a silica supported Fe catalyst obtained by using Fe(NO₃)₃ catalyst precursor but prepared under the same conditions (see Figure 12c). The surface area of the silica supported iron oxide (Fe₂O₃) obtained from FeCl₃ precursor was 193 m²/g and the crystallite size of Fe₂O₃ based on the strongest line (104) was 72.6 nm (mean Fe₂O₃ crystallite size was 74.2 nm). The surface area

of the silica supported iron oxide (Fe₂O₃) obtained from Fe(NO₃)₃ precursor was 303 m²/g while the crystallite size was very small (ca.1 nm) indicating that the nitrate salt is preferred.

Example 5-10: Supported catalyst generation within the pores of macroporous foams

In chemical reactors, catalysts are used in a fixed bed or fluidised bed. Alternatively catalysts can be fixed on the walls of so-called structured or monolithic microreactors. However in such reactors, catalyst fixation on the reactor walls has drawbacks including low catalyst volume and tendency for catalyst erosion due to fluid flow and thermal/mechanical stress generation.

In order to prevent these drawbacks, catalyst can be incorporated within the pores of metallic or ceramic foam which can then be fabricated into microreactors (such as micro-capillary reactors). Microreactor fabrication using metallic foams containing catalysts is especially straightforward since a series of parallel half capillaries or other types of channels can be formed and subsequently these plates can be assembled to form microchannel reactors. The main bulk flow of the reactants will be in these channels but they will readily diffuse into the foamed regions where the catalyst is present. The flow field can be tailored to promote heat and mass transfer through the geometry or architecture of the foamed structures. Further facilitation in such reactors can be achieved by separating each structured plate by a non-porous thin metal plates so that a two sets of separate inlets-outlets can be obtained to carry out separate reactions in each sets. Such systems are useful for rapid heat transfer. These structured reactors are illustrated in Figure 13. In such foamed channel reactors, catalyst removal due to stresses generated through fluid flow and/or thermal gradients are prevented since the transport processes (momentum, heat and mass transport) are not by convection but by diffusion and the foam structure allows the absorption of thermal and mechanical stresses.

A nickel-based foam (Retimet 80 grade) was used to incorporate silica supported cobalt catalysts. This system allows the foam support (Ni) to be distinguished from the catalyst (Co) in XRD analysis. A solution of Bindzil CC30 and Co(NO₃)₂ was prepared at a molar ratio of [Co]:[Si] = 1:4. Flat nickel foam (Retimet) plates measuring 10 cm X 10 cm were pressed against a set of 1 mm diameter stainless steel rods separated by 2 mm spaces in a hot press at 300 °C and 10 bar pressure for 2 minutes to form an imprint of the rods in the form of half capillaries. These plates were then soaked in the solution for 10 minutes and placed in flat dishes with sufficient solution covering them. These plates were then put into a furnace and heat treated at 600 °C (with 1 hour heating time at a rate of 10 °C/min and 1 hour dwell time at 600 °C followed by 24 hour of cooling). Excess catalyst from the surface was removed in an air stream and then examined under SEM and by XRD for the crystallite size of the silica supported cobalt oxide catalyst. Figure 14 shows the presence of cobalt catalyst within the pores of the nickel foam while Figure 15 illustrates the XRD-pattern of this catalyst system. Very sharp dominant peaks represent nickel while the smaller and broader peaks represent Co₃O₄ with a crystallite size of 20.9 nm based on the dominant cobalt oxide peak.

24

The technique proves that in order to obtain very small crystallite size, film formation is necessary as film formation within the pores of the foam is suppressed.

EXAMPLE 6 - Supported highly porous catalyst oxide generation using solar radiation or solar radiation simulant

Solar radiation can be used to induce catalyst precursor decomposition in the presence of coated silica support precursor solution provided that the decomposition gases are removed continuously.

Fe(NO₃)₃ was used as catalyst precursor and Bindzil CC 301 as the support precursor. The molar ratio of [Fe]:[Si] was 1:4. Under solar radiation, the solution of support and catalyst precursor appeared to bubble and flakes of mixed silica and iron oxides rose over the liquid similar to the foam extraction process. In the meantime, the liquid became highly viscous.

In order to replicate these experiments an agricultural plant growth cabinet which simulates solar radiation and atmospheric conditions (such as temperature and humidity) was used for the model solar irradiation. The growth cabinet operated continuously and to prevent the rapid evaporation of water from the solution, the relative humidity was kept at 50% while the temperature was kept constant at 25 0 C. Two types of dishes were used to contain the solution.

Method 1.1: To round bottom 9 cm diameter watch glasses were added 5 ml of the solution.

Method 1.2: To 50 ml capacity glass beakers were added 10 ml of the solution.

The solutions were place on the sample tray of the agricultural growth cabinet (Fitotron Model SGC097.CPX.F model manufactured by Weiss Gallenkamp) and the solar radiation was started. The radiation level of the growth cabinet was set at the maximum giving radiation dose at LUX= 82,000 lx as measured by a digital Illuminance Meter (supplied by Iso-Tech, type ILM 1332A). The temperature of the cabinet was 25 0 C and the relative humidity was 50%. Radiation was continued for 120 hours. The solutions had the following compositions:

- 1. SiO_2 (Bindzil CC301) + $Fe(NO_3)_3$ at a molar ratio of [Fe]:[Si] = 1:4
- 2. SiO_2 (Bindzil CC301) + $Fe(NO_3)_3$ + $Ca(NO_3)_2$ at a molar ratio of [Fe]:[Ca]:[Si] = 1:1:8
- 3. SiO_2 (Bindzil CC301) + $Fe(NO_3)_3$ + $Mn(NO_3)_2$ at a molar ratio of [Fe]:[Mn]:[Si] = 1:1:8

It was found that when the round bottom watch glasses were used, a dense but porous mixed oxide was obtained with the evolution of gases in all of the solutions. However when Fe(NO₃)₃ with Bindzil CC301 was used by itself in the glass beaker, iron oxide flakes started to form and travelled to the top of the beaker where they accumulated or fell over the side towards the end of the irradiation.

The samples in each category were brought together and their XRD patterns were analysed which revealed that non-decomposed nitrate was present. The samples were washed in deionized water and subjected to surface area, XRD, SEM and TEM analysis.

Table 6 indicates the surface area of various samples. All samples have very large surface area with no significant variation as a result of composition or method. The surface area of Fe/Mn/Si supported catalyst system processed through combined thermal and microwave irradiation at 600 0 C is included for comparison.

Sample	Fe/Si	Fe/Si	Fe/Ca/Si	Fe/Mn/Si	Fe/Mn/Si
	Method-1	Method-2	Method-1	Method-1	Method- TμW*
Surface Area					/ ***
(m^2/g)	267	254	240	268	233*

Table 6: Surface area of photocatalysed silica supported iron catalysts

The XRD data of the above samples using method-1 and method-2 are shown in Figures 16a-d. Also shown is the chemical structure associated with each XRD peak which indicates that although the crystallite size remains similar (*ie* very broad peaks with crystallite size approximately below 4 nm), the method of combined thermal and microwave irradiation forms MnFe₂O₄. In the case of Fe/Si (1:4), FeFe₂O₄ (magnetite) is the only iron oxide formed despite the fact that the microwave treated Fe/Si system was heat treated at 600^oC.

EXAMPLE 7 - Types of catalyst support

High temperature reactions accelerate catalyst size enlargement. If the catalytic reaction is at low temperature, all stages of the catalyst preparation should be carried out at low temperature. The following example demonstrates catalyst preparation using low temperature plasma. If the catalytic reaction is also carried out using low temperature plasma, all stages of the catalyst generation itself can be achieved within the same reactor.

The low temperature plasma reactor used to demonstrate supported catalyst generation at low temperatures is shown in Figure 17. Plasma is generated between two disk electrodes (25 mm in diameter separated by 25mm) in a cylindrical reactor. Plasma is generated in the space between the electrodes (one or both can be isolated in order to prevent any arching) which also contains the powdered or particulate supported catalyst precursor together with a plasma catalysis promoter PCP (3 mm diameter BaTiO₃ balls). The electrode separation was adjusted to ensure plasma generation.

^{*}Note: Method- $T\mu W$ refers to combined thermal and microwave radiation (see example 5-6 and XRD in Figure 16e).

4ml of Bindzil CC30 solution was placed in a 9 cm diameter round bottom watch glass and microwave irradiated in a kitchen microwave oven for 4 minutes at 1kW power input. The surface area and XRD spectrum of the resulting powder were obtained to give values of 234 m²/g and 1.13 nm respectively. 1.5 g of this material was placed in the plasma reactor with 40.3 g of 3mm diameter BaTiO₃ balls as PCP. The electrode separation was 25 mm. The applied voltage across the electrodes was 10 kV. Oxygen gas at a flow rate of 50 ml/min was passed through the reactor and the plasma power of 37 W was established. After the start of the plasma, the temperature of the reactor was kept at 175±5 °C. The gases evolved during the oxidative degradation of the organic coat around silica particles were identified by on-line gas chromatography.

The silica powder obtained from the decomposition of Bindzil CC30 or CC 301 under microwave irradiation was white initially but became brown (due to oxidative degradation of the organic coating around the silica particles) and then black as a result of char (carbon) formation. It then turned white again due to the oxidation of the char. These changes were accompanied by the formation of carbon dioxide and low carbon hydrocarbons as detected during the colour change from white-to-brown-to-black-to-white. No more gases were detected afterwards.

The above experiment was repeated with nickel catalyst precursor Ni(NO₃)₂. A solution of support precursor (Bindzil CC30) and catalyst precursor solution was prepared to obtain [Ni]:[Si] = 1:4. The pH of the solution was reduced to 0.2 by the addition of concentrated nitric acid in order to delay nickel nitrate decomposition during microwave irradiation at 1 kW using a kitchen microwave oven. To a 9 cm diameter glass watch dish was added 5 ml of the solution which was irradiated for 90s to just before the nitrate decomposition started. 1.5 g of the resulting green solid silica supported catalyst precursor was placed in the plasma space of the reactor with 3mm BaTiO₃ plasma promoter. Oxygen gas at a rate of 50 ml/min was used to decompose the nickel nitrate precursor. The plasma power was 37 W. The reaction gases were analysed by on-line gas chromatography using nitrogen as carrier gas. It was observed that there was a surge of NO2 as the colour of the powder changed from green to black as a result of nickel nitrate decomposition. As the concentration of NO₂ decayed, the emerging gases also contained carbon dioxide as result of the oxidation of the coating present on the catalyst support. When no more reaction was present, the plasma reactor was purged with nitrogen and hydrogen gas was substituted to reduce nickel oxide to metallic nickel. During this period, only water was formed which could be recovered by cooling the gases emerging from the reactor.

It was found that the size of the NiO crystallites was 3.16 nm after Ni(NO₃)₂ decomposition and burning of the organic coating around the silica particles. Compared with the thermal oxidation this crystallite size is considerably lower (see Table 5).

EXAMPLE 8 - Structure of the catalysts by Transition Electron Microscopy

The physical nanostructure of the catalysts can be evaluated by Transition Electron Microscopy (TEM). However such studies need to be extensive in order to ascertain that the observed nanostructure is common. In classical supported catalysts, since the catalyst deposition is on an existing solid support, catalysts appear as distinct circular particles.

Through extensive TEM studies, it was found that the support material (SiO₂) when processed under film forming conditions (through thermal, microwave or solar/UV radiation or their combination) formed *inter alia* layered or tubular nanostructures. With the rate of film formation and subsequent film collapse, the dimensions of these structures are small (nanometers to micrometers). In the case of solar/UV radiation when the liquid is spread on a plate, very large visible and continuous film strands are formed with lengths reaching several centimetres covering the whole plate where the film was formed. In all cases where the film formation was allowed, these structures are present. In the presence of catalyst, the supported catalyst system appears to have a mixture of isolated catalyst regions as well as layered structures with alternating silica and catalyst layers. The length of these layered structures can be greater than 10 nm but the thickness of the catalyst layers is typically a few nanometers. Typical SEM images of the catalyst are shown in Figures 20a-d whilst the hierarchical pore structure and nanostructure based on TEM are shown in Figures 20e-i. A summary of these structures is shown in Figure 20j.

EXAMPLE 9 - Plasma Reactor

A low temperature and low pressure plasma based process was developed to demonstrate the effectiveness of catalysts prepared according to embodiments of the invention. A plasma reactor (201) illustrated in Figures 18a and 18b comprises two cylindrical tubes (215, 216) made from quartz. A cross-sectional view of the plasma reactor (201) is shown in the inset of Figure 18a and in Figure 18b where three different electrode arrangements are illustrated. The outer tube (215) has an inside diameter (ID) of 32mm and a length of 300mm. The inner tube (216) has an outside diameter (OD) of 17mm thus leaving an annular discharge gap (209) of 7.5mm. The gap (209) could be packed with a catalyst (210) or a mixture of catalyst (217) and plasma-catalysis promoter PCP in the form of glass balls or barium titanate balls (210) (se Figure 18b). The ground electrode (206) was in the form of a wire mesh wrapped around the outer tube (215) in the middle of the concentric tubes. The high voltage electrode (207) was either a wire mesh or a stainless steel rod (as in Figure 18b) occupying space in the inner tube (216). The length of the ground electrode (206) was 17.3 cm. Plasma was generated only in the region where the ground electrode (206) is present giving an effective reactor volume of 100 ml. The remaining volume not occupied by the catalyst/PCP was packed with glass balls and glass wool. In Figure 18b, it can be seen that the electrodes (206, 207) are isolated from the reactor space by quartz walls of thickness 1.5mm which act as a dielectric barrier. It is also possible to place the ground electrode (206) inside the outer tube (215) to provide more electrical efficiency especially when PCP balls are used.

Reactant gases are supplied from gas bottles (202) which are fitted with mass flow controllers (203). The gases are mixed in a mixer unit (204) before being fed into the reactor inlet. Both

the reactor inlet and outlet contained contain glass wool (205) to prevent catalyst escape. The electrodes (206, 207) are connected to a high voltage source (208) able to supply 0-150W by adjusting the amplitude of the applied voltage. An alternating sinusoidal high voltage of up to 20 kV amplitude (peak-to-peak) and about 20 kHz frequency was applied to the electrodes (206, 207).

Reaction products from the reactor (201) were analysed using on-line gas chromatography (Varian 450-GC - (211)) and finally extracted into a fume cupboard. The data from the Varian 450-GC (211) were stored in a computer (212) and analysed subsequently. The reference gas to the Varian 450-GC (211) was supplied from a gas tank (213) at constant mass flow rate via a mass flow controller (214). Reaction products were also recovered at two stages using two sequential cold traps either at 0 $^{\circ}$ C using ice cold water or dry ice at 78.0 $^{\circ}$ C. The products could also be analysed off-line by gas chromatography.

EXAMPLE 10 Fischer-Tropsch (F-T) synthesis for gas-to-liquid conversion

The plasma reactor (201) described in Example 9 was used to demonstrate the conversion of a mixture of carbon monoxide and hydrogen gas to liquid hydrocarbons (*ie* gas-to-liquid conversion) in a Fischer-Tropsch (FT) synthesis. The simplified conversion can be represented through the formation of alkanes:

$$(2n + 1) H_2 + n CO \rightarrow C_n H_{(2n+2)} + n H_2O$$

In this Example is demonstrated the use of low temperature dielectric barrier discharge plasma in FT-synthesis in the presence of a nanostructural metal catalyst supported on a microporous solid support exhibiting a very high surface area and high porosity.

Co-Si Catalyst

Silica (SiO₂) supported cobalt catalyst was prepared from a solution of Bindzil CC 30 and $Co(NO_3)_2$ as catalyst precursor. A sufficient amount of $Co(NO_3)_2$ was dissolved in Bindzil CC30 to obtain a molar ratio [Co]:[Si] of 1:4. 10 ml of the solution was placed in a 19cm diameter watch glass and irradiated for 4 minutes at 1 kW using a kitchen microwave oven. $Co(NO_3)_2$ decomposed to cobalt oxide (Co_3O_4). This sample was coded as BB-9A. This supported catalyst oxide was heat treated at $600^{\circ}C$ for 2 hours in air to remove the coating material around the silica particles. This sample was coded as BB-9B and it was subsequently used in the plasma reactor for the conversion of a mixture of carbon monoxide and hydrogen (at a molar ratio of $[H_2]$:[CO] =2:1).

Before the reaction, the supported cobalt oxide was reduced to cobalt. The reduction was carried out in the plasma reactor (201) placed in a tubular furnace using hydrogen gas at a flow rate of 50 ml/min for 24 hours without plasma at two different temperatures 400 and 550 0 C. The sample reduced at 400 0 C directly from BB-9A was coded as BB-9C. The sample reduced at 400 0 C from BB-9B was coded as BB-9C1 while the sample reduced at 550 0 C from BB-9B was coded as BB-9C2.

After reduction, small amounts of the samples were removed for XRD analysis from which the crystallite size was determined using the strongest diffraction line (see Figure 8b). Figure 8c identifies the XRD peaks of BB-9C2. The very broad peak is silica and metallic cobalt and cobalt oxides exist. A summary of the oxidation state and the crystallite size of these samples at various stages is shown in Table 7. It is clear that the crystallite size of Co_3O_4 increases with heat treatment and that the reduction at $400^{\circ}C$ does not result in any detectible metallic cobalt. The crystallite size of Co_3O_4 increases

Table 7: Characteristics of the silica supported catalyst as a function of processing history evaluated from XRD patterns

Sample	Reduction	Reduction	Co (111)	CoO (200)	Co ₃ O ₄ (311)
Code	Temperature	from sample (Code)	Size	Size	Size
	(⁰ C)		(nm)	(nm)	(nm)
BB-9A	-	-	N/D*	N/D*	9.20
BB-9B	-	-	N/D*	N/D*	10.1
BB-9C	400	BB-9A		Not available	
BB-9C1	400	BB-9B	N/D*	N/D*	12.5
BB-9C2	550	BB-9B	15.6	5.01	ND*

Notes: N/D*:Not detected

FT-Synthesis using Co-Si catalyst

The plasma reactor (201) described in Example 9 was used in FT-synthesis. No plasma catalysis promoter (PCP) was used. 20 g of BB-9C, BB-9C1 or BB-9C2 was placed in the 100ml plasma zone of the reactor (201). The size of the catalyst particles was 1-3 mm. Outside the plasma zone were packed 3 mm diameter glass balls. The reactor (201) was used in a fume cupboard without insulation so as to allow heat dissipation generated by plasma as well as by FT-synthesis. The surface temperature of the reactor (201) was controlled at 150 ± 5 $^{\circ}$ C whereas the temperature at the centre of the reactor (201) where the catalyst bed was located was $240 \pm 10^{\circ}$ C (as measured at the end of each experimental run). Temperature measurements were made at various locations and averaged to obtain a nominal mean reactor temperature.

The wall power consumed by the plasma reactor (201) was measured by a plug-in power meter. The plasma power dissipated in the discharge was calculated by integrating the

product of voltage and current. The applied voltage was 20 kV at a frequency of 20 kHz and power consumption was 90W.

The reactor (201) was fed a mixture of carbon monoxide and hydrogen at a molar ratio of $[H_2]$:[CO] = 2. The gases were introduced into the reactor (201) at a total gas flow rate of 25.2 ml/min. The reaction products were analysed using the Varian 450-GC (211) from which the carbon monoxide conversion was determined.

The Varian 450-GC (211) was equipped with 2 ovens, 5 columns and 3 detectors (2 TCDs and 1 FID). One oven housed 3 columns (hayesep T 0.5 m x 1/8" ultimetal, hayesep Q 0.5 m x 1/8" ultimetal and molsieve 13 x 1.5 m x 1/8" ultimetal) to detect permanent gases. The second larger oven housed a CP-SIL 5CB FS 25 X.25 (.4) column for hydrocarbons and a CP-WAX 52CB FS 25 X.32 (1.2) for alcohols. The mass balance of the reaction was obtained by adding a controlled flow of nitrogen (20 ml/min) as a reference gas to the exit of the reactor (20 ml) in order to monitor the change of volume flow due to the reaction. All results are reported in mole percent.

The conversion of CO is defined as

CO Conversion (mole %) =
$$100 * \frac{CO (mole input) - CO (mole output)}{CO (mole input)}$$

The conversion of H₂ is defined as

H2 Conversion (mole %) =
$$100 * \frac{\text{H2 (mole input)} - \text{H2 (mole output)}}{\text{H2 (mole input)}}$$

The product selectivity is defined as

Selectivity (product)
$$_{i} = 100 * \frac{(Number of carbon atoms in product i)*(Mole af product i)}{Carbon atom number onverted}$$

 $i = CO_2$, CH_4 , C_2H_4 , C_2H_6 , C_3H_6 , C_3H_{10} , C_4H_8 , C_4H_{10} . The selectivity to C_5 + hydrocarbons was calculated from the carbon balance of the reactions.

Results

Table 8 illustrates carbon monoxide and hydrogen conversion for the catalysts BB-9C, BB-9C1 and BB-9C2 after 100 hours of continuous FT-synthesis at 240° C under identical conditions. It was found that 100 % conversion was obtained when the catalyst BB-9C2 was used even after 150 hours of continuous reaction. In the case of the catalyst BB-9C1, 100% conversion was initially observed (in the first 15 hours) but the conversion decayed gradually. This was followed by a slight increase after 95 hours reaching 67.7% Co and 39.2 H_2 conversion. The catalyst BB-9C initially showed some activity (30% carbon monoxide conversion after 30 min) which rapidly decayed to zero after 24 hours.

31

Methane, carbon dioxide, and higher hydrocarbons including ethylene, propylene, propane, butylene and butane were detected in the outlet gas stream. These results refer to 100 hours of reaction in the presence of plasma and 17hrs in the absence of plasma since the conversion in the absence of plasma decays to zero within 24 hours. The product distribution for BB-9C and BB-9C1 was also evaluated when the reaction temperature was 240 0 C and plasma power was 90W.

Table 8: Carbon monoxide and hydrogen conversion as a function of plasma power and time when the reactor temperature was 240 0 C using the catalysts described in Table 7

Catalyst system →	BB-9C2	BB-9C1	BB-9C		
Plasma power →	90 W	90 W	P=90 W	P=0 W	P=0 W
Reaction time →	100 h	100 h	100 h	17 h	25 h
Conversion ↓					
Carbon monoxide conversion (mol%)	100	67.7	29.6	15.1	0
Hydrogen	63	39.2	15.5	8.1	0
conversion (mol%)					
	Product Se	lectivity (m	ol %)		
Methane (C ₁)	56.0	37.4	40.6	22.4	-
Carbon Dioxide	31.3	24.1	31.2	14.7	-
C ₂	2.5	0.3	1.0	1.2	-
C ₃	1.4	0.2	0.4	0.5	-
C ₄	2.3	0.3	0.6	0.8	-
C ₅ +	6.5	37.7	26.2	60.4	-

EXAMPLE 11 - Conversion of methane to hydrocarbons and hydrogen

As shown in Example 10 (Table 8), the FT-synthesis yielded a considerable amount of methane and carbon dioxide as well as liquid hydrocarbons with carbon number 5 or greater. This synthesis also resulted in 100% carbon monoxide conversion. It is possible to remove all of the oxygenated carbons (*ie* CO and CO₂) through plasma FT synthesis at atmospheric pressure and low reaction temperature using catalytic plasma reactors and carbon dioxide separation by well known techniques. Essentially the oxygenated carbons are removed by de-oxygenation of the syngas and enhancement of hydrogen either as free hydrogen (H₂) or as chemically bound hydrogen in the form of methane (CH₄). Hydrogen is itself essential for FT-synthesis since the [H₂]:[CO] ratio in syngas is not sufficient to achieve optimum reaction conditions.

Another important property of hydrogen is that it can be separated easily from other gases. Hence the required hydrogen for FT-synthesis can be either provided from other sources of hydrogen such as methane or through steam reforming of carbon dioxide and/or carbon monoxide or by electrolysis of water.

When methane was subjected to catalytic plasma reaction, it was converted to hydrogen and non-oxygenated hydrocarbons. In this example the plasma reactor (201) described in Example 9 was used with only 5 mm soda lime glass balls acting as plasma catalysis promoter (PCP) in the plasma space between the electrodes. Methane gas (CH₄) was fed into the reactor at a constant flow rate of 25 ml/min. The emerging gases were analysed using gas chromatography. The concentration of hydrocarbons with carbon number equal or greater than 5 was calculated through mass balance in order to obtain product selectivity. The results are shown in Table 9 where the variation of methane conversion and the selectivity for hydrogen and C2, C3, C4 and C5+ are shown as a function of plasma power. It is clear that the methane conversion increases with increasing plasma power and that selectivity for C5+ hydrocarbons also increases. Table 10 shows the effect of total flow rate of methane on conversion and selectivity when the plasma power is 100 or 120 W.

Table 9: The effect of plasma power on methane conversion and non-oxygenated hydrocarbon selectivity when the total flow rate is 25 ml/min

Plasma Power (W)	80	100	120						
CH ₄ Conversion (mol. %)	22.4	28.0	33.7						
Product Selectivity (mol. %)									
H ₂ selectivity (mol %)	59.4	59.0	55.7						
Hydrocarbon selectivity (mol%)	40.6	41.0	44.3						
Carbon Number Selectivity (mol %)									

C ₂	20.0	18.4	16.6
C ₃	19.2	19.0	18.0
C ₄	17.6	18.0	17.2
C ₅ +*	43.2	44.6	48.2

C₅+*: calculated from carbon number balance.

Table 10: The effect of total flow rate of methane on conversion and selectivity when the plasma power is 100 or 120 W

Plasma Power (W)	120	100	100	100		
Total flow rate (mL/min)	25		37.5	50		
CH ₄ Conversion (mol. %)	33.7	28	20	15.6		
Product Selectivity (mol %)						
H ₂ selectivity (mol %)	59.0	55.7	59.1	60.1		
Hydrocarbon selectivity (mol %)	41	44.3	40.9	39.9		
Carbon Number Selectivity (mol %)						
C ₂	18.4	16.6	40.7	43.7		
C ₃	19.0	18.0	19.7	20.3		
C ₄	18.0	17.2	19.2	19.2		
C ₅ +*	44.6	48.2	20.4	16.8		

EXAMPLE 12 Plasma promoted Fischer-Tropsch synthesis of hydrocarbons at low temperature and ambient pressure

Experimental

Cobalt supported on silica (Co:Si = 1:4) was used as a catalyst. The process for its preparation is described in preceding Examples and uses microwave at 1000W (max

temperature 270°C). The resulting catalyst was oxidised at 600°C for 2 hours. The density of the catalyst was 0.2g/ml.

Catalytic Reactions

The discharge volume of the reactor (201) described in Example 9 was filled with 100ml of the porous Co based catalyst (20 g) with a particle size of 2-3mm. Prior to plasma reaction, the catalyst was reduced at 400°C in a flow of hydrogen (50 ml/min) for 12 hours. After catalyst reduction, the furnace was switched off and the reactor (201) was allowed to cool down to room temperature. The catalyst is identified as PR1.

CO and H_2 were introduced at a total gas flow rate of 20 to 100 mL/min. A back pressure valve at the inlet was used to regulate the pressure in the reactor (201) up to a maximum pressure of 5 bar. The preselected temperature of the reactor (201) was maintained by a tubular furnace. The Varian 450-GC was equipped as described in Example 10. The conversion of CO and H_2 and the product selectivity is as defined in Example 10.

Results

Methane, carbon dioxide and higher hydrocarbons including ethylene, propylene, propane, butylene and butane were detected in the outlet gas stream.

Figure 19a shows the influence of reaction time on CO conversion over the catalyst PR1. It demonstrates that the CO conversion dropped quickly from 74% to 46% in the early hours in plasma. CO conversion was then stabilized at about 40% until 60 hours after which the activity decreased slowly with an increase in the reaction time. At 100 hours, CO conversion was 30%. The production distribution (carbon number selectivity) of the reaction is listed in Table 11. It is clear that the product selectivity to methane decreased initially and stabilized at about 40%. Carbon dioxide decreased and stabilized at about 30% with an increase of the reaction time. The carbon number selectivity to C2, C3 and C4 increased although an increase of the reaction time had no apparent influence on the product selectivity to C5+ hydrocarbons which stabilised at 27%.

It is important to note that the temperature of the reactor (201) increased due to the dielectric barrier heating in the reaction. At 100 hours, the wall temperature of the reactor (201) was 150°C. For a better understanding of the reaction and to eliminate the influence of dielectric heating on the reaction over Co based porous catalyst in plasma, the reaction was carried out at a reaction temperature of 150°C in a furnace in the absence of plasma. From Figure 19a, it can be seen that there is no CO conversion at such a temperature indicating that it is dielectric barrier discharge that promotes the CO conversion at 150°C.

The reaction was also carried out at 250°C to explore the effect of reaction temperature. The results are listed in Table 12 and shown in Figure 19a. The initial conversion of CO was 31% which dropped quickly with an increase in the reaction time. At 17h, the conversion decreased to 15%. It is different from the reaction carried out under plasma conditions. Carbon number selectivity to methane, C2, C3, and C4 increased whilst selectivity to CO₂

and C5+ hydrocarbons decreased with an increase in reaction time. After reaction, a lot of carbon formed on the surface of the deactivated catalyst was detected which indicates that the higher selectivity to C5+ hydrocarbons is due to the formation of carbon on the surface of the catalyst under thermal conditions.

Effect of catalyst reduction temperature

For a better understanding of the reaction under plasma conditions, the catalyst was reduced at 350, 400 and 550°C (catalysts PR1, PR2 and PR3 respectively). Figure 19b shows that the catalyst reduction temperature plays a key role in its performance in the reaction. Higher reduction temperatures (catalyst PR3) favour higher conversion of CO. It is quite possible that some Co species generated at higher reduction temperatures in hydrogen contribute to the high CO conversion in the combination of plasma and catalysts in the process. Reducing the catalyst at higher temperatures also improved the stability of the catalyst. For example, 100% CO conversion for 150 hours was achieved over the catalyst reduced at 550°C. The catalyst reduced at 400°C (PR2 - see Table 13) demonstrated 100% CO conversion initially which then dropped to 81% after 50 hours in plasma. The CO conversion decreased further and stabilized at about 66% until 120 hours.

The reduction temperature not only influences the catalyst activity but also influences its selectivity. Compared with the catalyst reduced at 350°C (PR1), the one reduced at 400°C (PR2) showed higher CO conversion and higher carbon selectivity to methane and ethylene in the beginning. The minimum selectivity to methane reached 29.9% at 72 hours. Further increases in the reaction time led to an increase of the selectivity to methane. The maximum selectivity to CO2 (36%), C2 (2.52%) and C3 (0.19%) was obtained at 25hours. With an increase in the reaction time, the selectivity to C5+ increased initially and reached a maximum (39.3%) at 72 hours. Further increases in the reaction time decreased the selectivity to C5+.

Catalyst regeneration

Table 14 summarizes results of F-T synthesis over the Co-based catalyst reduced at 550°C for 24 hours in hydrogen under differing conditions. Even at a total flow rate of 100ml/min (H₂:CO=2:1), 100% CO conversion at a plasma power of 90W is still obtained. When the plasma was switched off and the reaction was carried on at 250°C, the catalyst lost activity within 24 hours.

Further experiments revealed that a combination of hydrogen and plasma cannot totally regenerate the catalyst. Only a part of the activity can be restored after treatment with hydrogen in plasma and the catalyst activity was lost quickly in the following F-T synthesis in plasma.

When the used catalyst is activated in air with plasma and then reduced with hydrogen in plasma, the catalyst activity was restored totally and gave CO conversion of 100% at a plasma power of 90W for more than 24 hours.

Conclusions

The catalyst reduction temperature plays a key role in F-T synthesis in plasma. Plasma can promote the Fischer-Tropsch reaction over a Co based porous catalyst at low temperature. Plasma can maintain the reaction activity for a longer time. At the same CO conversion level, the reaction under plasma generates more methane and more carbon dioxide than a thermal reaction at 250°C which demonstrates that the mechanism of the reaction under plasma conditions is different from that under thermal conditions.

Hydrogen conversion is higher in a plasma reaction than that in a thermal reaction which indicates that a dielectric barrier discharge can promote the hydrogenation of CO for more methane and higher hydrocarbon formation. By optimizing the plasma parameters and the catalyst property, it is possible to develop a new route for Fischer-Tropsch reactions at lower temperature and ambient pressure.

Table 11: Product distribution over PR1 catalyst with plasma

, , , , ,	Time (h)								
	1	2	21	50	75	100			
CO Conversion (mol %)	73	46.7	40.2	39	35.8	29.6			
H ₂ Conversion (mol %)	37	24.8	22.6	22	19.7	15.5			
Converted H ₂ /CO (mol)	1.1	1.2	1.3	1.3	1.2	1.2			
Carbon Containing Product Selectivity (%)									
CO_2	35.9	32.7	30.2	29.8	29.9	31.2			
CH ₄	48.4	39.3	41.5	41.8	40.8	40.6			
C ₂	0.27	0.45	0.54	0.68	0.85	1.01			
C ₃	0.14	0.23	0.28	0.29	0.32	0.39			
C ₄	0.23	0.38	0.44	0.47	0.51	0.63			
C ₅ +	15.1	27	27	26.9	27.6	26.2			

Reaction conditions: CO 8.4 SCCM; H₂: 16.8 SCCM; Porous Catalyst: 20 g

Power 90W; Reactor at 150°C

Table 12: Production distribution over PR1 catalyst without plasma

	Reaction Time (h)				
	1	17			
CO Conversion (mol %)	31	15.1			
H ₂ Conversion (mol %)	6.7	8.1			
Converted H ₂ /CO (mol)	0.2	0.7			
Carbon Contain Product	Selectivity	y (Mol %)			
CO_2	23	14.7			
CH ₄	11.6	22.5			
C_2	0.39	1.21			
C ₃	0.17	0.46			
C ₄	0.30	0.76			
C ₅ +	64.4	60.4			

Reaction conditions: CO 8.4 SCCM; H₂: 16.8 SCCM; Porous Catalyst: 20 g

Reaction temperature: 250°C

Table 13: Product distribution over PR2 catalyst

	Time (h)								
	1	2	3	25	50	72	95	120	
CO Conversion (mol %)	100	100	100	92	81.4	66.3	66.5	67.7	
H2 Conversion (mol %)	79.9	80	80	40.9	51.3	33.8	39	39.9	
Converted H ₂ /CO (mol)	1.8	1.8	1.8	1.0	1.4	1.1	1.3	1.3	
Carbon Containing Product Selectivity (mol %)									
CO_2	15.2	15.3	15.8	36	21.5	29.7	24.7	23.5	
CH ₄	78.1	79.2	79.2	36.3	39.3	29.9	36.7	41.2	

C_2	1.82	1.85	1.85	2.52	0.55	0.61	0.28	0.96
C ₃	0.13	0.14	0.14	0.19	0.00	0.17	0.16	0.16
C ₄	0.15	0.16	0.16	0.21	0.19	0.25	0.24	0.31
C ₅ +	4.6	3.4	2.9	24.8	38.4	39.3	37.9	33.9

Reaction conditions: CO 8.4 SCCM; H₂: 16.8 SCCM; Porous Catalyst: 20 g

Power 90W; Reactor at 150°C

Table 14: Plasma-assisted FT synthesis over a Co-based catalyst

Prior to the reaction the catalyst was reduced in hydrogen (50ml/min) at 500 C for 24 hours

Experiment	Flow rate	H ₂ :CO	Temperature	Catalyst Type	Plasma Reactor Power	Time on Stream (h)	Notes	Catalyst Characterization
PR3	25	2:1	240	BB-9D	90	150	100% CO conversion	
PR4	100	2:1	240	PR3	90	25	100% CO conversion	
PR5	100	2:1	240	From PR4	0	24	Catalyst lost activity	
PR6	100	2:1	150	From PR5	90	24	No activity	
PR7	100	H2 Only	240	From PR6	90	48	Release of C/HC by H ₂ , but some heavier HC still appear after 48 h.	
PR8	100	2:1	240	From PR7	90	24	Some activity restored. Lost activity with time.	
PR9		Air only	240	From PR8	90	24	Oxidize C/HC and catalyst by O ₂ plus plasma	Carbon/HC to CO/CO ₂ re- activation
PR10	100	H2 Only	240	From	90	24	Reduce catalyst by	Re-activate

				PR9			H ₂ Plus Plasma	catalyst
PR11	100	2:1	240	From PR10	90	24	100% CO conversion with more methane and CO ₂ produced	

CLAIMS

1. A process for preparing a metal catalyst precursor or a decomposition product thereof supported on a microporous solid support comprising:

- (A) adding together a metal catalyst precursor and surface-modified nanoparticles of the material of the microporous solid support to form an aqueous supportedcatalyst precursor solution; and
- (B) subjecting the aqueous supported-catalyst precursor solution to a source of energy at a power sufficient to cause repeated formation and collapse of films in the supported-catalyst precursor solution and to facilitate the emergence of the metal catalyst precursor or the decomposition product thereof supported on the microporous solid support.
- 2. A process as claimed in claim 1 wherein step (B) is carried out by subjecting the aqueous supported-catalyst precursor solution to a source of energy at a power instantly sufficient to cause repeated formation and collapse of films in the supported-catalyst precursor solution and to facilitate the emergence of the metal catalyst precursor or the decomposition product thereof supported on the microporous solid support.
- 3. A process as claimed in claim 1 or 2 wherein in step (B) the source of energy is at a power sufficient to facilitate the emergence of the decomposition product supported on the microporous solid support.
- 4. A process as claimed in any preceding claim further comprising: (C1) removing organic surface modifiers from the surface-modified nanoparticles of the material of the microporous solid support.
- 5. A process as claimed in claim 4 wherein step (C1) is carried out by applying an electric field to the metal catalyst precursor or decomposition product thereof supported on the microporous solid support in the presence of plasma.
- 6. A process as claimed in any preceding claim further comprising: (C2) applying an electric field to the metal catalyst precursor supported on the microporous solid support in the presence of plasma whereby to decompose the metal catalyst precursor into the decomposition product thereof.
- 7. A process as claimed in any preceding claim further comprising: (D) reducing the decomposition product supported on the microporous solid support to a metal catalyst supported on the microporous solid support.
- 8. A process as claimed in claim 7 wherein step (D) is carried out using hydrogen by applying an electric field in the presence of plasma at a temperature of 250°C or less.

9. A process as claimed in any preceding claim wherein step (B) is carried out in a continuously curved vessel.

- 10. A process as claimed in any preceding claim wherein the source of energy capable of achieving the requisite power may be selected from one or more of the group consisting of microwave irradiation, thermal energy, ultrasound, solar irradiation and ultra-violet irradiation.
- 11. A process as claimed in any preceding claim wherein the source of energy is (or includes) microwave irradiation.
- 12. A process as claimed in any preceding claim wherein the metal catalyst contains one or more metal elements selected from the group consisting of Co, Fe and Ni.
- 13. A process as claimed in any preceding claim wherein the metal catalyst precursor is a metal nitrate.
- 14. A process as claimed in any preceding claim wherein step (B) is carried out in the presence of a film-forming promoter.
- 15. A process as claimed in any preceding claim wherein the nanoparticles of the material of the microporous solid support are surface-modified with an organofunctional silane.
- 16. A process as claimed in any preceding claim wherein in step (A) the molar ratio of metal to material of microporous solid support is in the range 1:5 to 1:3.
- 17. A process as claimed in any preceding claim wherein the metal catalyst supported on the microporous solid support has a hierarchically interconnected micro-mesoporous architecture or a micro-meso-macroporous architecture.
- 18. A metal catalyst supported on a microporous solid support obtained or obtainable from a process as defined in any preceding claim.
- 19. The use of a metal catalyst defined in claim 18 for cleaning syngas, producing syngas or converting syngas into liquid hydrocarbons.
- 20. The use as claimed in claim 19 for converting syngas into one or more liquid hydrocarbons in a Fischer-Tropsch synthesis.
- 21. The use as claimed in claim 19 or 20 wherein the Fischer-Tropsch synthesis is carried out in the presence of plasma at a temperature of 240°C or less.

WO 2013/108045

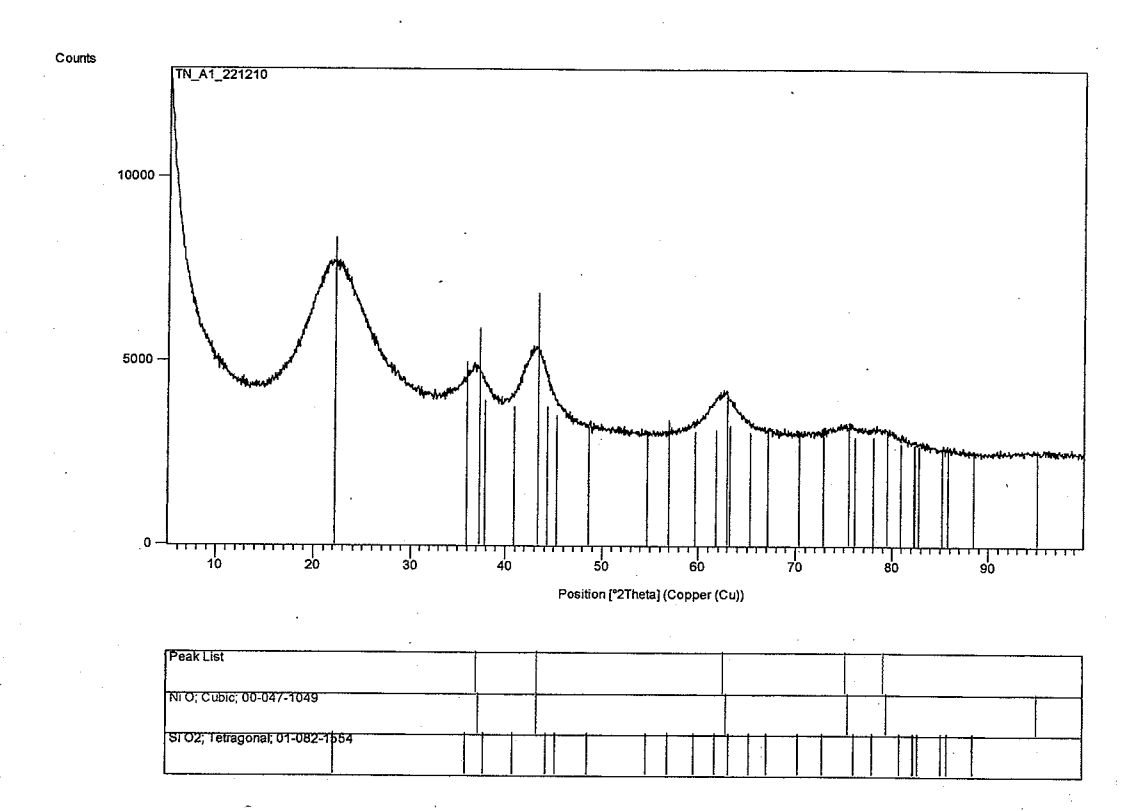


Fig. 1 (a)

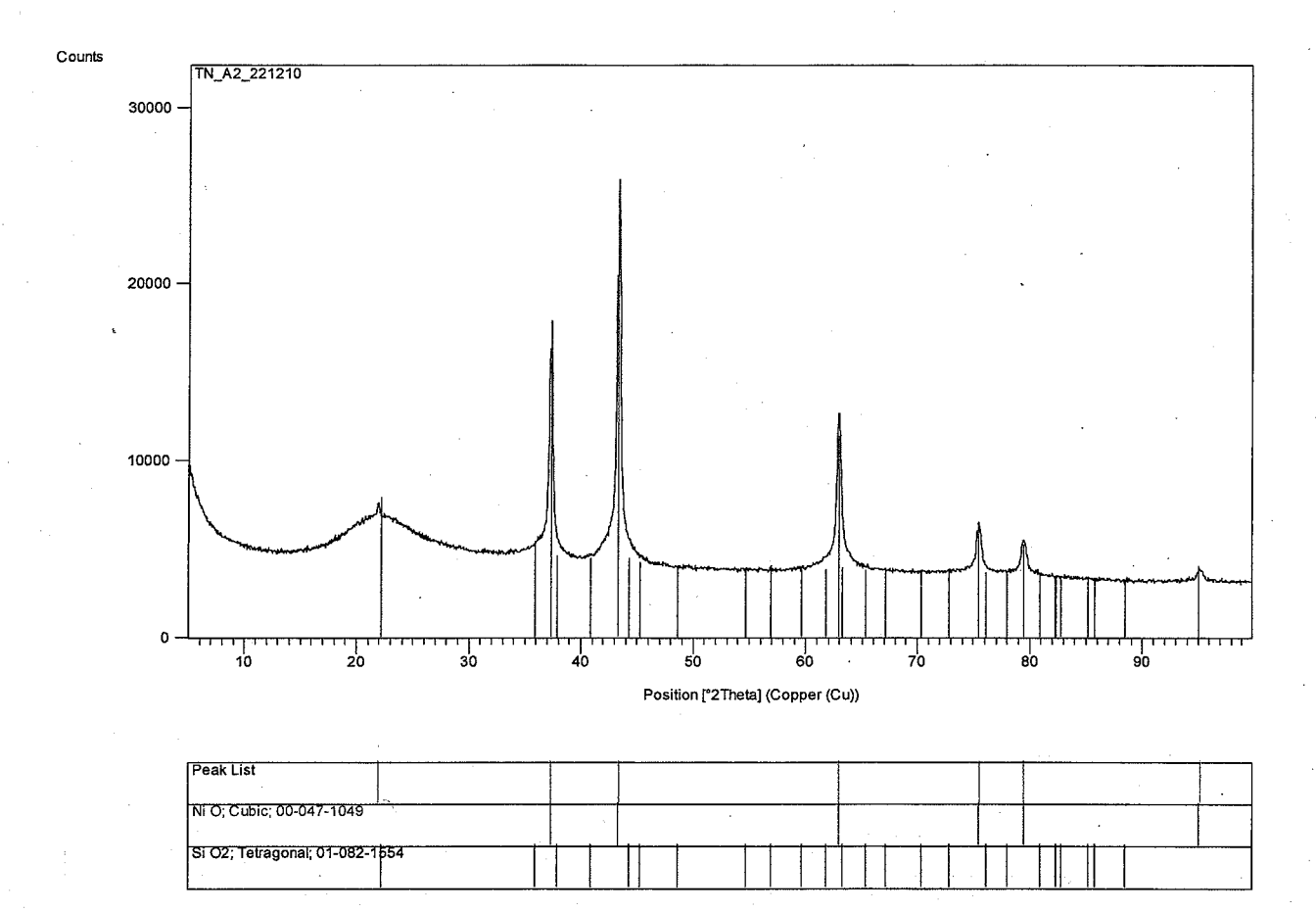


Fig. 1 (b)

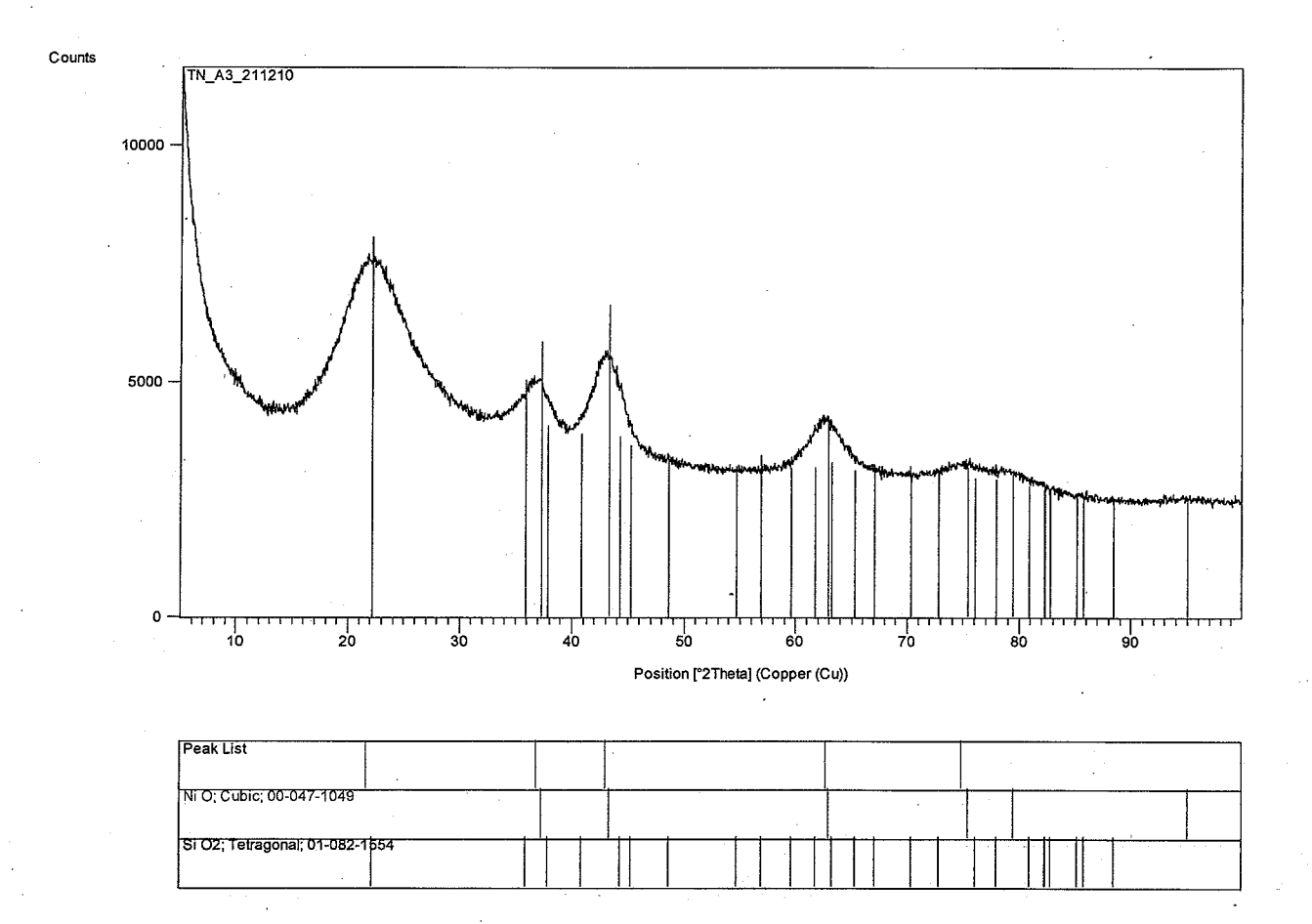


Fig. .1 (c)

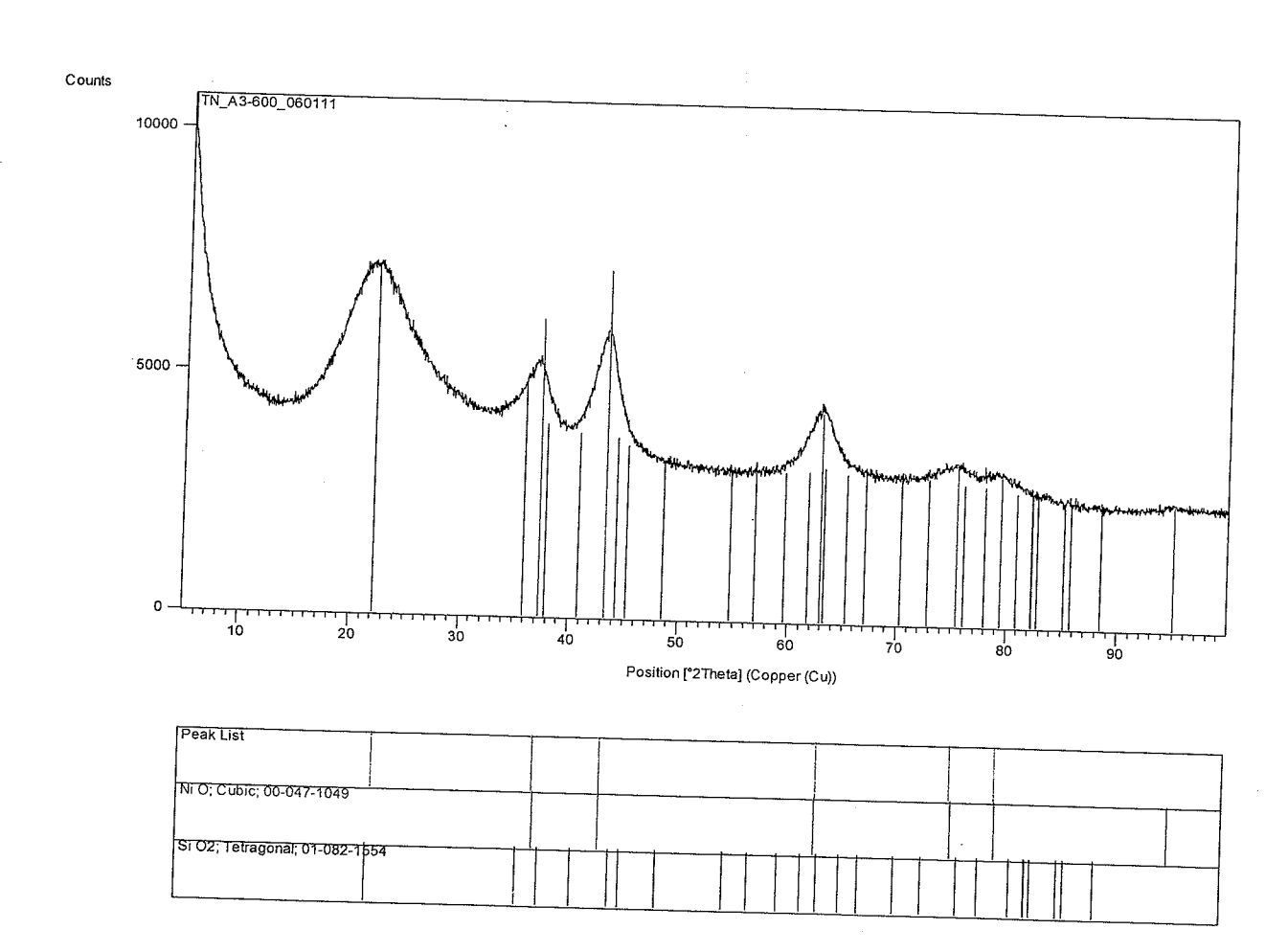
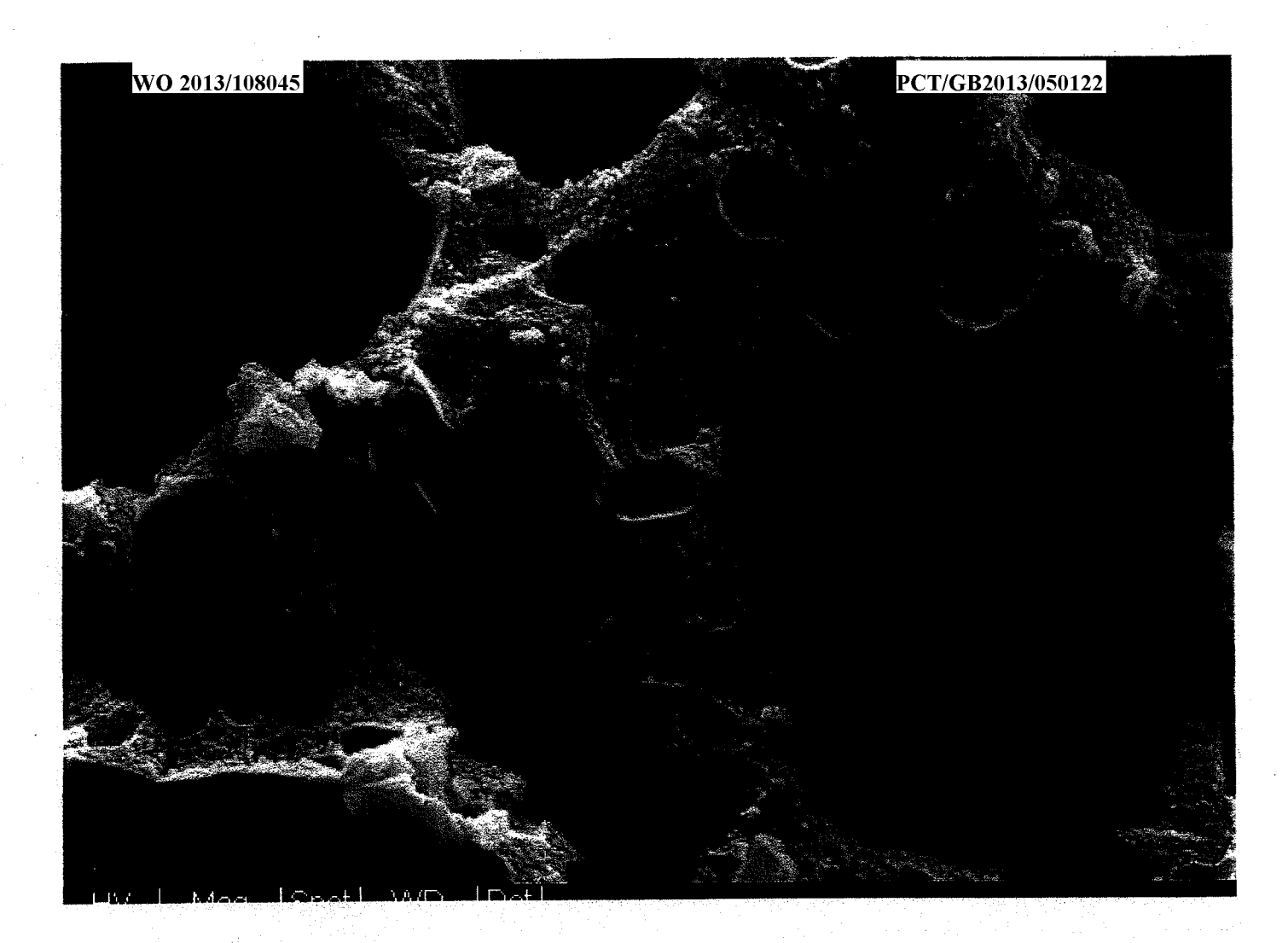


Fig. 1 (d)



Fiq 2(a)

Fiq 2(b)

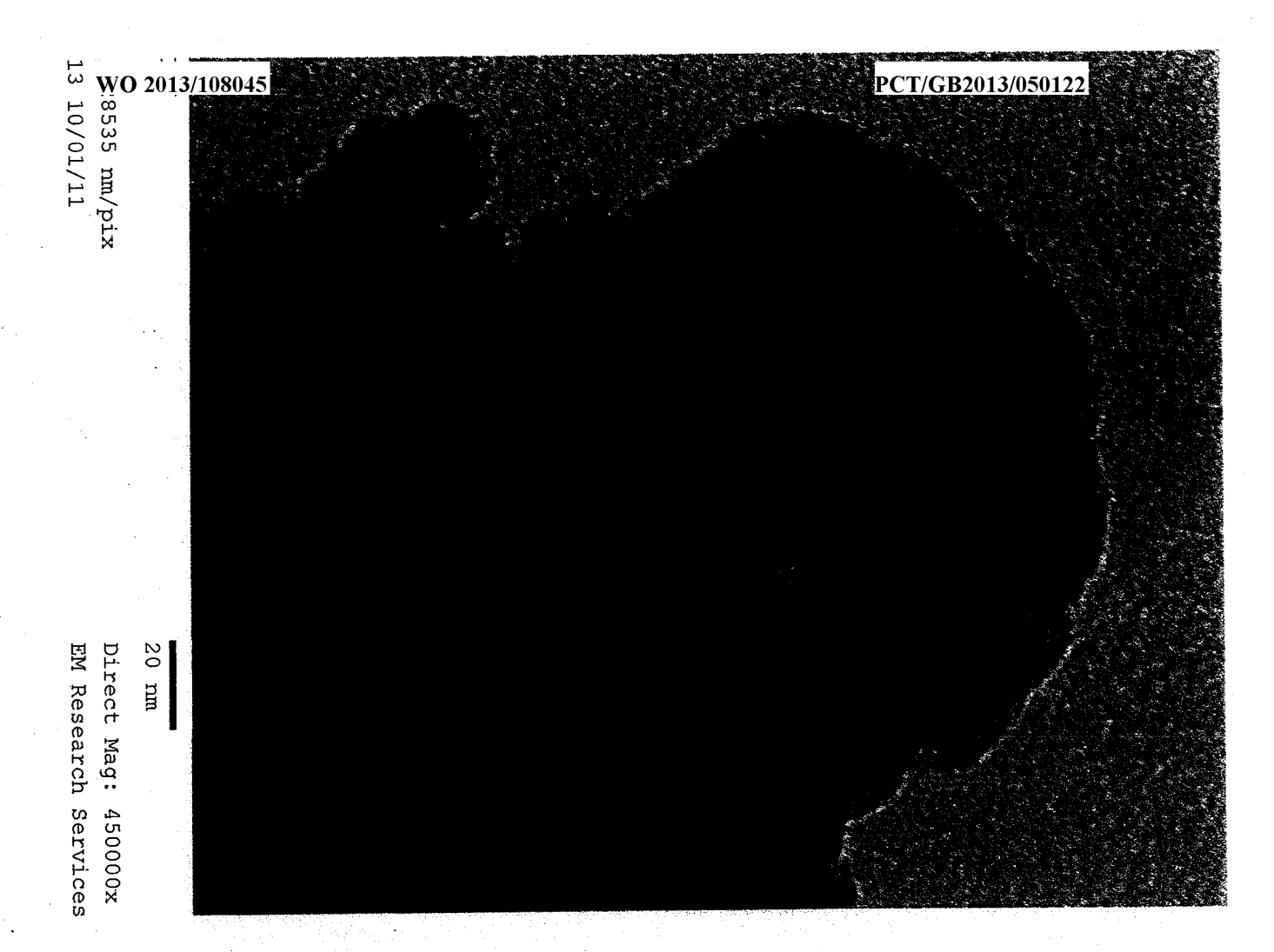


Fig d(c)

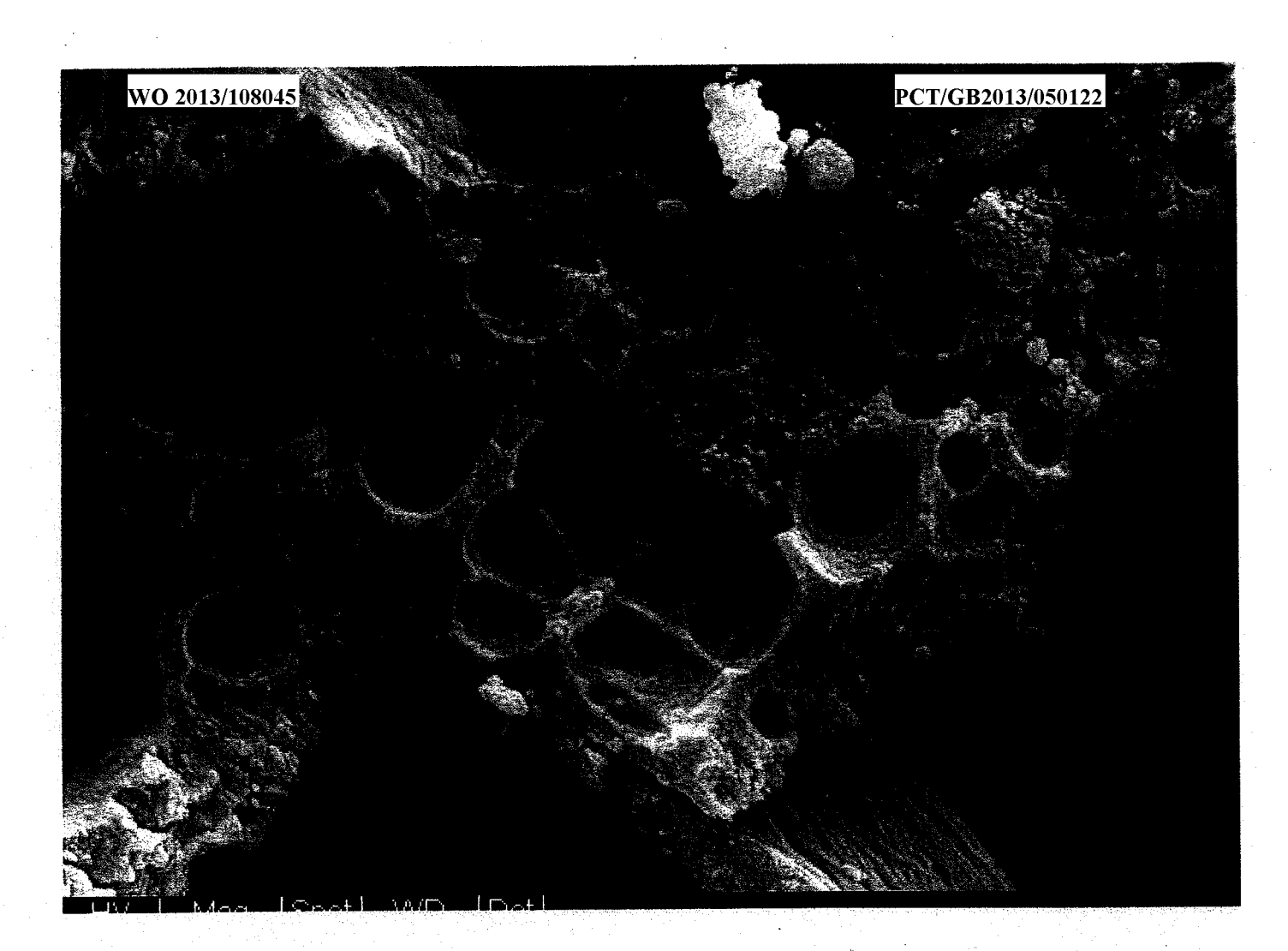


Fig 3(a)

Fig. 3(b)

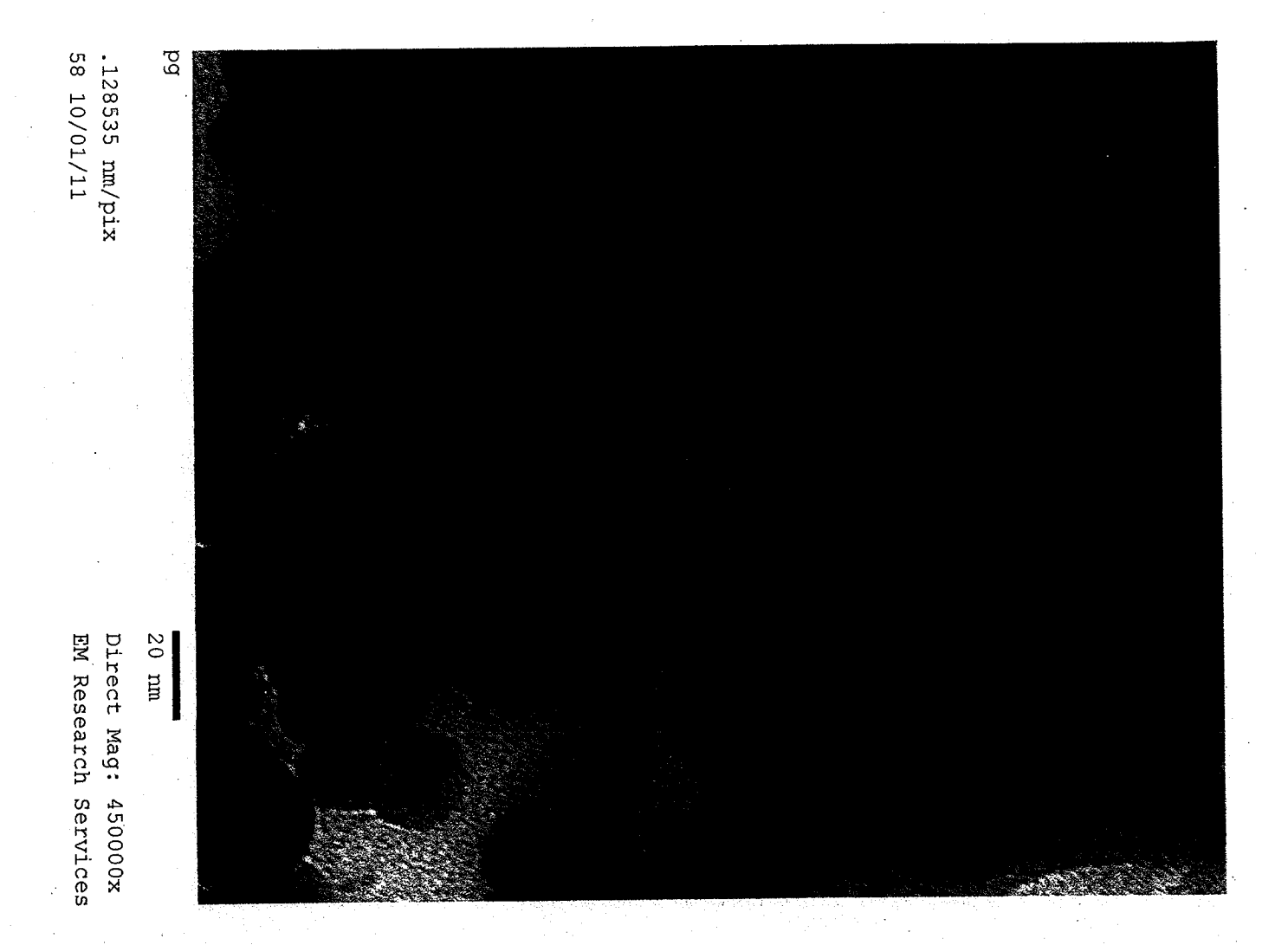


Fig 3(c)

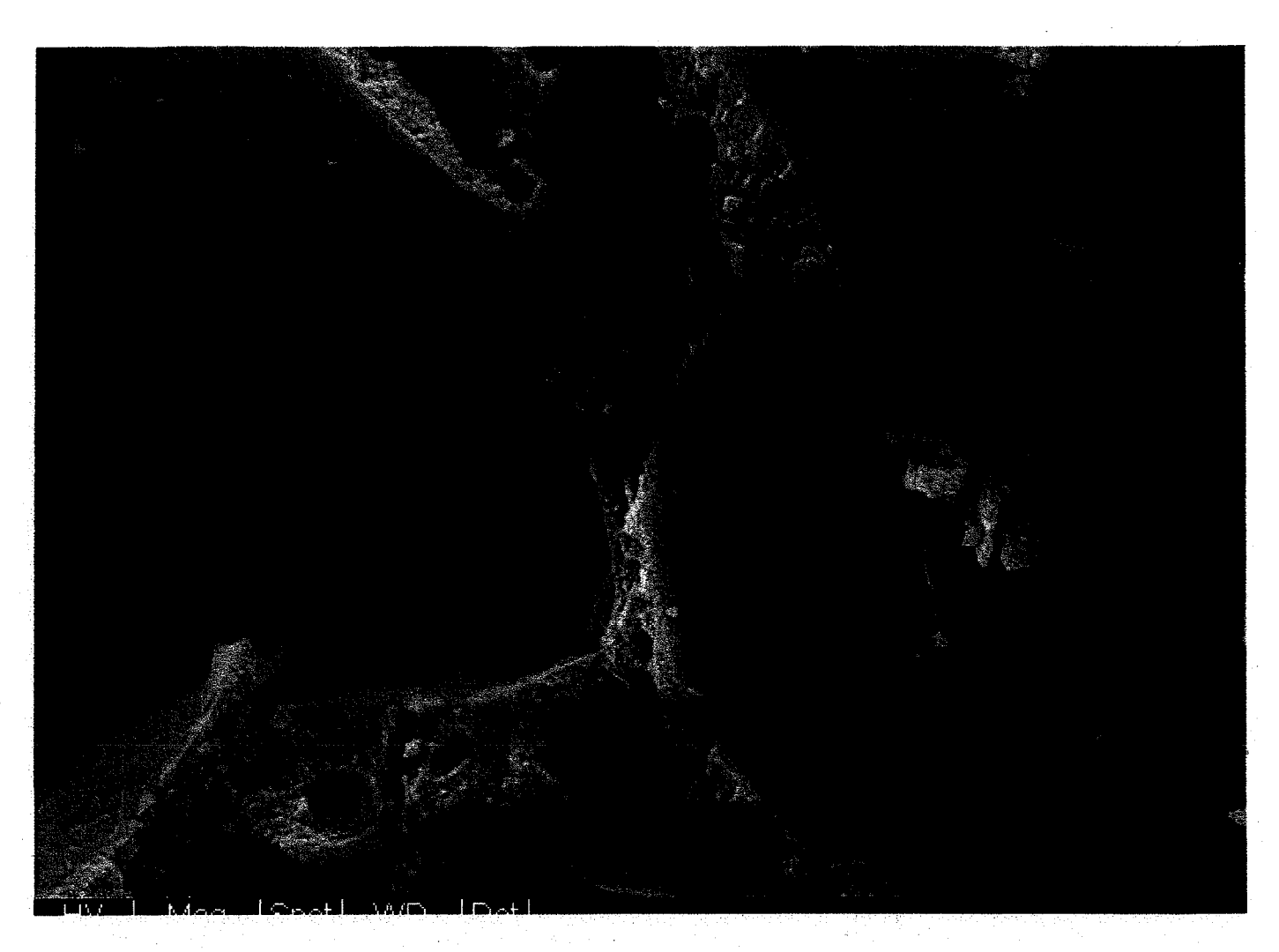
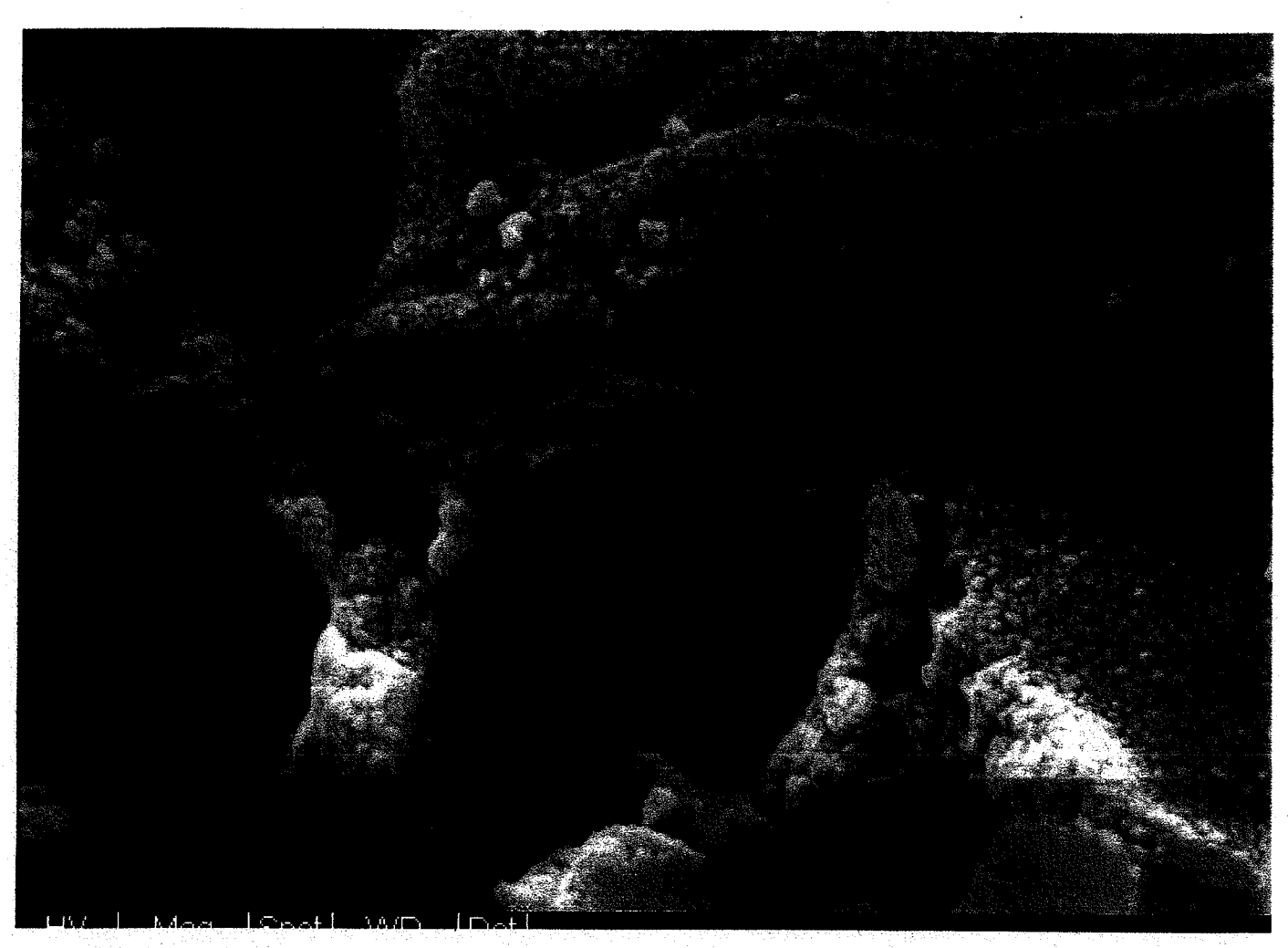


Fig H(a)



V.a 4(b)

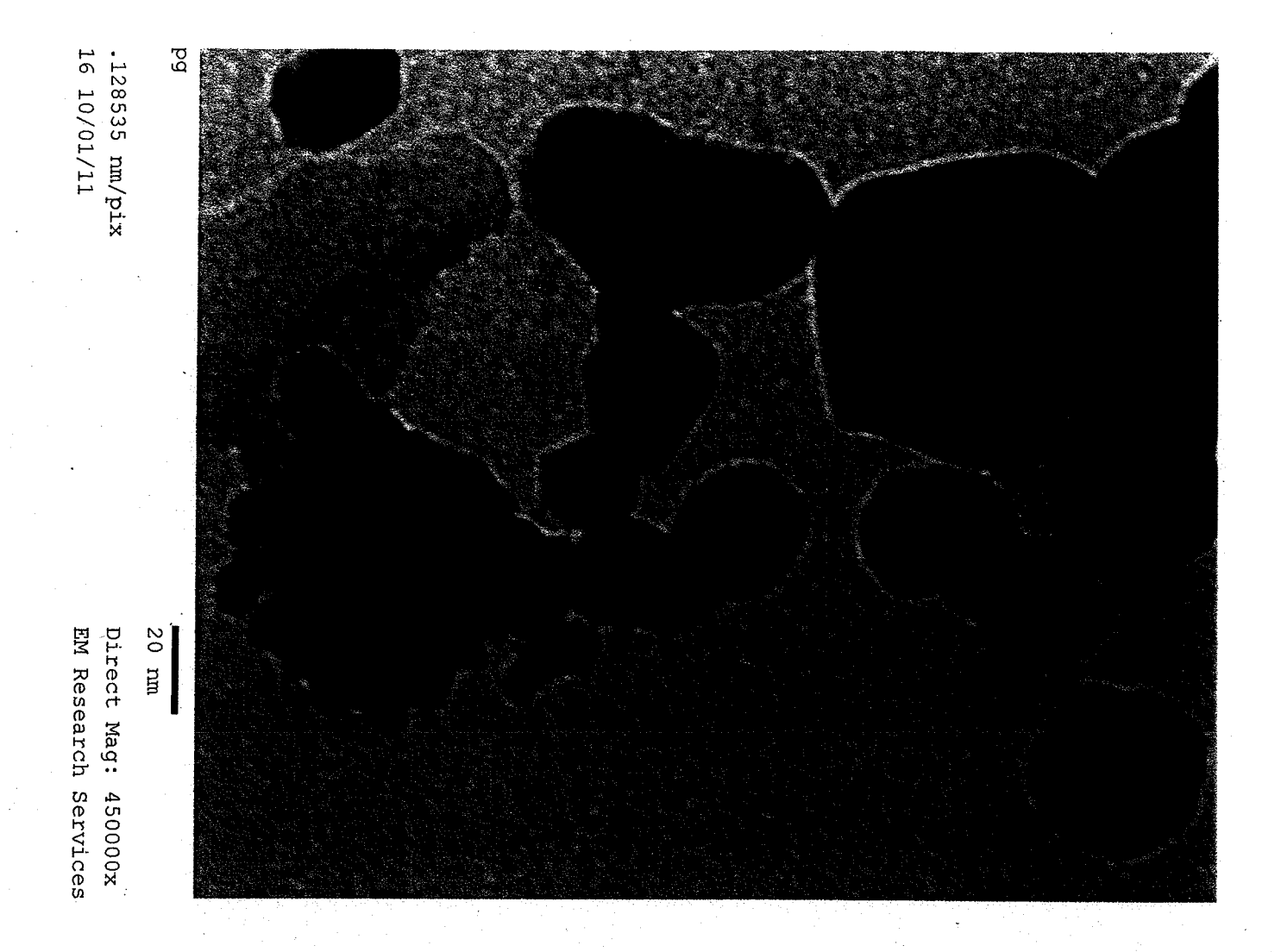
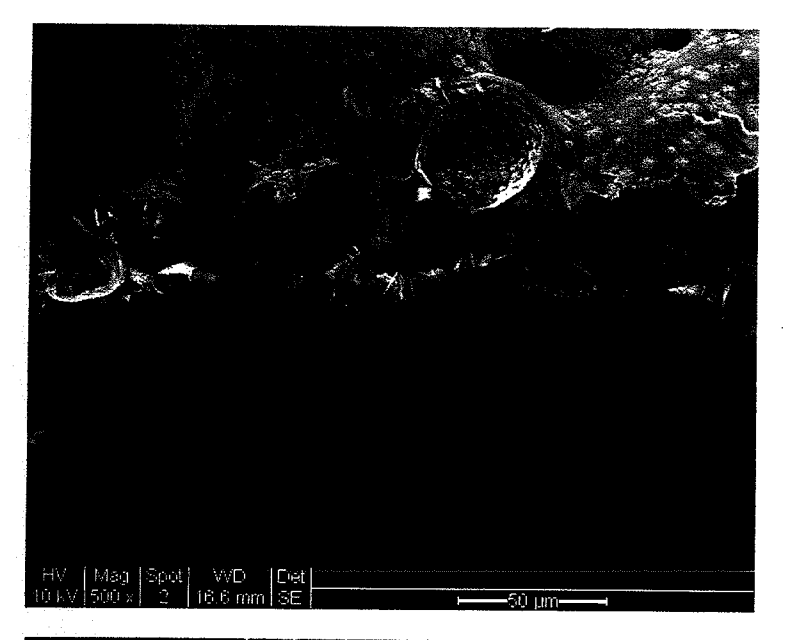


Fig H(c)



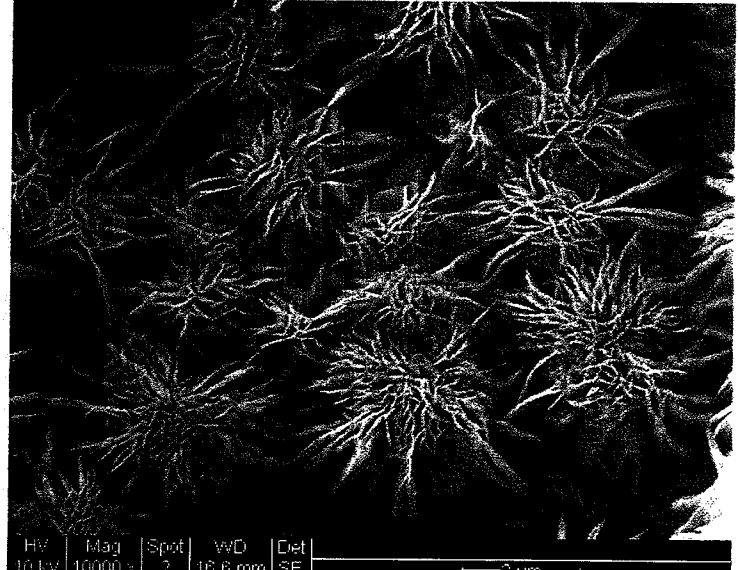


Figure 5

Figure 6a

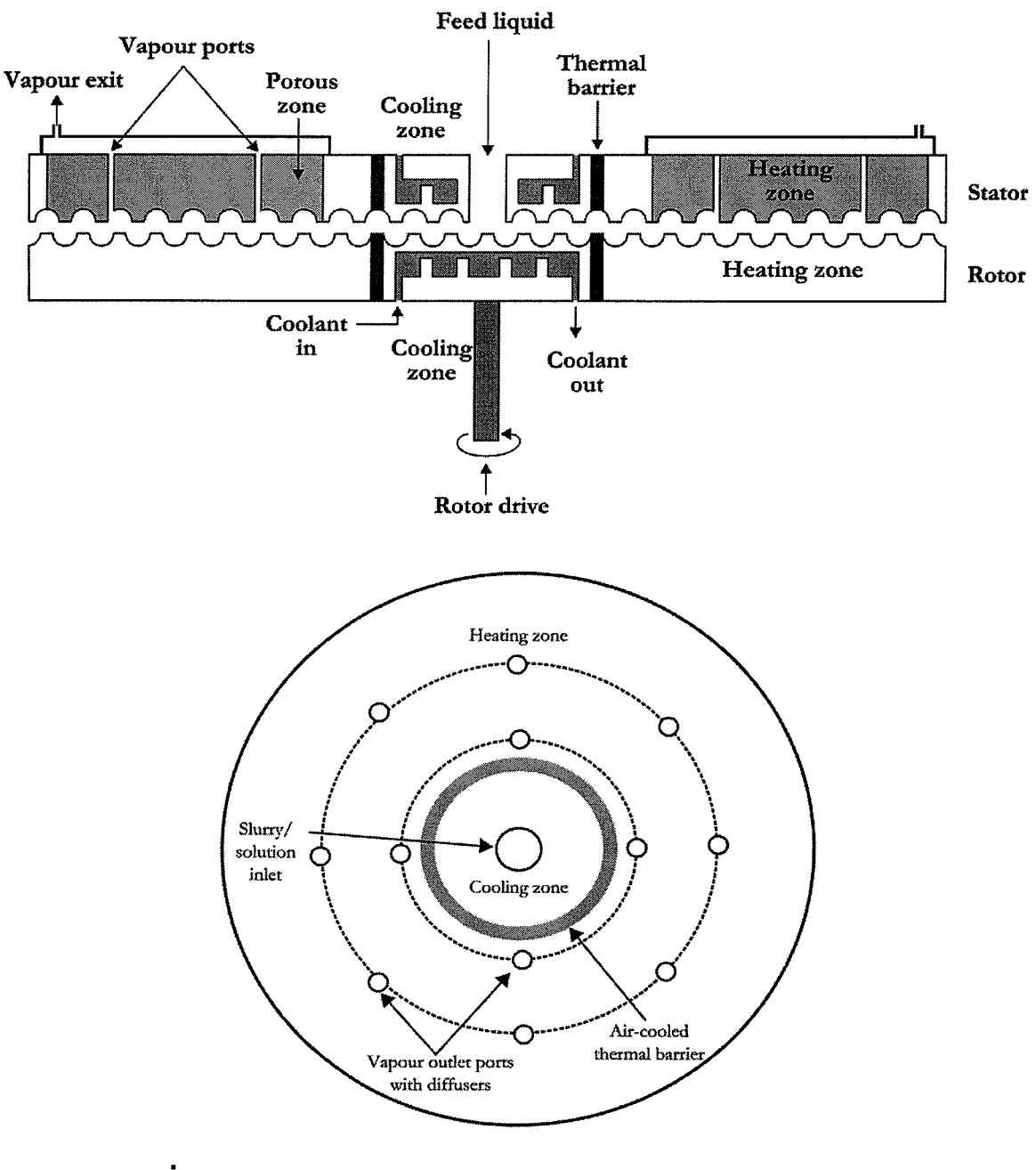
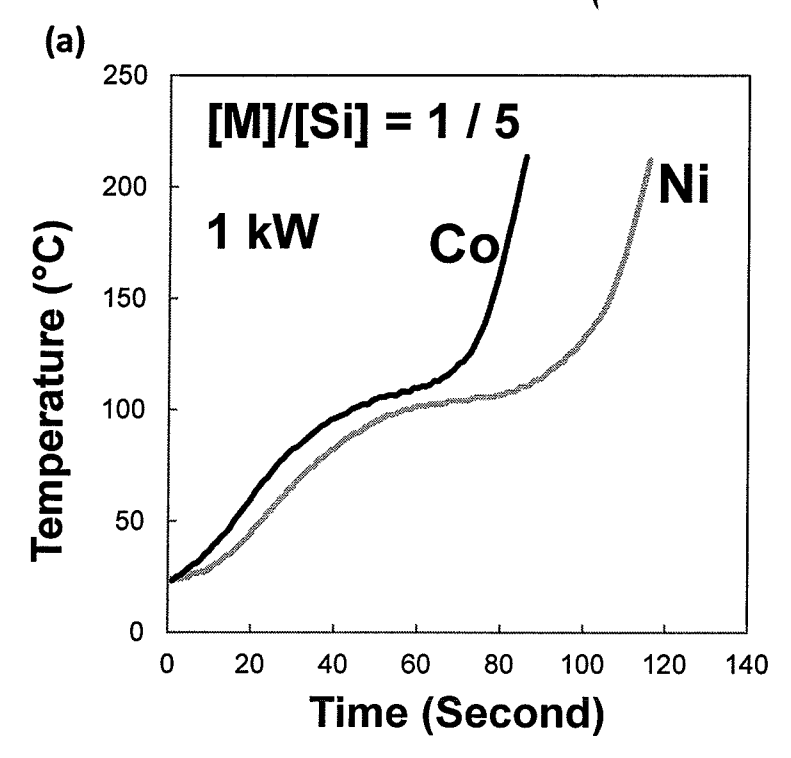
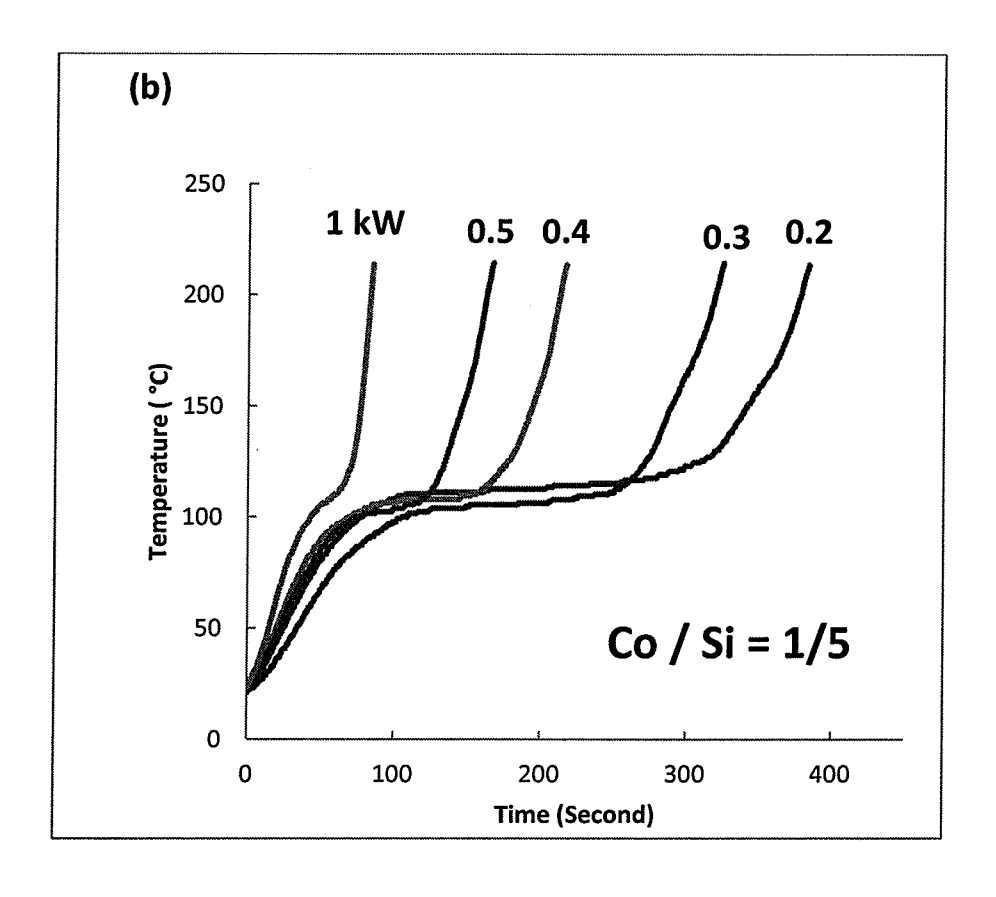
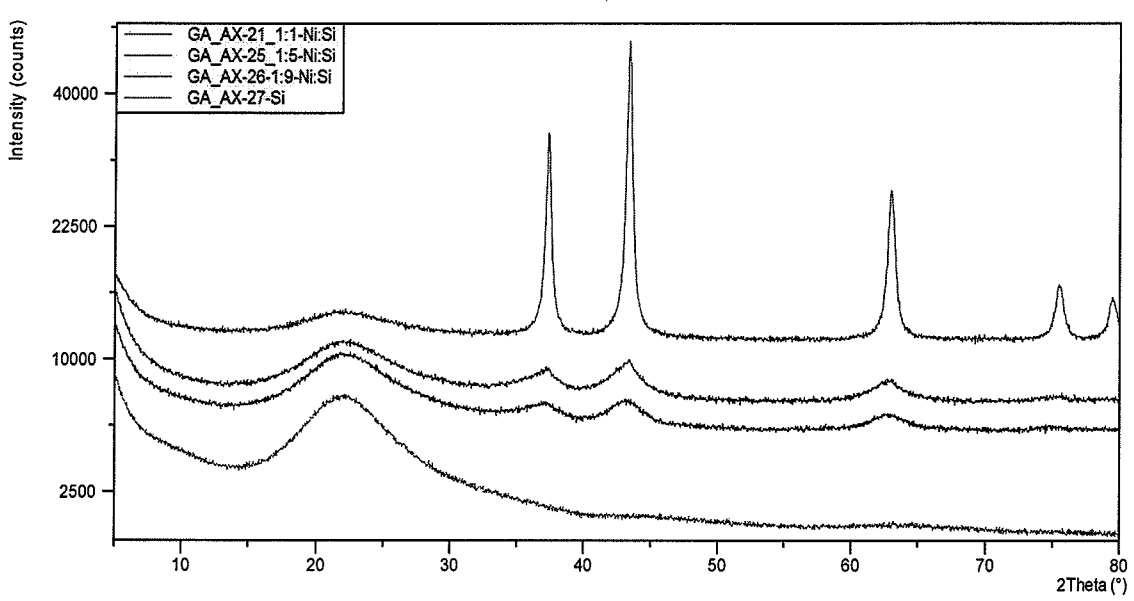


Figure 66







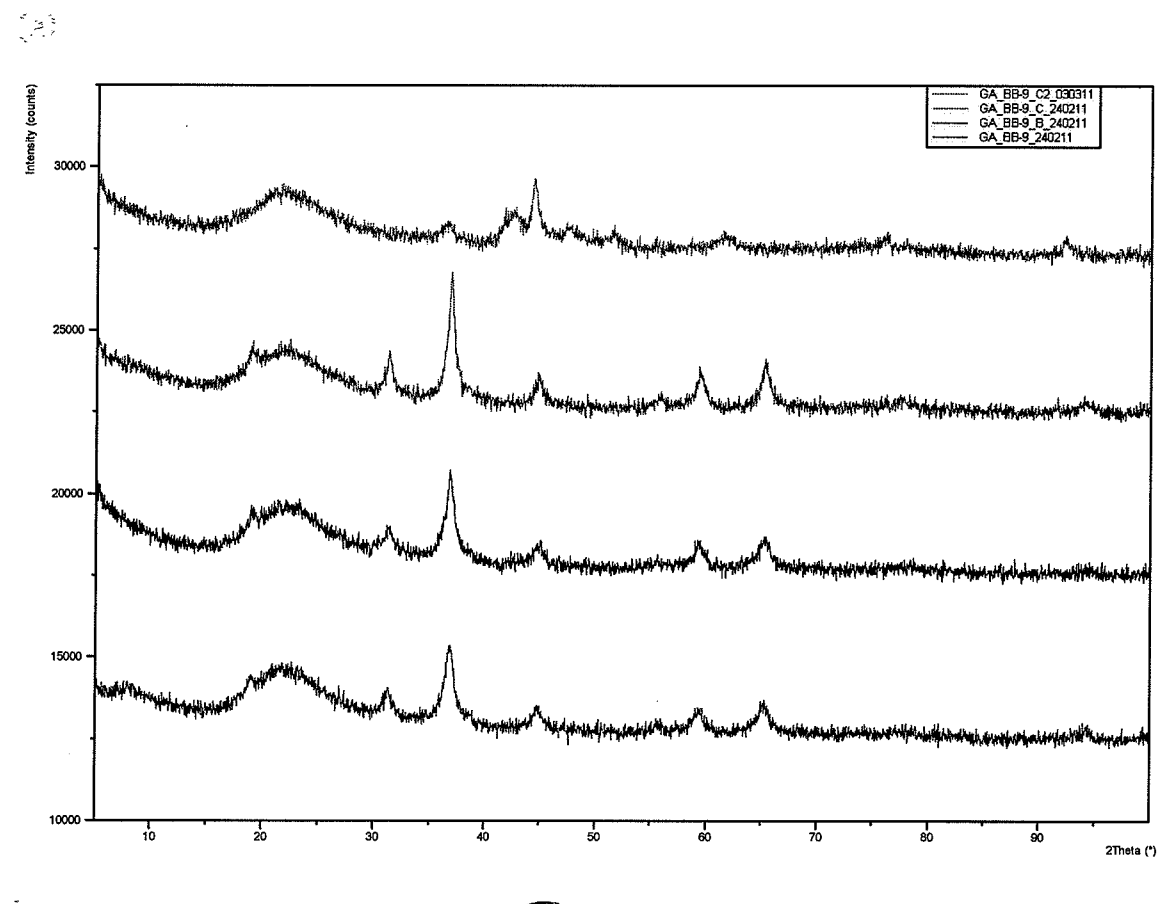
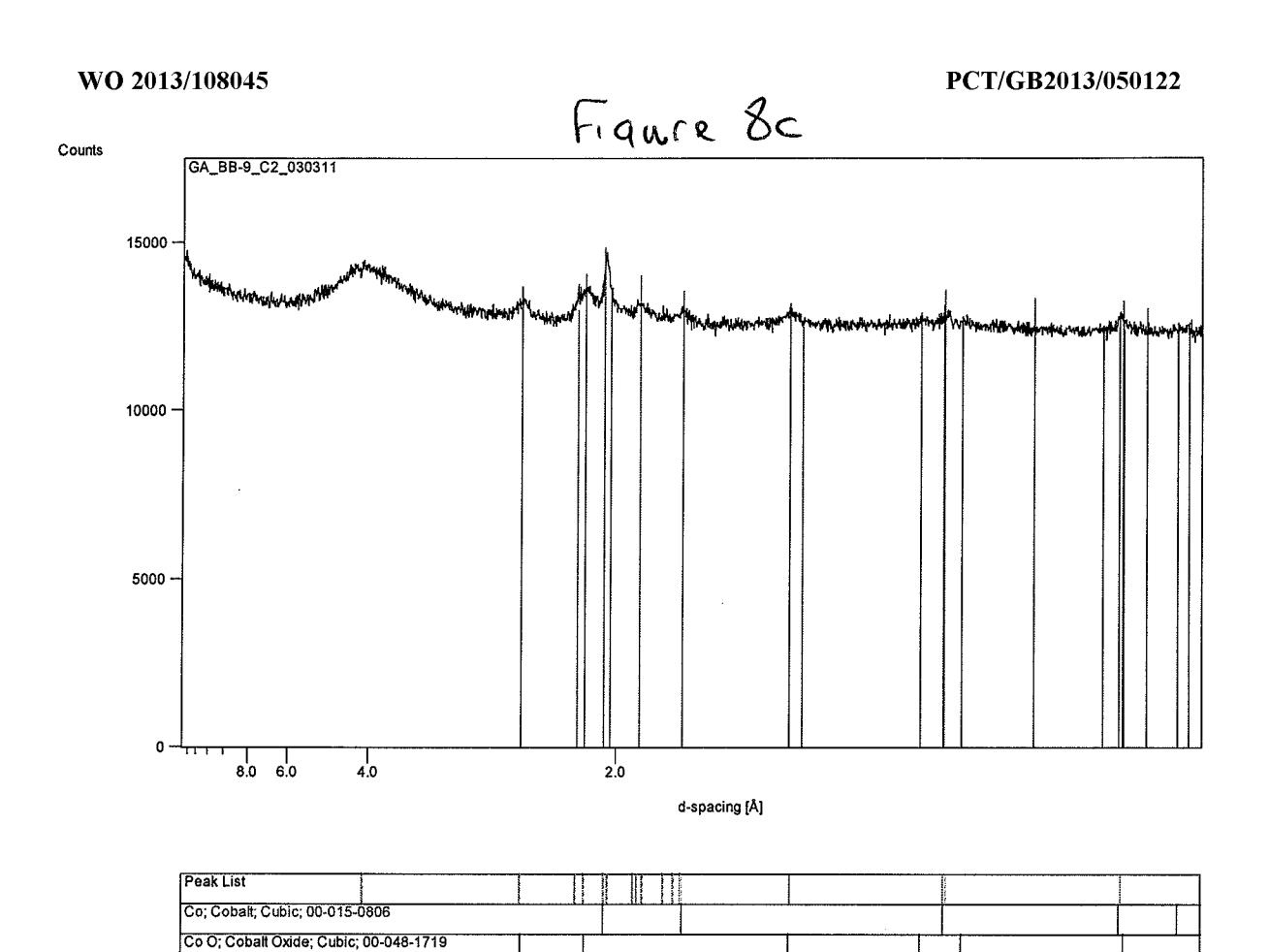


Figure 86



(c)

Co; Cobalt; Hexagonal; 00-005-0727

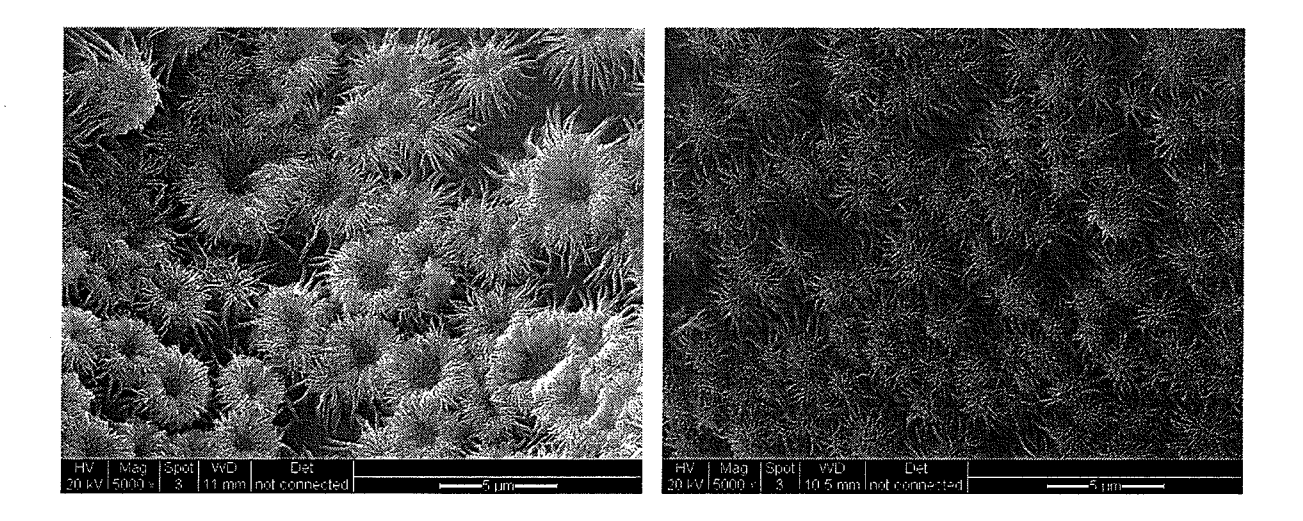


Figure9

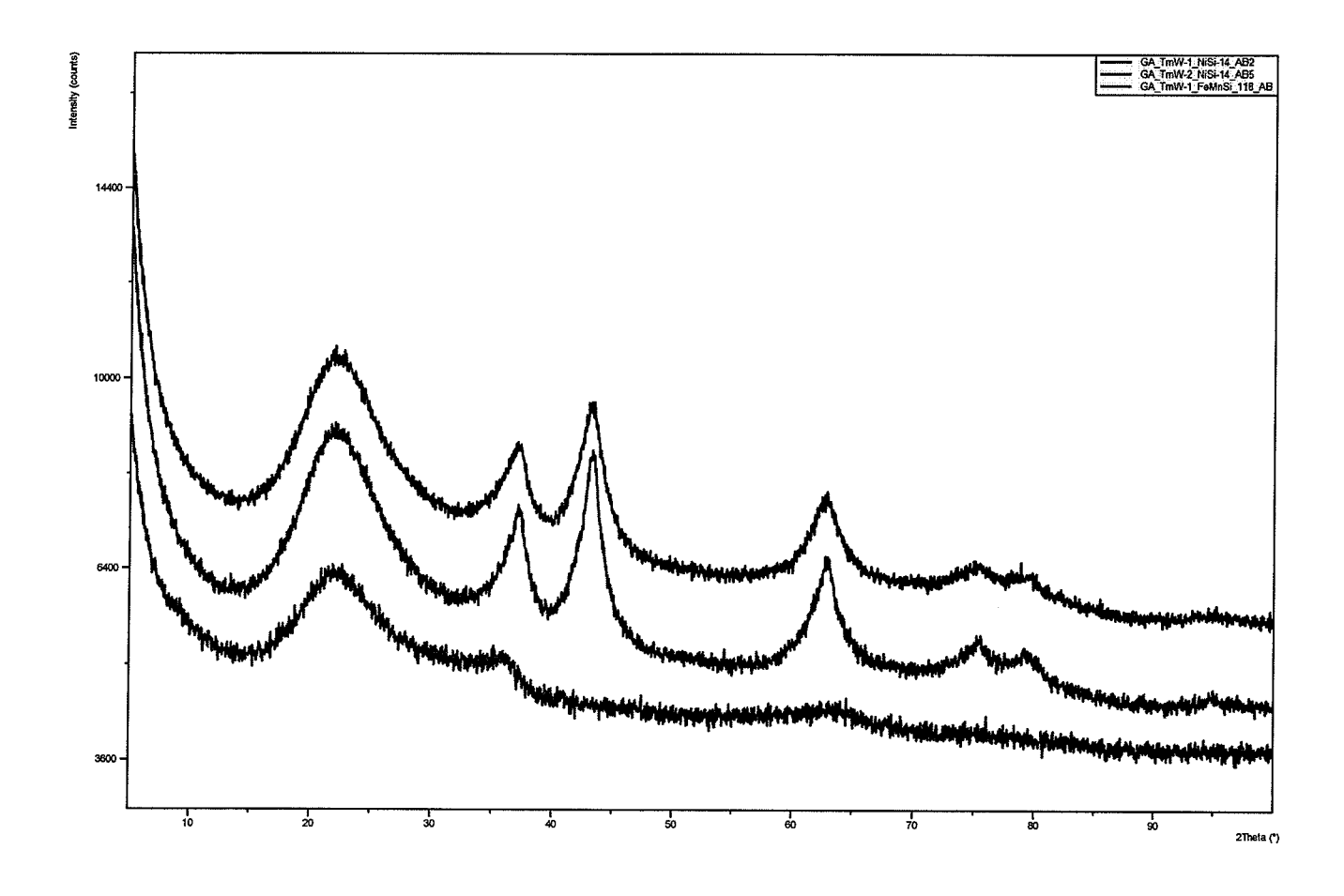


Figure 10

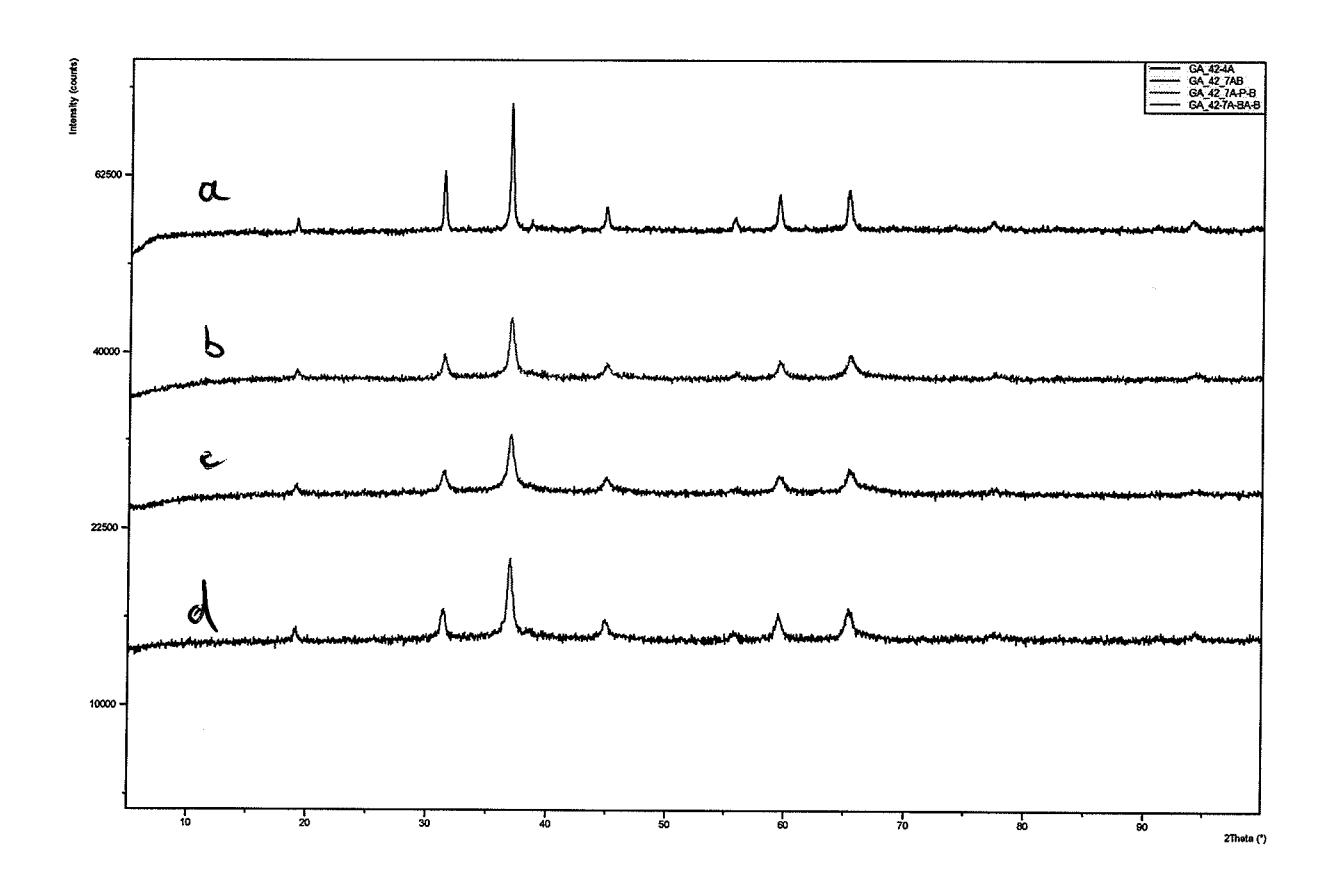
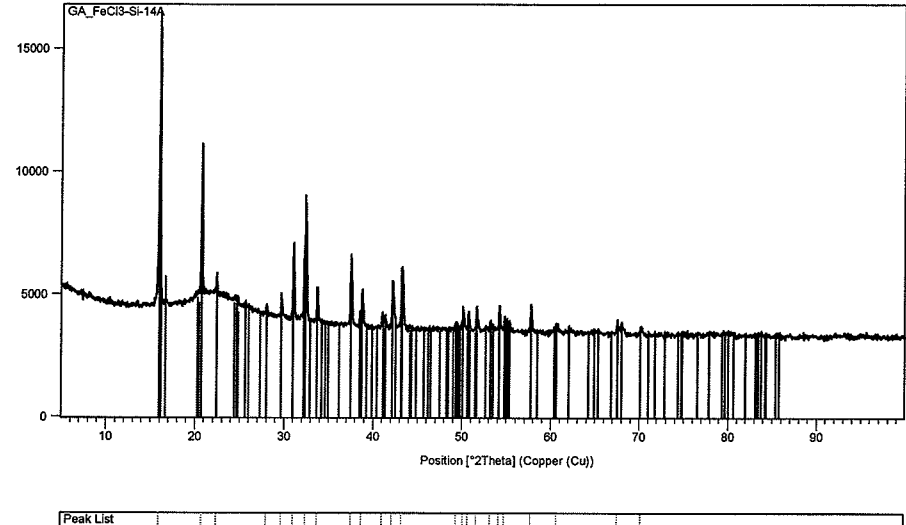


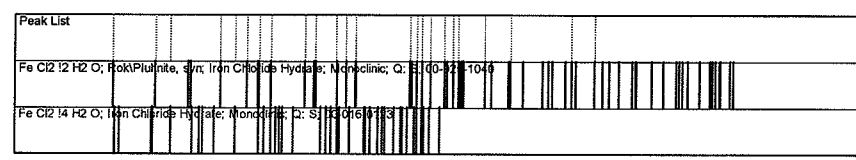
Figure 11

WO 2013/108045

Figure 12

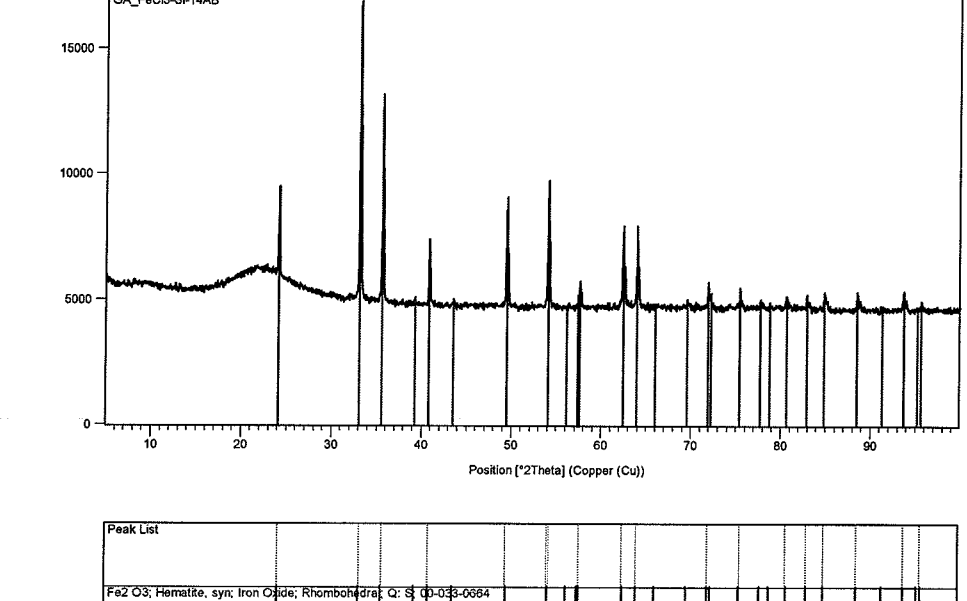




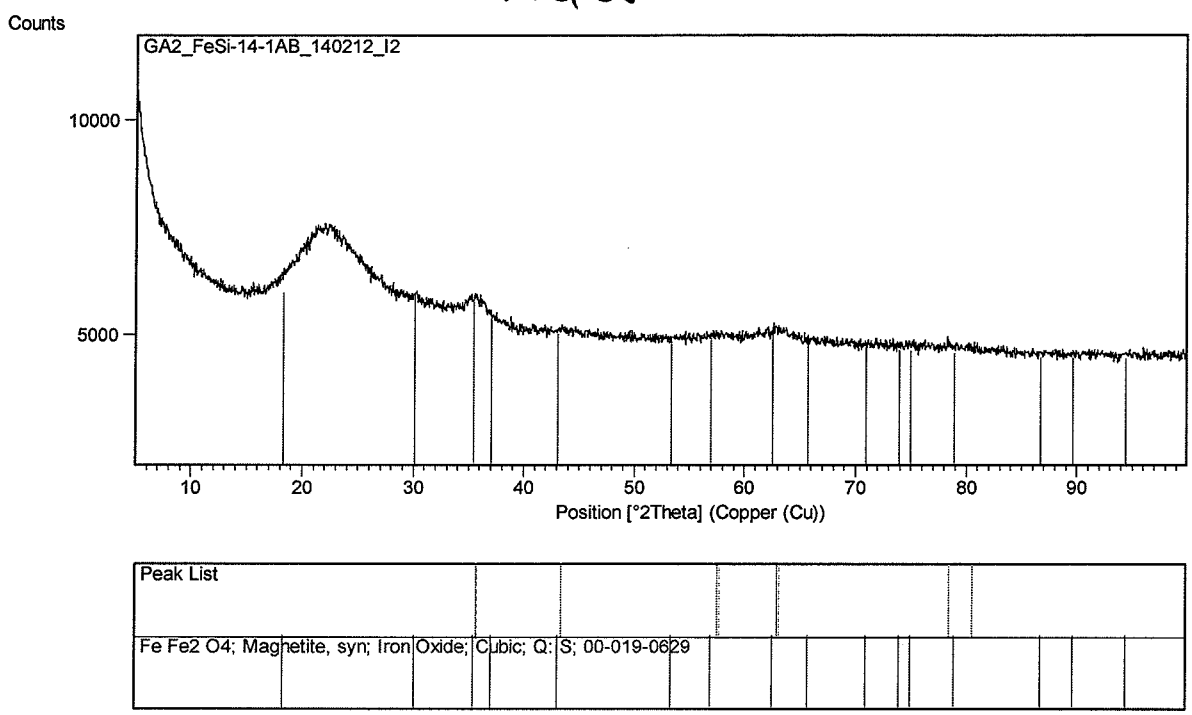


(a)

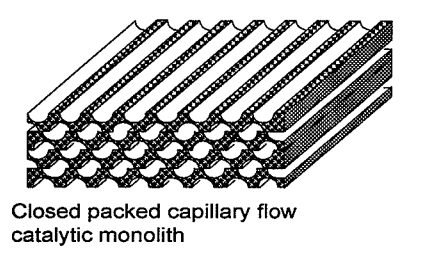




(b)

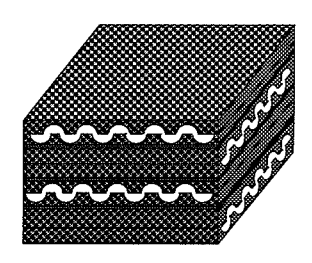


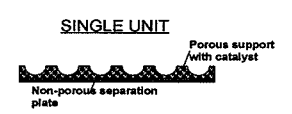
(c)



Single unit (cross sectional view)

CAPILLARY CROSS-FLOW CATALYTIC MONOLITH





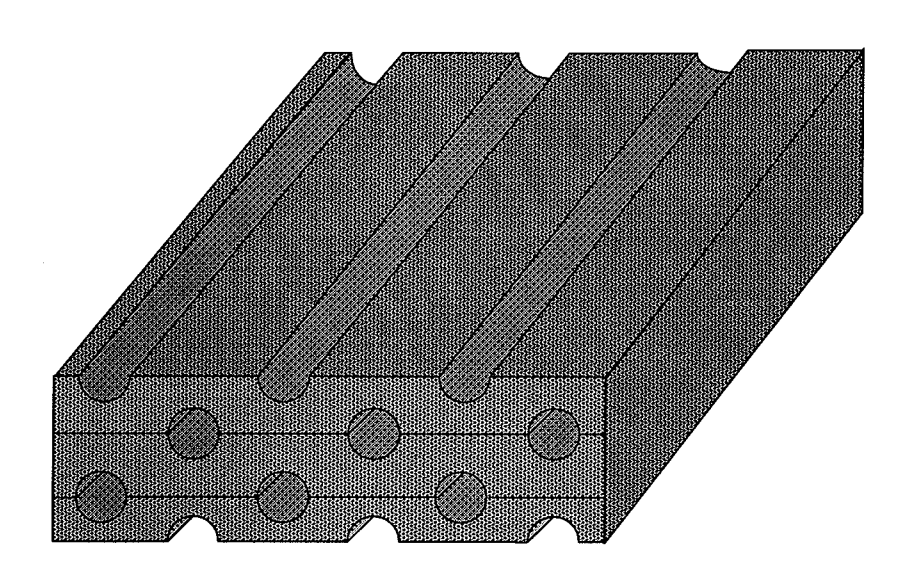
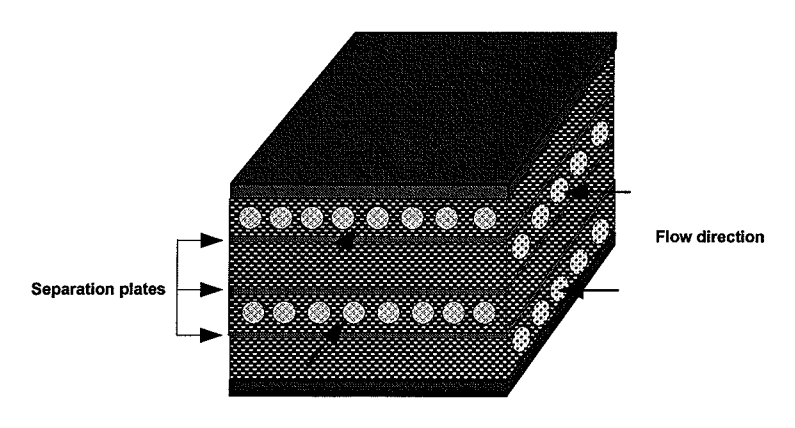
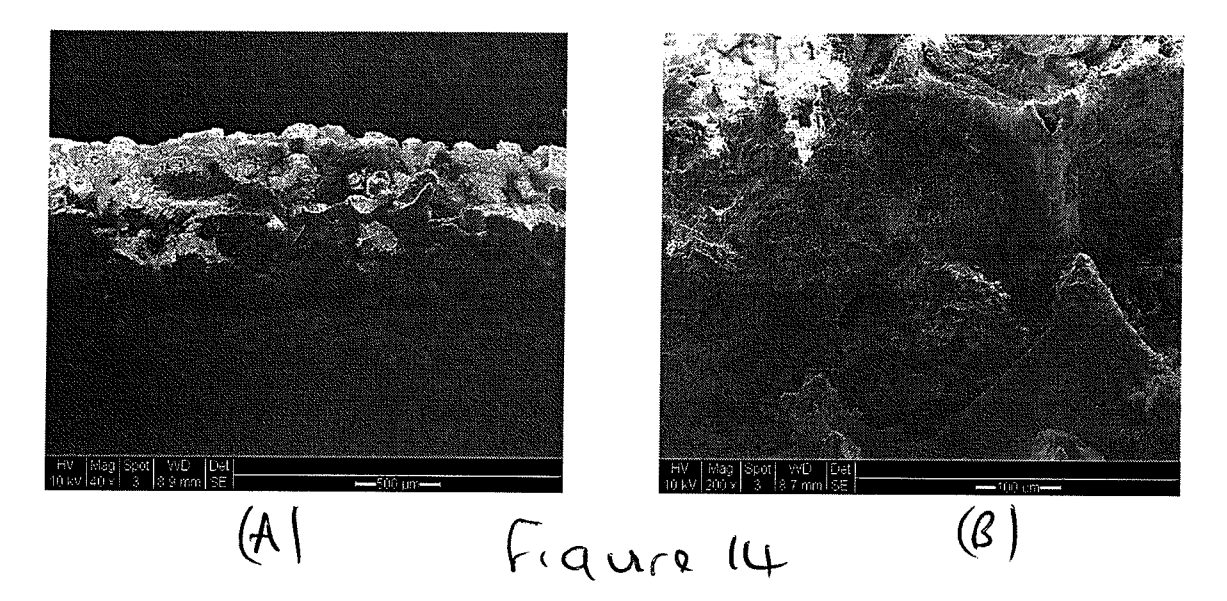


Figure 13

Close packed capillary flow





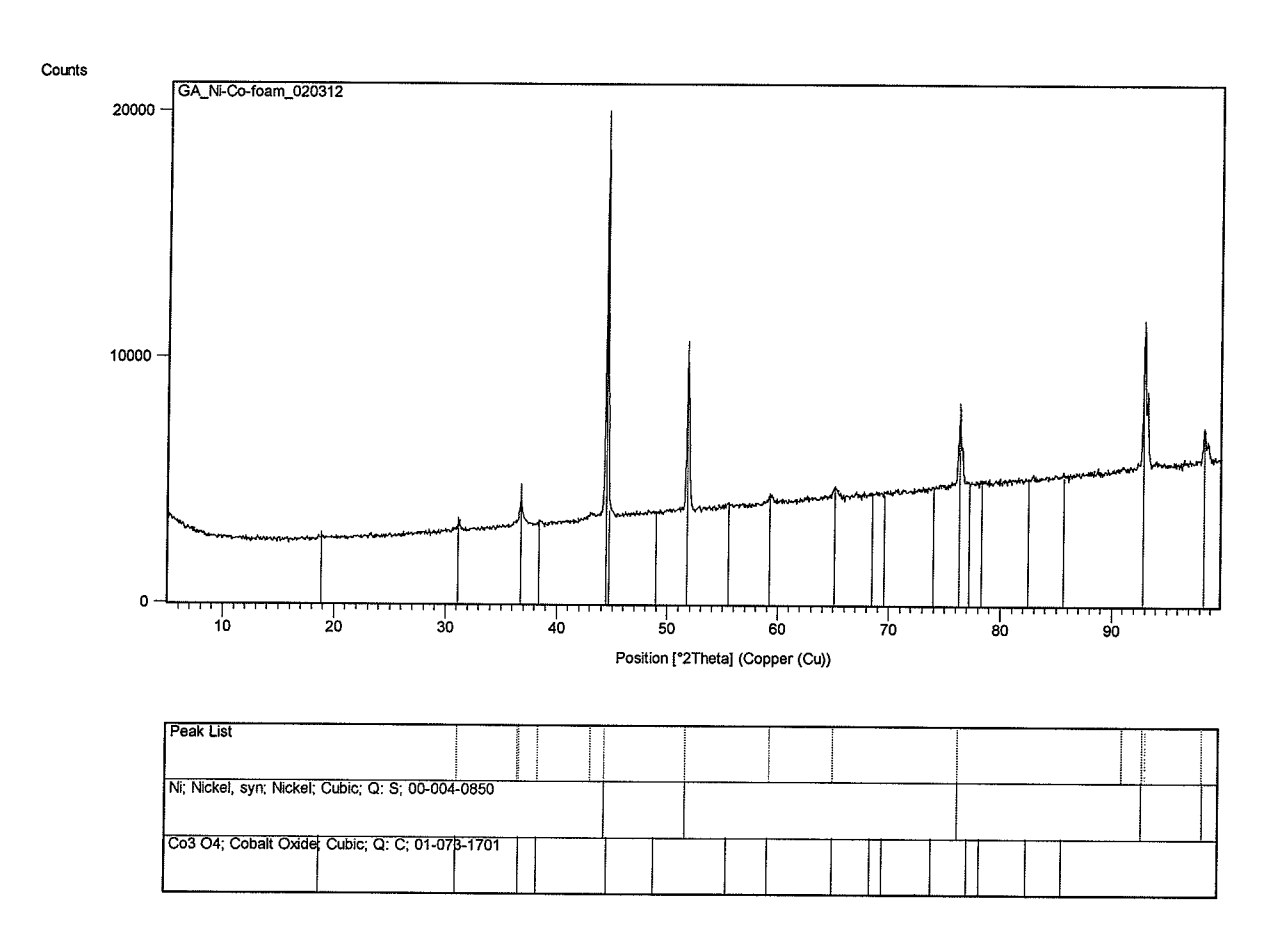
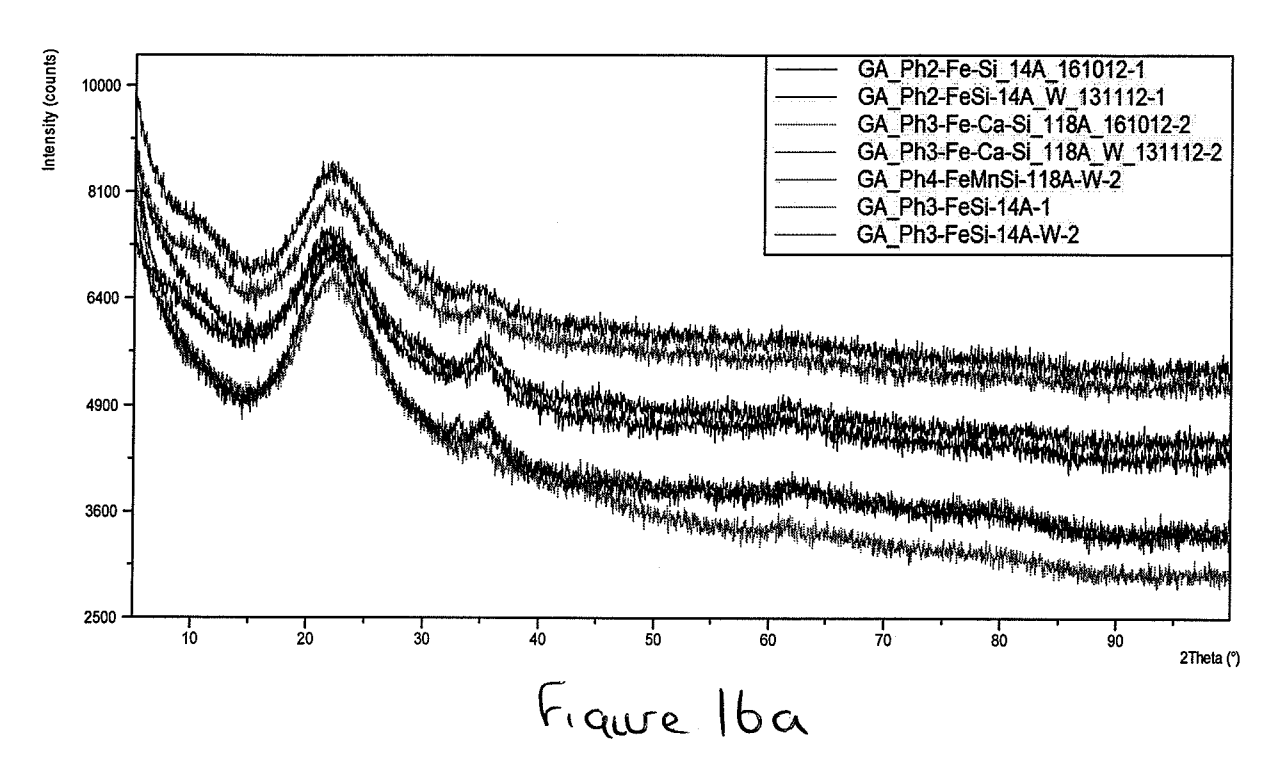


Figure 15



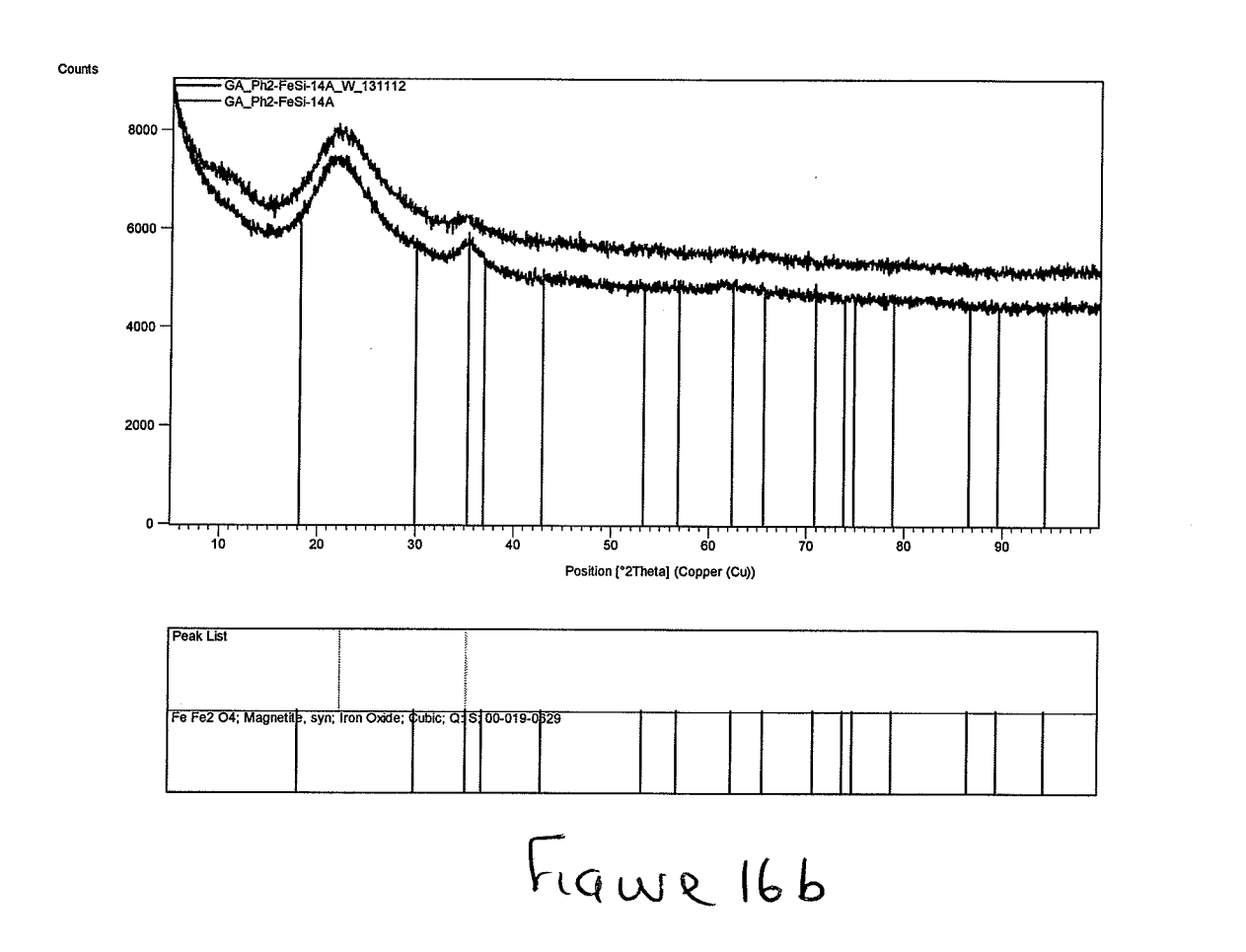
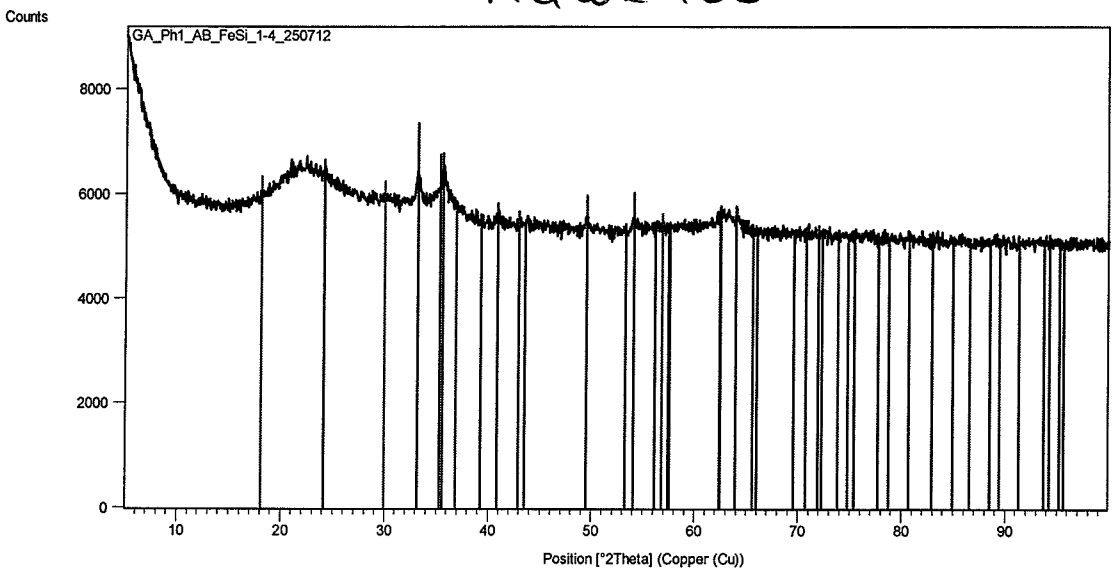
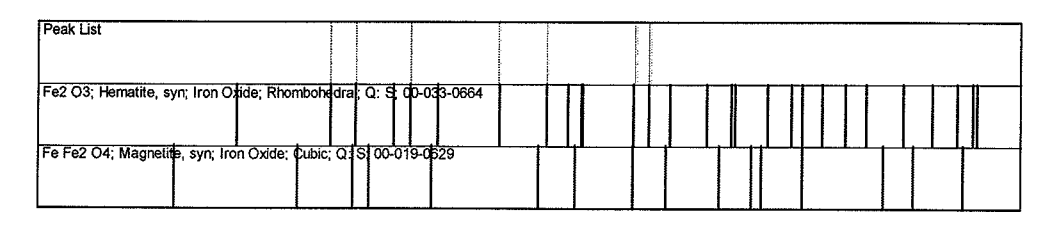
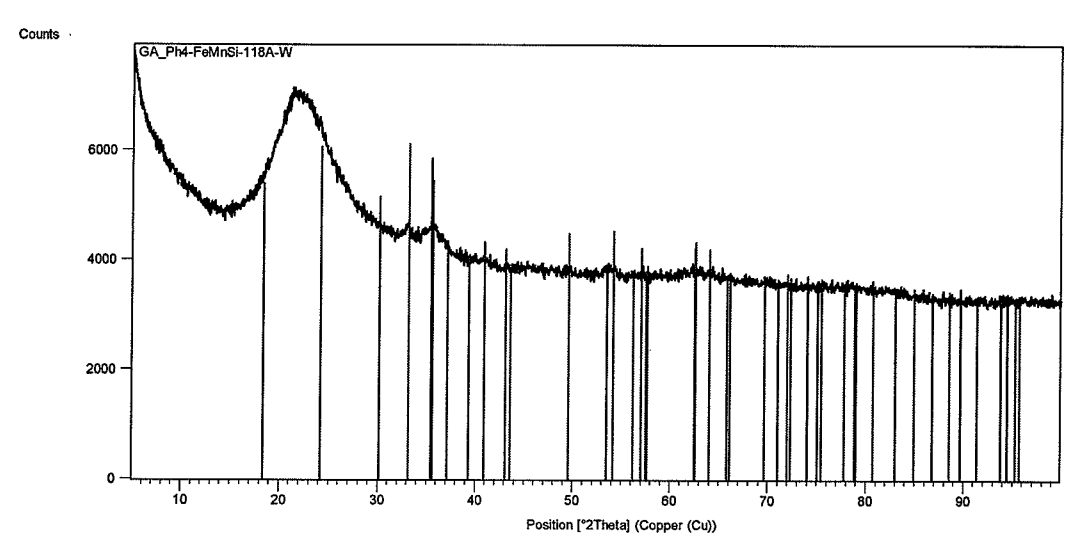


Figure 16c

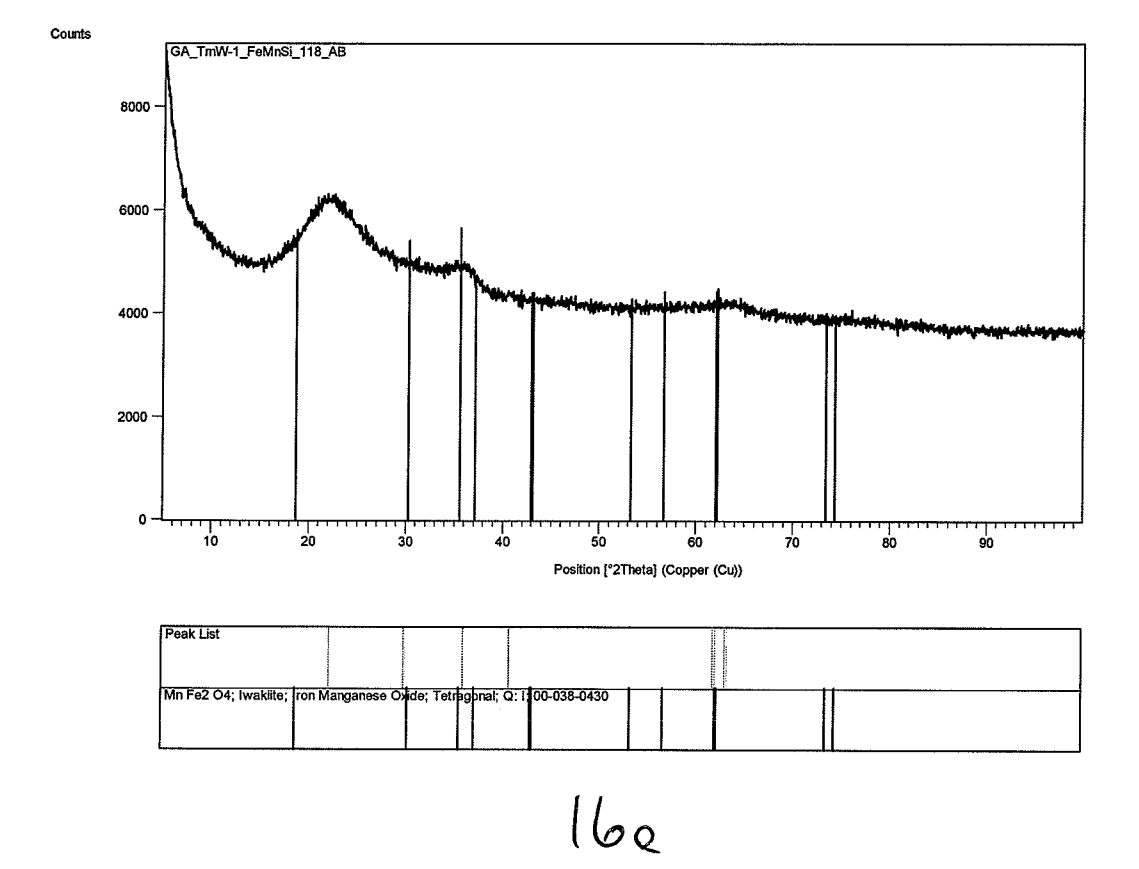






Peak List	Annual An	ATTENDED TO THE PARTY OF THE PA	Share de constituente de const	
Fe Fe2 O4; Magnetite, syn; Iron Oxide;				
Fe2 O3; Hematite, syn; Iron Oxide; Rhoi	mbohedral, Q; S; 00-0	33-0664		

Figure 16d



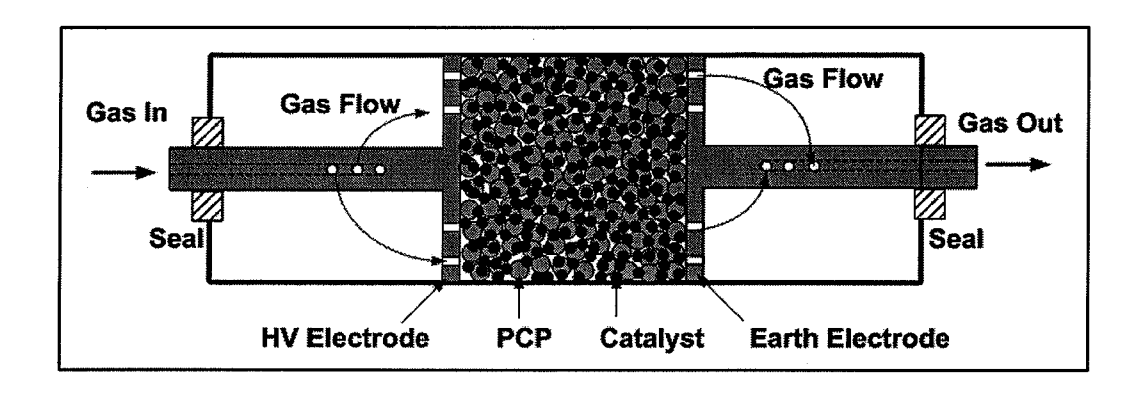
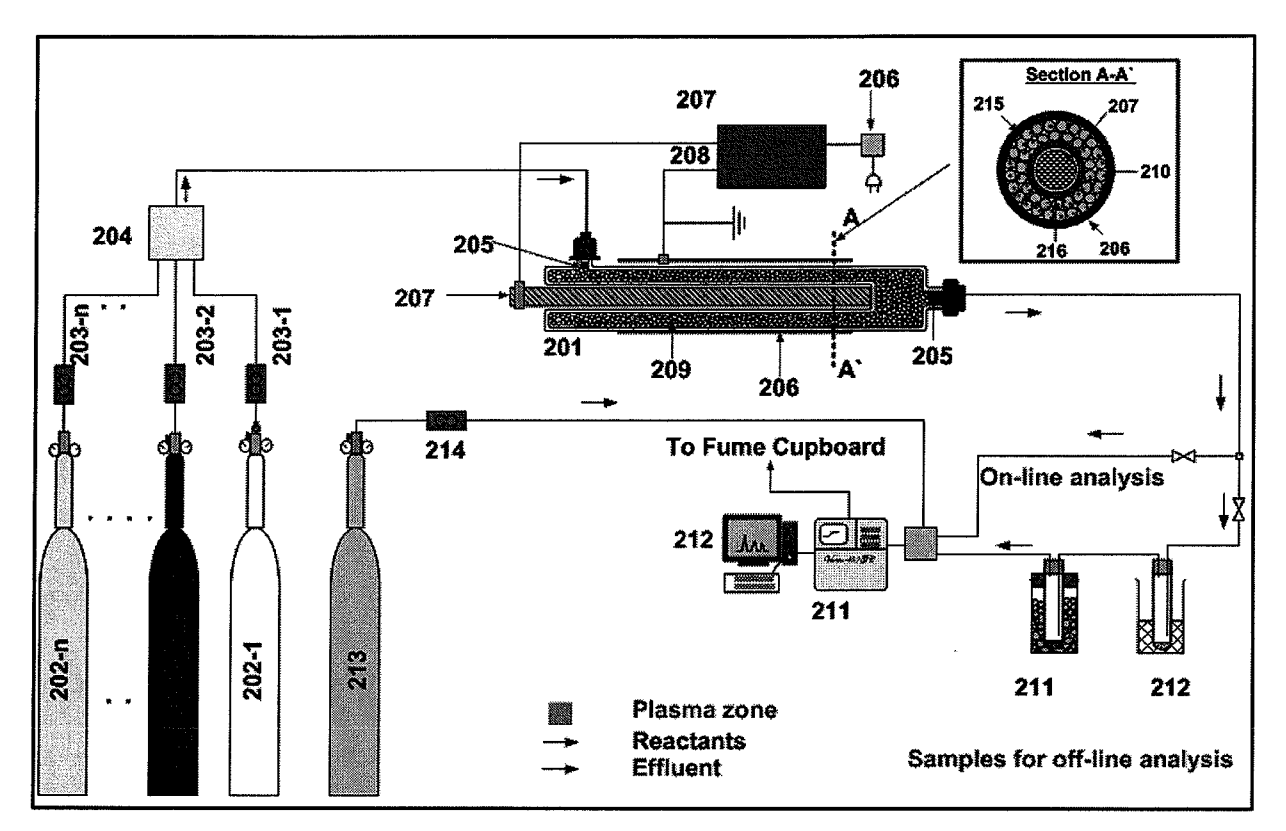


Figure 17



have 18a

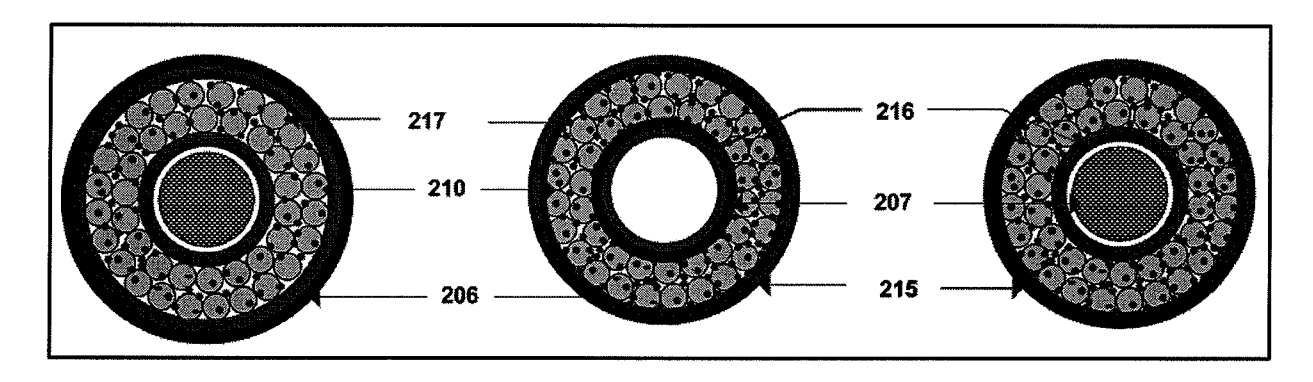
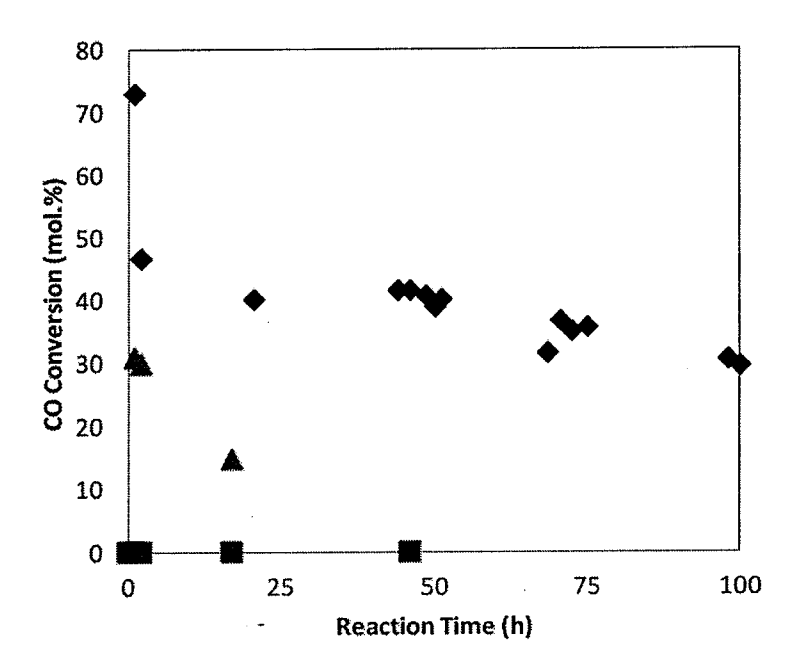


Figure 186



♦ PR1 Plasma 90W ▲ PR1 Thermal (250C) ■ PR1 Thermal (150C)

hawe 19a

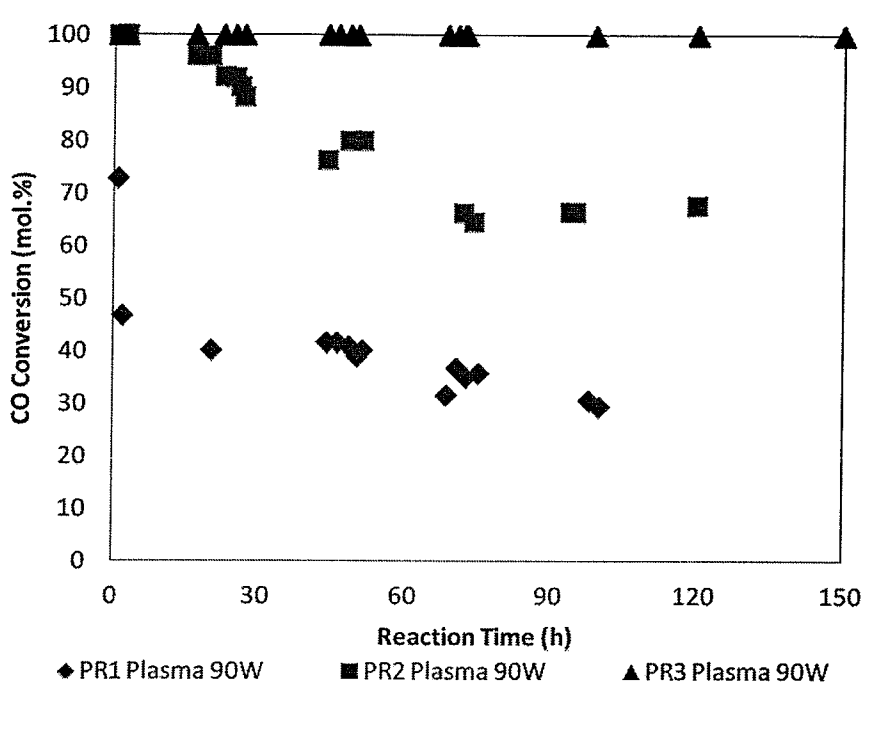


Figure 196

31/38

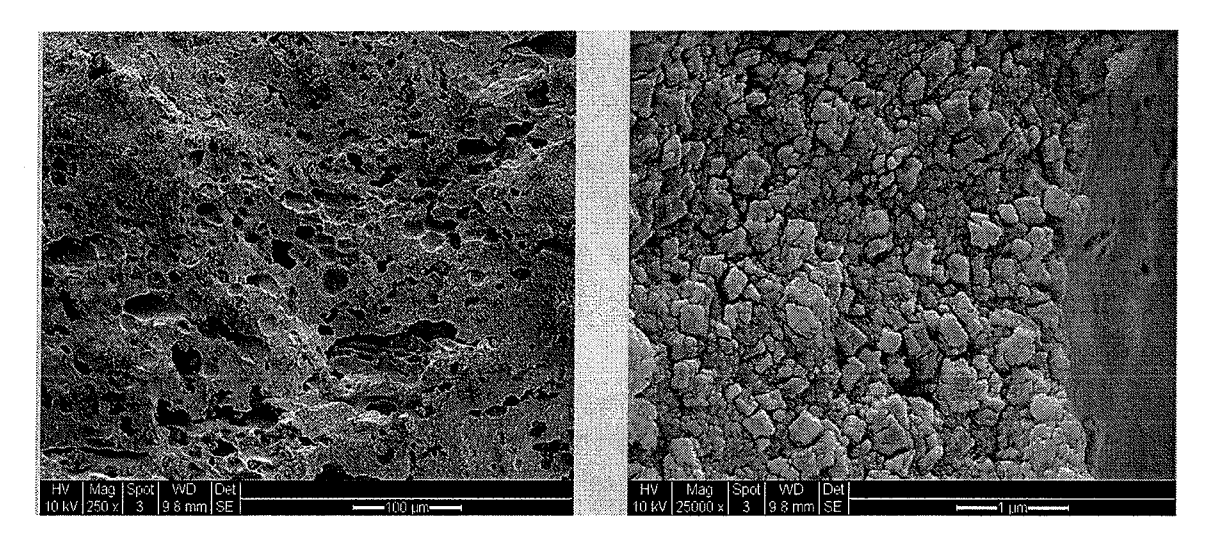


Figure 20a, b

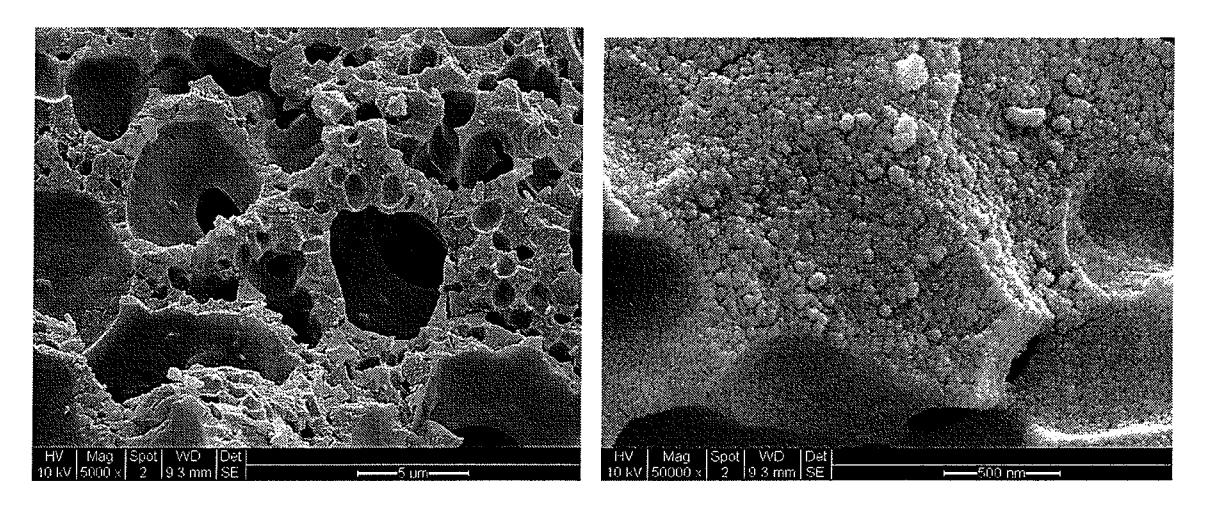


Figure 20c, d



4.tif Si

Cal: 0.130242 nm/pix 8:57:03 07/12/12 20 nm

Direct Mag: 450000x EM Research Services

Figure 20e



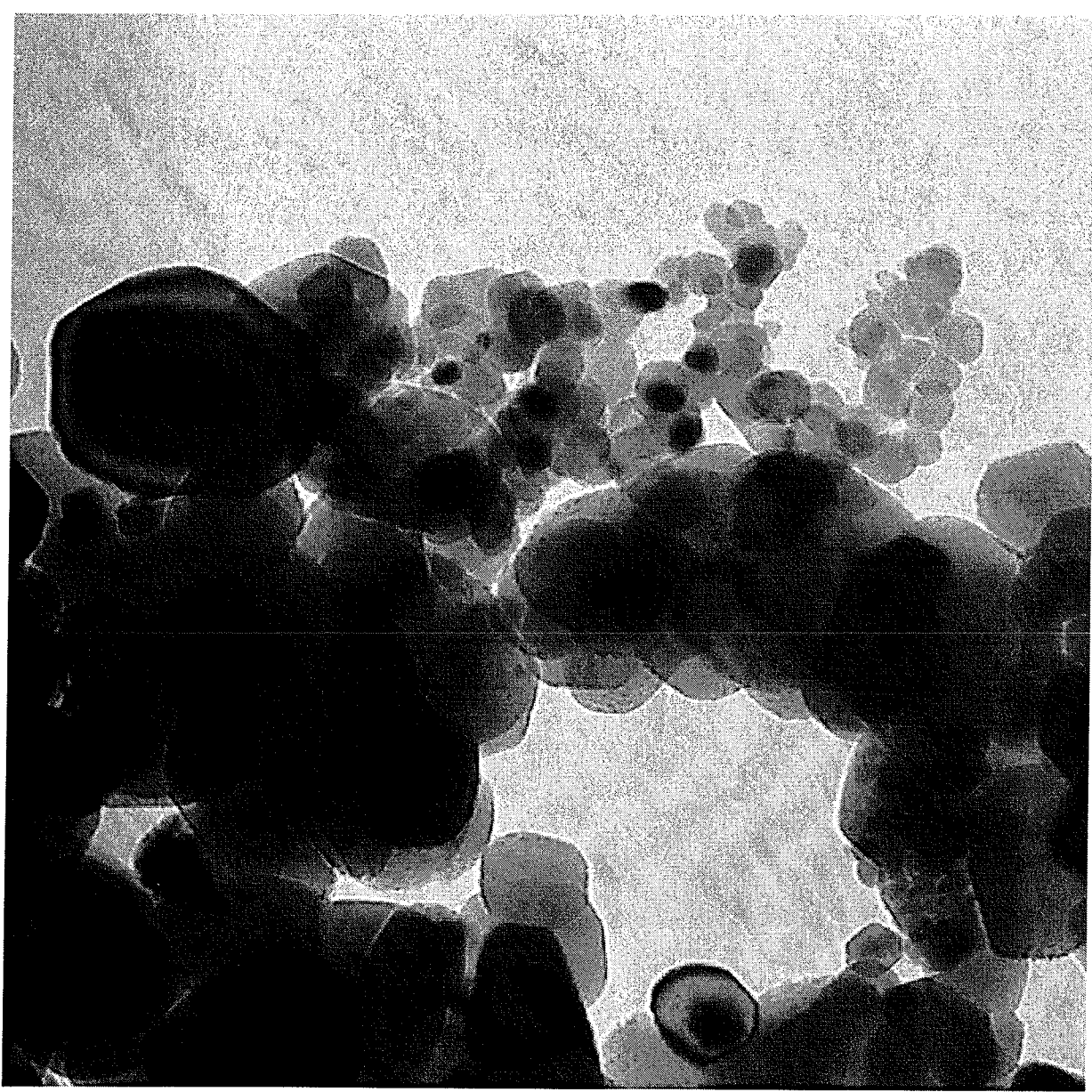
1.tif AA-1AG B

Cal: 0.130242 nm/pix 15:07:54 14/12/12

20 nm

Direct Mag: 450000x EM Research Services

Figure 20f



A2-5.jpg

A2

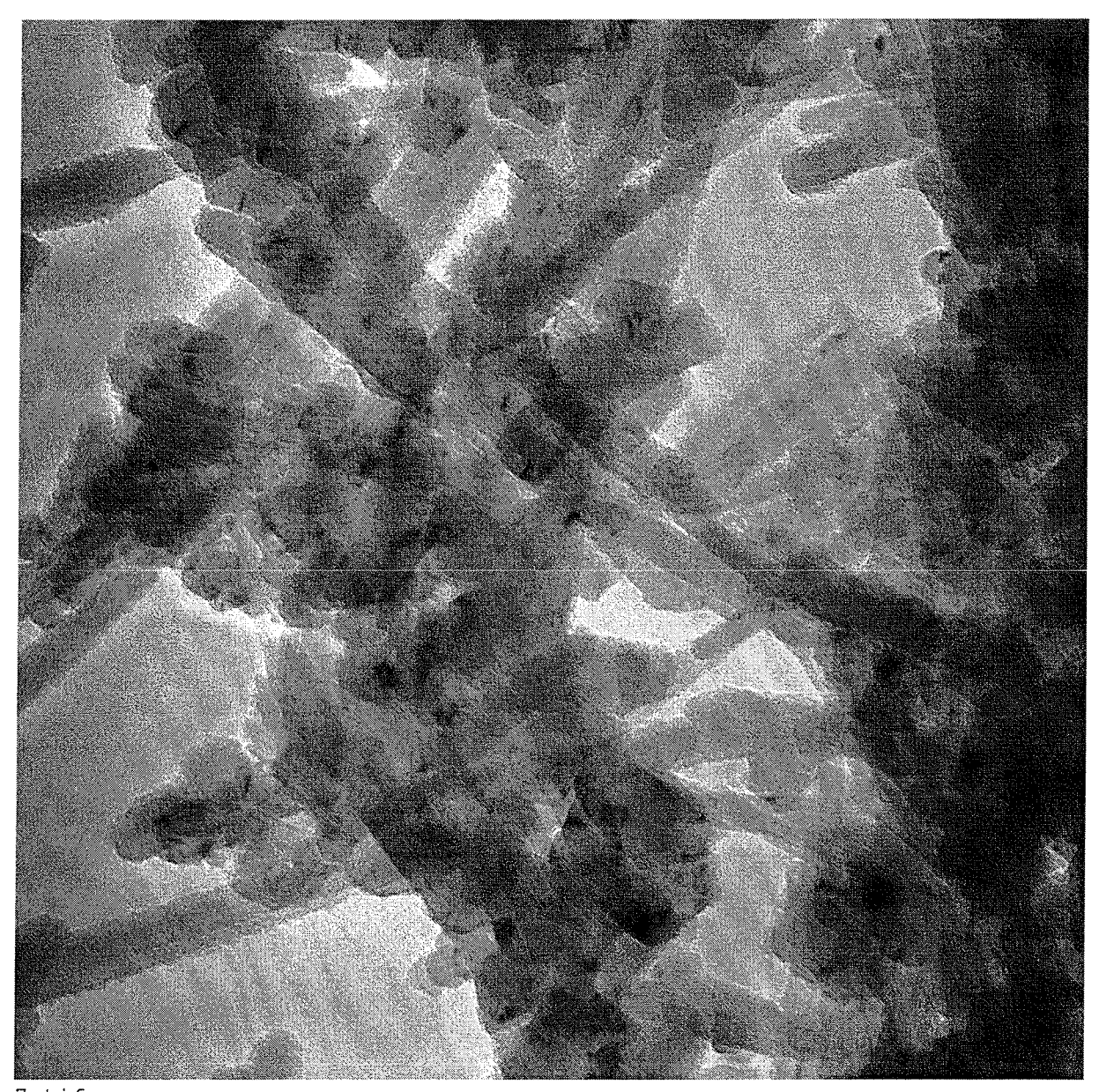
Cal: 0.236072 nm/pix

16:53:18 10/01/11

100 nm

Direct Mag: 245000x EM Research Services

Figure 20g



7.tif BB-10 ABC

Cal: 0.325627 nm/pix 10:16:48 11/12/12

100 nm

Direct Mag: 180000x EM Research Services

Figure 20h

36/38



4.tif FeCl3Si14 A

Cal: 0.130242 nm/pix 11:16:38 17/12/12

20 nm

Direct Mag: 450000x EM Research Services

Figure 20i

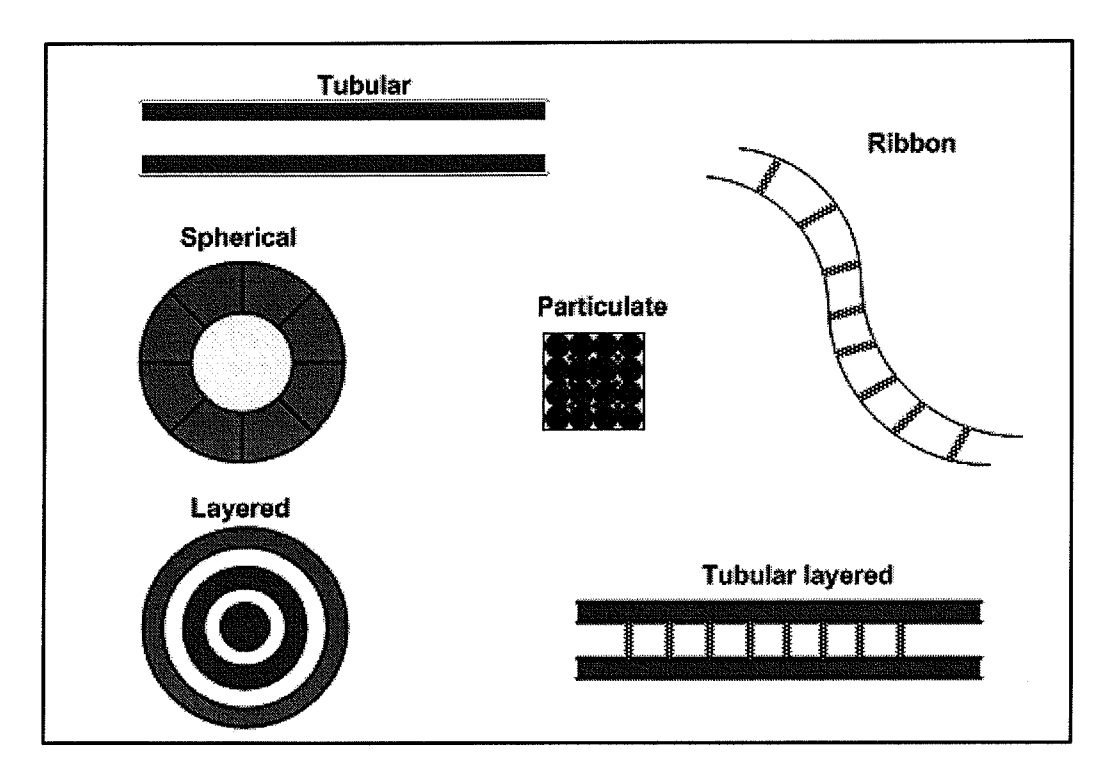


Figure 20j